AD-A194 425 DETECTABILITY OF A DIRECT SEQUENCE EMITTER WITHIN A NETWORK OF DIRECT SEQ (U) M/A-COM SYSTEMS ENGINEERING CENTER VIENNA VA D L NICHOLSON ET AL JAN 88 1/2

UNCLASSIFIED ARO-25331 EL DAAL03-87-C-0020 F/G 17/4 NL

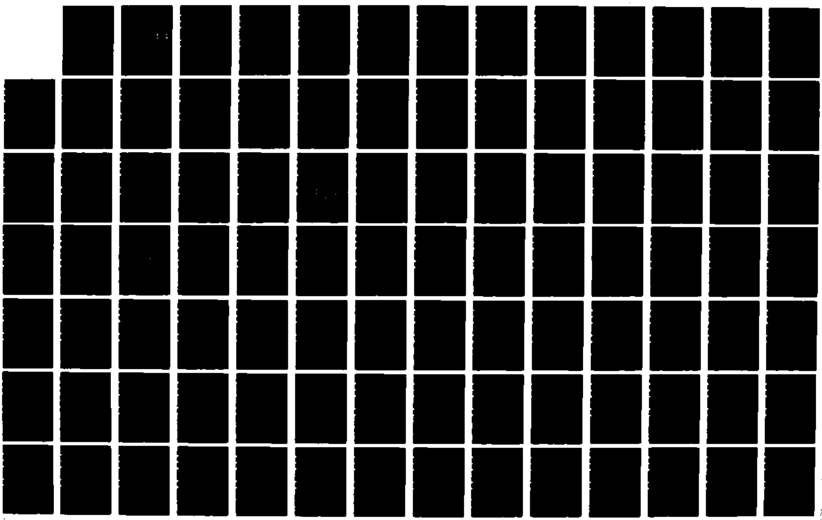

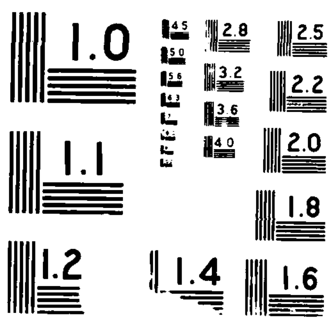

1.0
1.1
1.2
1.4
1.6
1.8
2.0
2.2
2.5
2.8
3.2
3.6
4.0

ARO 25331.1-EL

(2)

DETECTABILITY OF A DIRECT SEQUENCE EMITTER WITHIN A NETWORK OF DIRECT SEQUENCE EMITTERS

FINAL TECHNICAL REPORT

David L. Nicholson and Edgar H. German, Jr.

January 1988

U. S. Army Research Office
Research Triangle Park, NC

Contract No. DAAL03-87-C-0020

M/A-COM ~~Government~~ Systems, Inc.
Systems Engineering Center
8619 Westwood Center Drive
Vienna, VA 22180

FINAL TECHNICAL REPORT ON DETERMINING

DETECTABILITY OF A DIRECT SEQUENCE EMITTER WITHIN A NETWORK OF DIRECT SEQUENCE EMITTERS

Submitted to

United States Army Research Office
Research Triangle Park, NC

M/A-COM Government Systems, Inc.
System Engineering Center
8619 Westwood Center Drive
Vienna, VA 22180

January 1988

EXECUTIVE SUMMARY

This report analyzes the ability of unintended intercept receivers to isolate individual Direct Sequence (DS) emitters within a network of DS emitters. The report demonstrates that interception over $1/R^4$ propagation paths requires very large, ground-based antennas in order to achieve a usable intercept Signal-to-Noise Ratio (SNR). On the other hand, free space, $1/R^2$ propagation paths provide intercept receivers with signal power levels well above the thermal noise power even when the intercept antenna is quite small. However, these small antennas are not able to resolve individual emitters at typical intercept ranges. Antennas large enough to resolve individual emitters are too large to put on aircraft as required to achieve the necessary free space propagation. Hence, the report finds that the beamwidth of the intercept receiver will typically contain many DS emitters. Therefore the receiver bandwidth will contain many overlapping DS signals each typically with a power level which is well above the thermal noise power in the intercept bandwidth. This is the intercept context analyzed in this report.

The analyses therefore confirm that the many DS signals mask each other at linear receivers which attempt to find a spectral region in which the power of one signal is well above the combined powers of the other DS signals. This follows because if the number of DS emitters in the antenna beamwidth equals M+1, then the SNR for any one signal is on the order of 1/M, which is expected to be low. Hence, to be a serious threat, the intercept receiver must be able to detect and process signals which are weak compared to the total power in the intercept bandwidth. Such receivers are called nonlinear receivers.

Nonlinear receivers include the total power radiometer, the doubler, the single channel delay or autocorrelation receiver, the dual channel or cross correlation receiver, and a number of receiver subsystems called feature detectors. The most serious threat to DS emitters is found to be the cross correlation receiver. This receiver forms the cross correlation function of the signals received in its two channels.

First assume that the cross correlation receiver is contaminated only by thermal noise (no narrowband interference). In this idealized case, the cross correlator is expected to generate an autocorrelation spike for every DS emitter whose location is such that the differential propagation delay of its signal between the two intercept antennas is more than just a few nanoseconds. Each autocorrelation spike can be converted into a Line of Bearing (LOB). However, the detection of these autocorrelation spikes can be greatly complicated by using signal design steps. One signal design step is to use repeated, short composite codes to produce DS signals with multiple spikes in their autocorrelation functions. Common code segments can be inserted into all DS signals to produce many spikes in the cross correlation function which do not correspond to autocorrelation spikes. While such signal design does not avoid the largest autocorrelation spikes, it does dramatically increases the signal processing tasks at the intercept receiver.

The report shows that the major factor impacting the ability of the cross correlator to detect individual DS emitters is the presence of a dense environment of unwanted, dynamically varying, narrowband signals. Such is the signal environment expected at airborne interceptors. The report concludes that while not sufficient by themselves, signal design steps plus operation in a dense signal environment will seriously degrade the ability of cross correlators to resolve and identify individual DS emitters in a DS network.

Furthermore, to be a major threat, the LOB's from a DS emitter generated at several intercept sites must be coordinated to form estimates of emitter location. This coordination requires that the autocorrelation spikes be "tagged" with a signal feature as a means of identification. Typical tags which can be extracted in the low SNR environment by nonlinear feature detectors include the DS chip rate and recovery of the DS carrier. The process by which an unintended receiver can extract useful identifying tags can be very seriously degraded by the design of the DS signal. For instance design procedures which limit the performance of chip rate detectors include the following:

- Frequency Hopping to limit the bandwidth of the bandpass filter to a value equal to about twice the hopping rate;
- Time Hopping to limit the bandpass filter bandwidth to a value equal to about the reciprocal of half the burst duration;
- Tailoring the chip shape to approach a bandlimited spectrum such that the spectral line at the chipping rate is small as it is at all the harmonics of the chipping rate; and
- Jittering the chip rate such that again no strong spectral line exists at the chipping rate.

These design steps, in addition to the fundamental goal of operation in a dense signal environment, should make the combined processes of spike detection and tag extraction extremely unreliable and time consuming. In the case of the carrier recovery detector, signal design steps include the following:

- Using MSK or QPSK spreading to lower the output SNR for a given input SNR and TW product;
- Using digitized band-limited Gaussian noise as spreading sequences with essentially uniform phase distribution and Rayleigh distributed amplitude;
- Jittering the carrier frequency; and
- Time Hopping and Frequency Hopping to limit integration time as against the chip rate detector.

Again these steps should be combined with operation in a dense signal environment.

It is concluded that using some of the above design steps plus the inherent sensitivity of nonlinear detectors to dense environments can keep nonlinear receivers from performing adequately even when excision is used to prewhiten the input and remove distortion from the filter output.

TABLE OF CONTENTS

	PAGE
CHAPTER 1 - INTRODUCTION	1-1
CHAPTER 2 - BACKGROUND	2-1
2.1 Interference in Communications Networks	2-1
2.2 Interference at Unintended Receivers	2-3
CHAPTER 3 - TECHNICAL RESULTS	3-1
3.1 Introduction	3-1
3.2 Antenna Issues in Emitter Detection and Isolation	3-1
3.3 Emitter Detection and Isolation Using Non-Linear Receiver	3-15
3.3.1 Background to Non-Linear Intercept	3-15
3.3.2 Detection Using a Dual Channel Cross Correlation Receiver	3-19
3.3.3 Detection Using a Chip Rate Detector	3-29
CHAPTER 4 - CONCLUSIONS	4-1
APPENDIX A: PERFORMANCE OF CHIP RATE DETECTOR IN MULTIPLE SIGNAL ENVIRONMENT	A-1

CHAPTER 1

INTRODUCTION

A primary consideration in denying an enemy knowledge of friendly force position and movement, location of critical command centers, and Electronic Support Measures (ESM) is using communications signals with a low probability of detection and interception. One means of providing tactical Army communications with a Low Probability of Detection (LPD) and a Low Probability of Identification (LPI) is the use of Direct Sequence (DS) spread spectrum modulation. Not only does the wideband DS modulation lower the signal power spectral density, making the signal difficult to detect and identify, but the signals from the many emitters in a network also tend to overlap and mask the presence of each other. The purpose of the research reported here is to quantitatively assess and parameterize the LPD and LPI protection achieved by a single DS emitter within a network of DS emitters.

The research reported here focuses on two critical emitter detection and isolation issues. The first area investigates the feasibility of an intercept receiver capable of isolating an individual communications emitter using a highly directional antenna. The second area investigates the ability of an intercept receiver to somewhat limit the number of emitters in its antenna mainlobe and then to isolate on an individual emitter using signal processing techniques. This second area immediately results in consideration of signal processing techniques capable of performing well when the power of the Signal of Interest (SOI) is lower than the sum of the powers of the other signals present. This is the case because it would not be unlikely for the Signal-to-Noise Ratio (SNR) for one emitter among M emitters in the antenna mainlobe to be approximately 1/(M-1), where M is the total number of emitters in the mainlobe.

BACKGROUND

2.1 INTERFERENCE IN COMMUNICATIONS NETWORKS

Earlier analysis of the design of an LPI network has confirmed that it is not unusual for the "noise floor" of a receiver in a network of DS radios to be established by self-interference caused by the reception of unwanted DS signals transmitted by other emitters in the network. This is particularly the case in the low UHF band (400 MHz) where the propagation attenuation is lower and the antennas are less directional than at higher UHF frequencies such as 1800 MHz. Mathematically this means that for communications power levels and ranges within a ground-to-ground network of direct sequence spread spectrum radios it is not unusual for the following condition to prevail

$$\frac{P_T W_{BB}}{1.36\ W_{SS}} \sum_{m=1}^{M} \frac{G_{TmR} G_{RTm}}{\beta(R_m)} > N_o W_{BB} = \text{Receiver Thermal Noise Power} \qquad (2.1)$$

where the left-hand side of Equation (2.1) is the interference power received at one DS radio as a result of the signal power transmitted by the other radios in the DS network. In Equation (2.1), P_T is the assumed equal transmitted power level of each emitter in the network, G_{TmR} is the gain of the antenna of the m^{th} emitter in the direction of a given receiver, G_{RTm} is the gain of the receive antenna in the direction of the m^{th} transmitter, $\beta(R_m)$ is the propagation attenuation assumed to follow a $1/R^4$ dependence over the path from the m^{th} transmitter to the given receiver, W_{SS} is the spread spectrum bandwidth, W_{BB} is the communications baseband bandwidth, and N_o is the thermal noise power spectral density at the receiver. Of particular concern is the attenuation of the signal from the nearest transmitter in the network whose message is unwanted at a given receiver. As long as the conditions indicated by Equation (2.1) prevail, the SNR at any receiver is not significantly increased or decreased by increases or decreases in transmitted power, assuming each emitter transmits at the same power. Of course, the condition will not be satisfied as the transmitted power is lowered substantially.

Since the transmitted power, P_T, equals the transmitted energy per bit, E_B, times the bit rate, R_b Equation (2.1) may be rewritten yielding the following equation:

$$\frac{E_B R_b}{1.36\ W_{SS}} \sum_{m=1}^{M} \frac{G_{TmR} G_{RTm}}{\beta(R_m)} > N_o \tag{2.2}$$

If the interference level at the communications receivers could be lowered, then the communications transmitted power could be lower to provide more protection against unwanted detection and interception. As noted earlier, one way to lower the interference is to lower the transmitted power. However, it is not always possible to lower the power enough that it is not a major source of interference at the nearest receiver and at the same time provide reliable communications at distant receivers to which it is transmitting. However, if the data rate is reduced then the power could be reduced by the same fraction without lowering the received energy per bit. If the data rate remains the same, then the power control issue is range dependent and needs to be addressed in the network routing control scheme.

Lowering the interference could also be accomplished, and is accomplished to a significant degree, by increasing the spread spectrum bandwidth W_{SS}. With power control so range dependent, Equation (2.2) suggests that the maximum possible spreading bandwidth be used. The interference can also be lowered by decreasing the values of the interference terms added and by reducing the number of interference terms added. Lowering the value of the summation may be achieved by lowering the number of emitters in the network. This lowers the number of terms added, but more importantly, it tends to increase the range to the nearest emitter in the network thus dramatically increasing the propagation attenuation $\beta(R)$ experienced by the interference. Hence the values of the interference terms in Equation (2.2) will typically be significantly decreased by reducing the number of transmitters in the network.

From the above discussion, it follows that both reducing the data rate and the number of emitters in the network will permit the transmitted power to be lowered. However, as determined below, the impacts of these two options on the probabilities of detection and interception at an unintended receiver may be very different.

2.2 INTERFERENCE AT UNINTENDED RECEIVERS

The total amount of power lying within the detection bandwidth, W_D, of an unintended intercept receiver is given approximately by

$$\frac{P_T W_D}{W_{SS}} \sum_{m=0}^{M} \frac{G_{TmI} G_{ITm}}{\beta(R_{Im})} + \sum_{k=1}^{K} P_{Ik} + N_{oI} W_D \tag{2.3}$$

where $N_{oI}W_D$ is the thermal noise power, P_{Ik} is the received power of the k^{th} source of narrowband interference, $\beta(R_{Im})$ is the propagation attenuation over the intercept range R_{Im} between the intercept receiver and the m^{th} DS communications emitter and G_{ITm} is the gain of the intercept receiver in the direction of the m^{th} emitter. If the DS emitters and sources of interference can all be separated or isolated from one another using a directional antenna, the power received at an intercept receiver from the m^{th} emitter would be given by

$$\frac{P_T W_D G_{TmI} G_{IT}}{W_{SS} \beta(R_{Im})} + N_{oI} W_D \tag{2.4}$$

where G_{IT} is the mainlobe gain of the highly directional intercept antenna when it is pointing directly at an individual emitter. In the situation suggested by Equation (2.4), it very likely will be possible to detect and extract the features of the DS signal from the m^{th} emitter needed to intercept or recognize it as a signal of interest. This possibility, and ways to reduce the probability of detection and intercept when this case arises, has been investigated earlier. The result was that increasing power would not result in significantly improved communications, assuming all emitters transmitted the same power level. Rather data rate or communications range had to be decreased assuming that the spread spectrum bandwidth had been maximized during design and was fixed by implementation.

The more general case suggested by Equation (2.3) is investigated here to see how feasible it is to field an intercept receiver capable of the isolation needed to achieve the near worst-case communication situation depicted by Equation (2.4).

One option, identified above, was to lower the number of users. However, this makes it more likely that the individual emitters remaining in the network will be separated enough in angle to permit the type of isolation suggested by Equation (2.4). Hence the advantage of self-masking may be lost when the level of self-interference is lowered by reducing the number of transmitters in the network. While the spread spectrum bandwidth, W_{SS}, is selected during the design stage to be large, it is not considered to be a candidate for adaptive variation during operation. This strongly suggests that adaptively lowering the data rate may be a much preferred way of lowering transmitted power to achieve LPD and LPI. This lowers the SNR at the intercept reciever and also has the potential of retaining the very desirable mutually self-masking aspects of the emitters within a network of DS radios. This possibility, and factors related to it, will be carefully studied in the next section of this report.

CHAPTER 3

TECHNICAL RESULTS

3.1 INTRODUCTION

This section of the report is divided into two major subsections. Subsection 3.2 analyzes the antenna issues relevant to the detection and isolation of individual emitters. This subsection derives the fact that at UHF frequencies near 400 MHz that antennas capable of isolating individual emitters in typical tactical geometries are prohibitively large. At 1800 MHz antennas capable of emitter isolation are unlikely, but possible. Subsection 3.3 considers the case when the intercept antenna is able to reduce the number of emitters in its mainlobe to a number M+1, where M is significantly larger than unity. Further isolation down to individual emitters would then depend on extracting an emitter feature or features by which the individual emitters could be identified.

3.2 ANTENNA ISSUES IN EMITTER DETECTION AND ISOLATION

The factors which most influence the ability of an unintended receiver to detect and isolate an individual emitter within a network of DS emitters are as follows:

a. the relative communications and intercept ranges;
b. the propagation over the communications and intercept paths;
c. the gain and beamwidth of the intercept antenna; and
d. the intercept bandwidth and signal processing strategy.

The first three of these issues will be addressed in this subsection and the fourth issue will be the focus of the next subsection. The approach taken in this subsection is to determine the relationships between the first three factors which result in the ability to detect and isolate individual emitters within a network of DS emitters. The realizability or ability to actually field an intercept system which embodies these factors will then be assessed.

The goal will be to see if any realizable combination of the above factors can be found which would permit individual emitters to be detected and recognized.

The three factors addressed in this subsection will be analyzed as follows. The intercept range expected will lead to an indication of the antenna gain necessary to achieve an adequate intercept Signal-to-Noise Ratio (SNR). Focus will also be placed on the minimum angular separation expected between emitters (as seen by the interceptor) for typical communications and intercept ranges. This angle will provide an indication of the antenna beamwidth needed to resolve or isolate the emitters in angle. Assuming communications center operating frequencies of 400 and 1800 MHz, both the gain required for adequate intercept SNR and the beamwidth required for emitter isolation lead directly to required values of the diameter of a parabolic intercept antenna dish. The size of the antenna dish required will be used as the principal measure of the realizability or fieldability of a candidate intercept system. The comparison between the antenna size needed to isolate emitters and the size needed to achieve a required intercept SNR is critical in determining the relative *risk of being* isolated in angle or being detected in a dense signal environment.

The second important factor is propagation. The propagation path for the communications will be assumed to be $1/R^4$ in all cases. The intercept propagation path will typically be assumed to be $1/R^2$, but the impact of a $1/R^4$ intercept path will be noted.

Two major detection strategies will be investigated. The first will be linear Fourier power spectral analysis as a means of detecting the DS signal in the noise and interference environment. The ability of the antenna to supply an adequate SNR will be a key issue. The second detection strategy, to be addressed in Subsection 3.3, will be the use of a nonlinear cross correlation receiver. In this case, the ability of the antenna to limit the number of other emitters and sources of nonwhite interference power in the mainlobe will be critical.

The first issue to be investigated is the size of antennas needed to isolate or resolve individual DS emitters within a network of DS emitters. This analysis will assume that the unintended receiver uses a parabolic dish or that the antenna reflector is at least parabolic in the azimuth plane. Under these assumptions, for a parabolic dish with an illumination factor of 0.54, the gain relative to an isotropic antenna in dB is given by [1]

$$G_{dB} = 20 \log f_{MHz} + 20 \log D_{ft} - 52.6 \tag{3.1}$$

where f_{MHz} is the frequency in megahertz and D_{ft} is the dish diameter (or aperture in the azimuth plane) in feet.

Two frequencies are of particular interest. These are 400 MHz and 1800 MHz. At these frequencies the gain in dB, from Equation (1) becomes

$$G_{dB} = 20 \log D_{ft} - 0.56 \quad \text{at 400 MHz} \tag{3.2a}$$

$$= 20 \log D_{ft} + 12.51 \quad \text{at 1800 MHz} \tag{3.2b}$$

The ability of an antenna to resolve an emitter depends on its 3 dB beamwidth. Generally, in a given geometry, emitters lying within the 3 dB beamwidth of an antenna are not resolvable in the given geometric situation using that antenna. The 3 dB beamwidth, in radians, of a parabolic dish antenna is given by [1]

$$\Delta_{\theta} = \frac{1.223 \times 10^3}{f_{MHz} D_{ft}} \tag{3.3}$$

which yields

$$\Delta_{\theta} = \frac{3.06}{D_{ft}} \quad \text{at 400 MHz} \tag{3.4a}$$

$$= \frac{0.679}{D_{ft}} \quad \text{at 1800 MHz} \tag{3.4b}$$

---

[1] Reference Data for Radio Engineers, ITT Corp., Fourth Edition, 1949, p.753.

Using Equations (3.2) and (3.4), the relationship between the gain in dB and the 3 dB beamwidth (resolution) in radians is given by

$$G_{dB} = 9.14 - 20 \log \Delta_\theta \tag{3.5}$$

Two approaches will be used to predict how small the antenna resolution must be in order to isolate individual emitters. The first approach, as used in the initial DS network investigation at E-Systems, assumes a network of M emitters is active over an area A. The average communications distance $\langle d_o \rangle$ is then defined as the diameter of the circle whose area is such that

$$M \left[\frac{\pi}{4} \langle d_o \rangle^2 \right] = A \tag{3.6}$$

From Equation (6), the average communication distance is given by

$$\langle d_o \rangle = 2 \sqrt{\frac{A}{M\pi}} \tag{3.7}$$

It follows that the antenna 3 dB beamwidth should satisfy the relationship

$$\Delta_\theta \leq \frac{\langle d_o \rangle}{R_I} \tag{3.8}$$

where R_I is the intercept range. To insure that consistent units are used, A will be given in square miles, d_o in miles, and R_I will be in miles. Using Equation (3.4) in (3.8) yields

$$D_{ft} \geq \frac{C_f}{\langle d_o \rangle} R_I = \left[\frac{C_f}{2} \sqrt{\frac{\pi}{A}} \right] \sqrt{M}\, R_I \tag{3.9}$$

where C_f equals 3.06 at 400 MHz and 0.679 at 1800 MHz.

Equation (3.9) is used to plot the antenna diameter, D_{ft}, as a function of the intercept range, R_I, for the case when A equals 100 square miles and M equals 10, 50 and 100. The result when the communication center frequency equals 400 MHz is shown in Figure 3-1. For an 1800 MHz center frequency, the results are shown in Figure 3-2. From these figures, it is clear that emitters at 1800 MHz are much more easily resolved than emitters at 400 MHz. Based on the "average-communications-range" model, it appears that 50 to 100 users at 400 MHz distributed over 100 square miles would be resolved by an

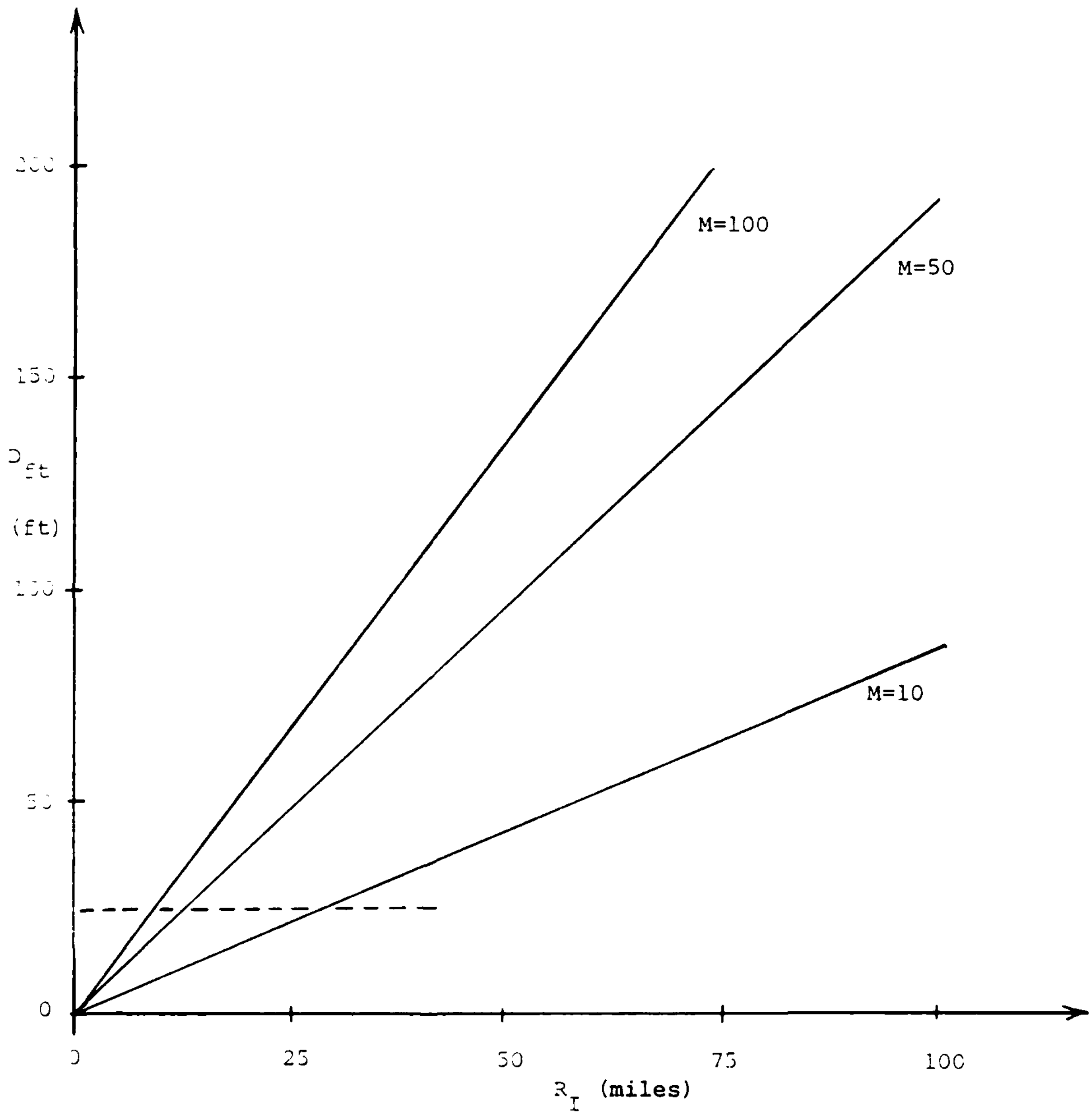

Figure 3-1. Antenna Diameter Required to Resolve Emitters at 400 MHz, A=100 Sq. Miles

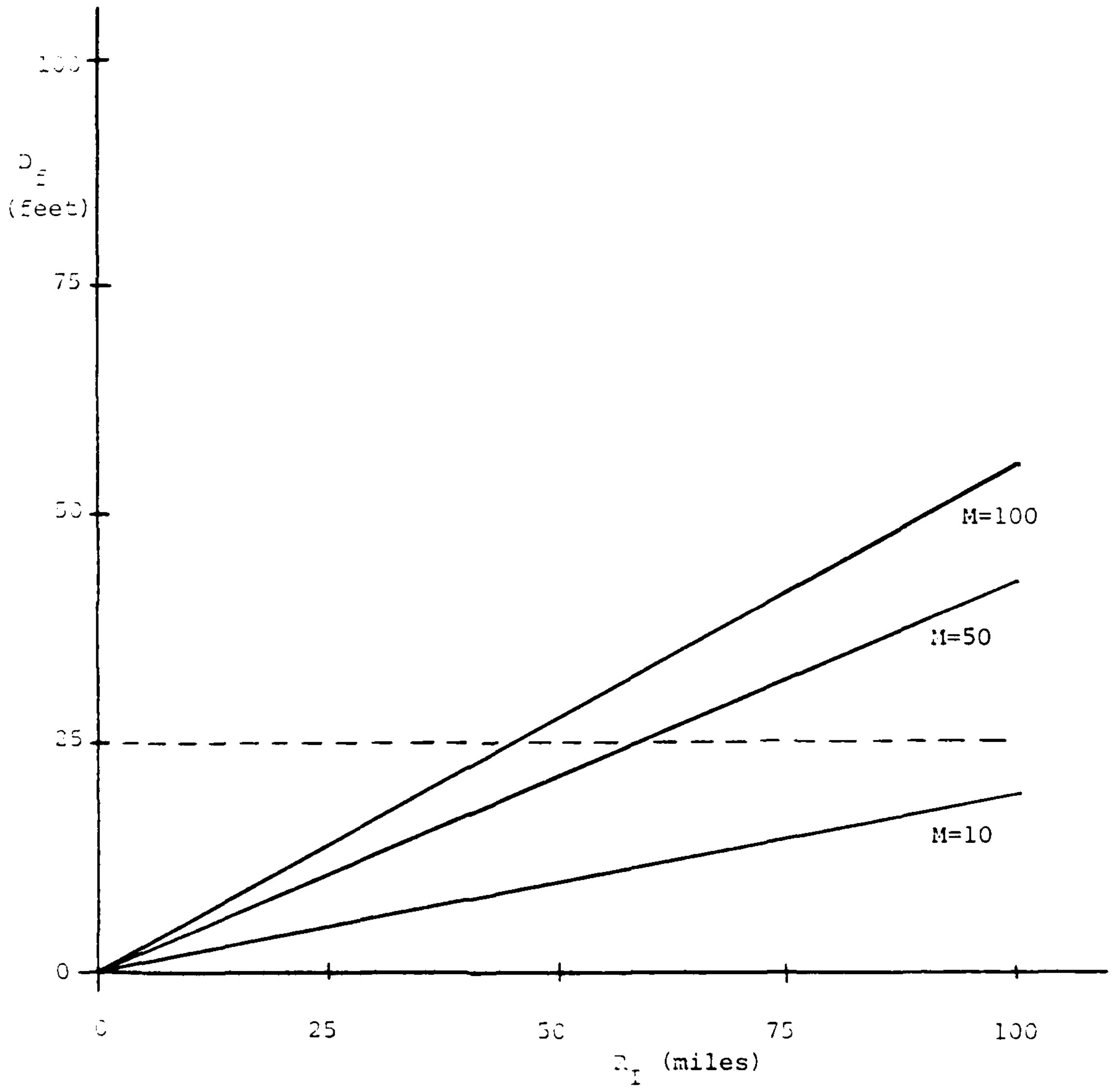

Figure 3-2. Antenna Diameter Required to Resolve Emitters at 1800 MHz, A=100 Sq. Miles

intercepter at a range of more than 10 miles only if the antenna diameter were greater than about 25 feet. The same 25 foot antenna would provide isolation out to about 50 miles at 1800 MHz.

The fact that a 25 foot antenna would almost surely not be airborne will be considered later when the impact of $1/R^4$ versus free space $1/R^2$ propagation is analyzed.

The second, more direct, approach to intercept antenna requirements is to set the antenna 3 dB beamwidth equal to the separation between emitters, R_c, divided by the intercept range, R_I. In this case, Equation (3.4) yields

$$D_{ft} \geq \left[\frac{C_f}{R_c}\right] R_I. \tag{3.10}$$

Equation (3.10) is used to plot D_{ft} as a function of R_I for various values of communication range, R_c. The results for 400 MHz communications is shown in Figure 3-3 and for 1800 MHz in Figure 3-4. From Figure 3-3, it is apparent that very sizable antennas are required for satisfactory resolution at 400 MHz. Note that if the communications link is not perpendicular to the line of intercept, even larger antennas are required. Hence, the antenna size plotted is the smallest capable of isolating the emitters with the specified separation. Figure 3-4 shows that an intercept range of less than about 20 miles is required if emitters at 1800 MHz separated by one-half mile are to be resolved with a 25 foot antenna.

Summarizing, Figures 3-1 through 3-4 reveal that to isolate communications centered around 400 MHz requires either very large antennas (greater than 25 foot diameter) or very close intercept locations (less than 5 or 10 miles). Antennas this large would not be mobile but could exist as fixed-site installations. For fixed sites, the intercept range is expected to increase resulting in even larger antennas. Hence, isolation of emitters at 400 MHz seems infeasible for most tactical communications emitters at 1800 MHz appears feasible, but not likely, except at intercept ranges less than about 10-20 miles for emitters separated by one-half mile. It appears that a 10 foot

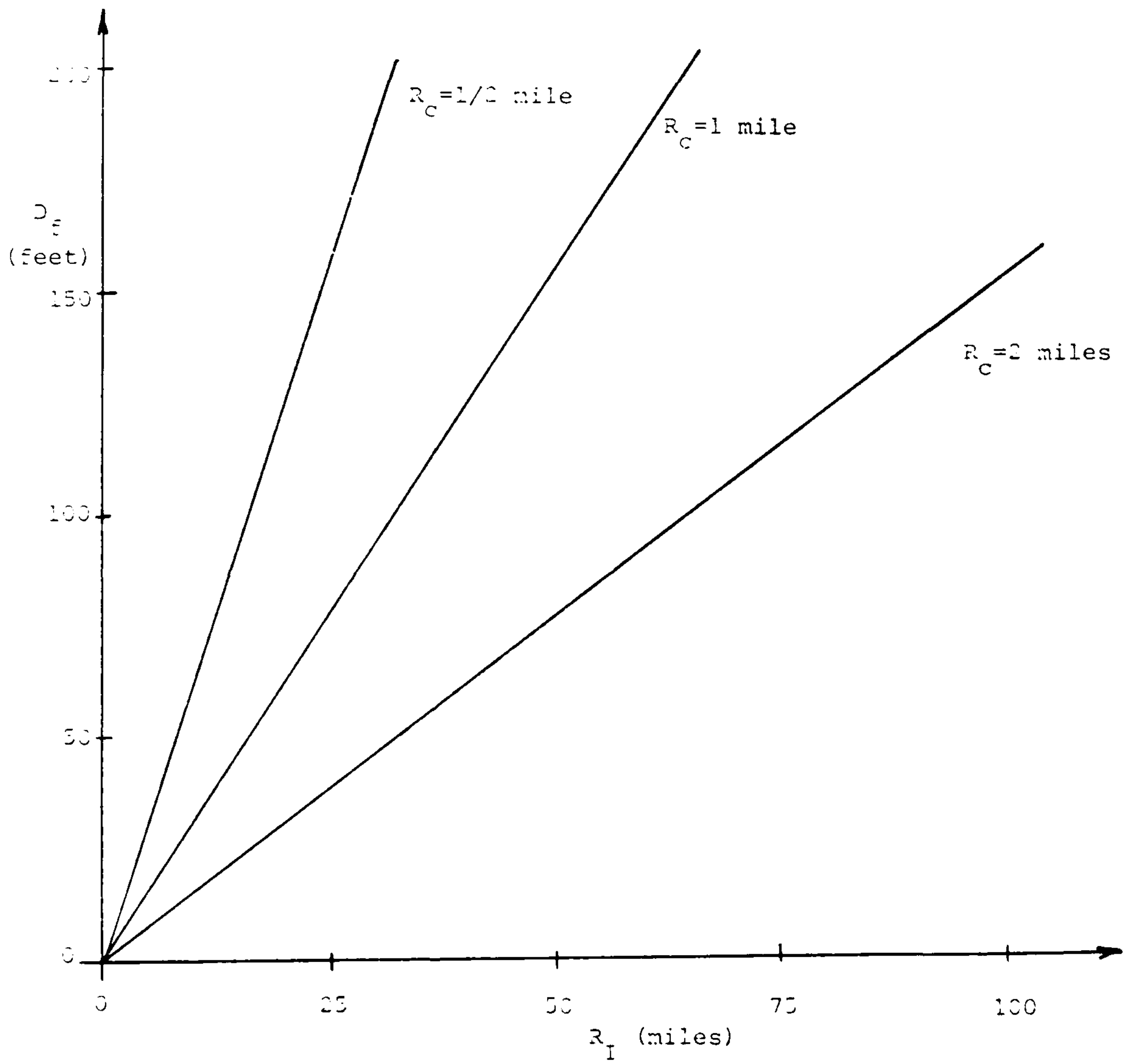

Figure 3-3. Antenna Diameter Requied to Resolve Emitters at 400 MHz at Indicated Emitter Separations

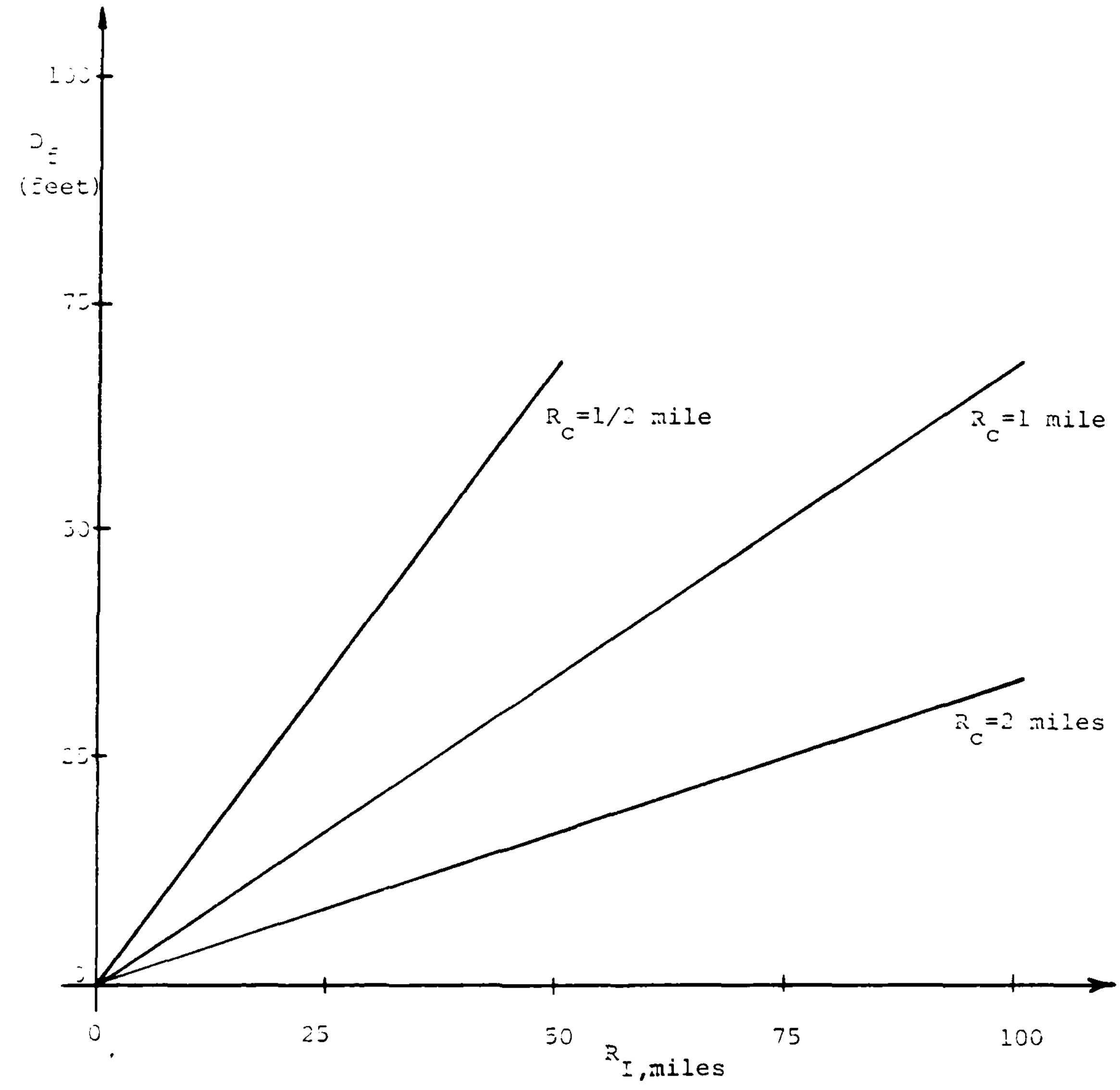

Figure 3-4. Antenna Diameter Required to Resolve Emitters at 1800 MHz at Indicated Cross Beam Separations

antenna, consistent with airborne intercept, would require an intercept range of 7.5 miles to resolve emitters separated by one-half mile and 15 miles for emitters separated by one mile. It should be noted that propagation and signal strength considerations as discussed in the next section relate directly to the ability of a receiver to isolate DS emitters.

The second issue critical to emitter isolation and detection is the intercept Signal-to-Noise Ratio (SNR). The SNR, in turn, is strongly dependent on the propagation mode between the emitters and the intercept receiver. These issues are discussed in this section of the report.

A DS emitter spread its transmitted power, P_T, over its spread spectrum bandwidth, W_{ss}. Assuming that the transmitted signal power spectral equals P_T/W_{ss}, the power in an intercept bandwidth, W_I, is given by

$$Q = \frac{P_T(W_I/W_{ss})\, G_{TI}G_{IT}}{\alpha_I(R_I)L_I} \tag{3.11}$$

where G_{TI} is the gain of the communications transmit antenna in the direction of the unintended intercept receiver, G_{IT} is the gain of the intercept antenna in the direction of the communications emitter, $\alpha_I(R_I)$ is the propagation attenuation over the intercept path of range R_I, and L_I is the loss in the intercept receiver. Assuming the intercept receiver is thermal noise limited, at noise power spectral density N_{oI}, the intercept SNR, denoted by Q/N_I is given by

$$\frac{Q}{N_I} = \frac{P_T G_{TI} G_{IT}}{\alpha_I(R_I)N_{OI}W_{ss}L_I} \tag{3.12}$$

since the intercept thermal noise is equal to $N_{oI}W_I$. In order for Q/N_I to exceed the required value, denoted by $(Q/N_I)^*$, Equation (3.12) shows that the intercept antenna gain must satisfy the relationship

$$G_{IT} \geq \frac{(Q/N_I)^*\ \alpha_I(R_I)W_{ss}N_{oI}L_I}{P_T G_{TI}} \tag{3.13}$$

However, the gain of a parabolic antenna can be written in the form

$$G = 0.54 \left[\frac{\pi D_I}{\lambda}\right]^2 \tag{3.14}$$

from which Equation (3.1) follows. Substituting Equation (14) into Equation (3.13) yields

$$D_{ft} \geq 2.87 \times 10^4 \sqrt{\frac{(Q/N_I)^* W_{ss} N_{oI} L_I}{P_T G_{TI} \; [G_{TI}/G_{TR}]}} \quad R_{I,mi} \tag{3.15}$$

when the intercept path is free-space and when $R_{I,mi}$ is the intercept range in miles. Equation (3.15) is used to plot D_{ft} versus $R_{I,mi}$ from typical values of the parameters under the radical sign. The assumed values are $(Q/N_I)^*$ equals 10, $P_T G_{TI}$ the transmitted Effective Radiated Power (ERP) is 10 watts, N_{oI} is -196 dBW/Hz, L_I is 3 dB and the gain ratio $[G_{TI}/G_{TR}]$ equals unity. The antenna diameter required to achieve the necessary value of $(Q/N_I)^*$ for three values of spread spectrum bandwidth are shown in Figure 3-5. Note that the diameter is quite small, relative to the diameter needed to resolve emitters, even with the reasonably low transmitted ERP of 10 watts. From Figure 3-5, it is clear that for free space propagation the size of the antenna required to achieve useful values of intercept SNR is small compared to the size needed to resolve emitters. The size is small even at ranges compatible with airborne intercept from many tens of miles.

When the intercept propagation path is not free space, the attenuation can be written in the form

$$\alpha(R_I) = C(f,R_o)\alpha_{fs}(f,R_o)(R_I/R_o)^4 \tag{3.16}$$

for typical $1/R^4$, lower UHF ground-to-ground communications over intercept ranges of about 0.1 miles to 10 miles. In Equation (3.16) , $C(f,R_o)$ is a constant which, depending on the heights of antennas, could reasonably equal 35 dB at a reference range, R_o, of 1 mile. The factor $\alpha_{fs}(f,R_o)$ is the free-space, $1/R^2$ attenuation at the communications center frequency and reference range of 1 mile. Therefore, it follows that,

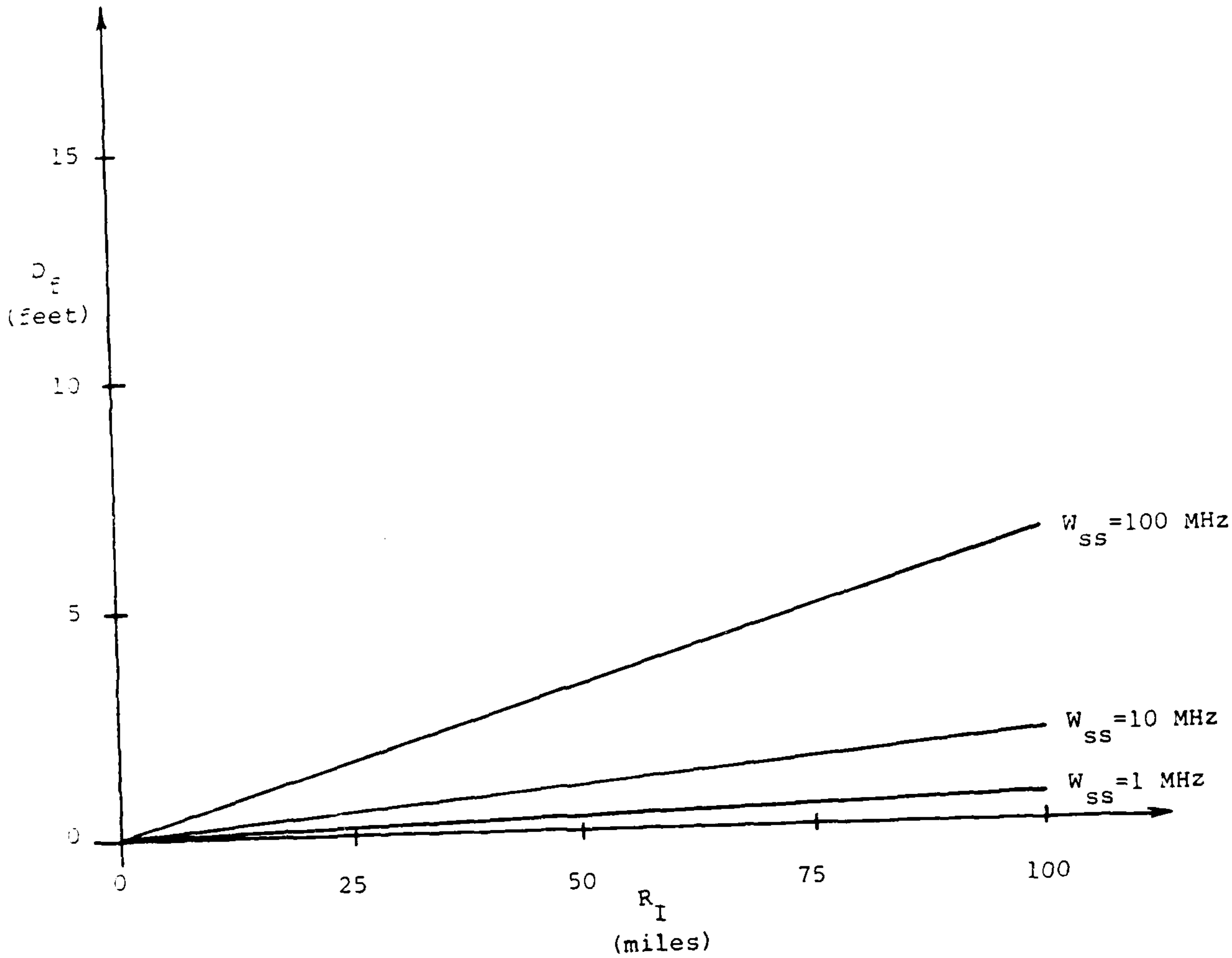

Figure 3-5. **Antenna Diameter Required to Achieve Useful Intercept SNR Against Signal with Indicates Spread Spectrum Bandwidth (Free Space Intercept Assumed).**

$$\alpha_{fs}(f,R_o) = \left[\frac{4\pi R_o}{\lambda}^2\right] = [36.58 + 20 \log f_{MHz} + 20 \log R_{o,mi}] \text{ dB} \quad (3.17)$$

$$= [36.58 + 20 \log f_{MHz}]_{dB}$$

at the referene range of 1 mile.

In, dB, the $1/R^4$ attenuation is therefore

$$\alpha(R_I) = 71.58 + 20 \log f_{MHz} + 40 \log R_{I,mi} \quad (3.18)$$

for $R_{I,mi}$ between about 0.1 and 10 miles. Using Equation (3.17), the diameter of the intercept antenna becomes

$$D_{ft} \geq 2.87 \times 10^4 \sqrt{\frac{(Q/N_I)*C(f,1)W_{ss}N_{oI}L_I}{ERP \quad [G_{TI}/G_{TR}]}} \quad R_{I,mi}^2 \quad (3.19)$$

Using C(f,1) equal to 35 dB, Equation (3.19) is used to plot D_{ft} versus the intercept range. Note the dependence on the square of the intercept range. For the same values of the parameters under the radical sign, Figure 3-6 is a plot of D_{ft} versus R_I for three values of the spread spectrum bandwidth. From Figure 3-6, note that the antenna diameter required is much larger for $1/R^4$ than $1/R^2$ propagation. For instance an antenna diameter of more than 25 feet is required to intercept a signal with a 10 MHz spread bandwidth from an intercept range of only 5 miles under the assumed conditions.

From Figures 3-5 and 3-6, the conclusion is that for free-space, $1/R^2$ propagation the intercept antenna diameter is quite small and easily realized. The antenna is much larger for ground-to-ground intercept of DS, UHF signals.

Overall, the conclusions from Figures 3-1 through 3-6 are that while resolving emitters at 1800 MHz is feasible, it is most likely that intercept antennas will be able to achieve intercepted signal power well above thermal noise levels but that several emitters would typically be within the antenna 3 dB beamwidth, particularly for communications at 400 MHz.

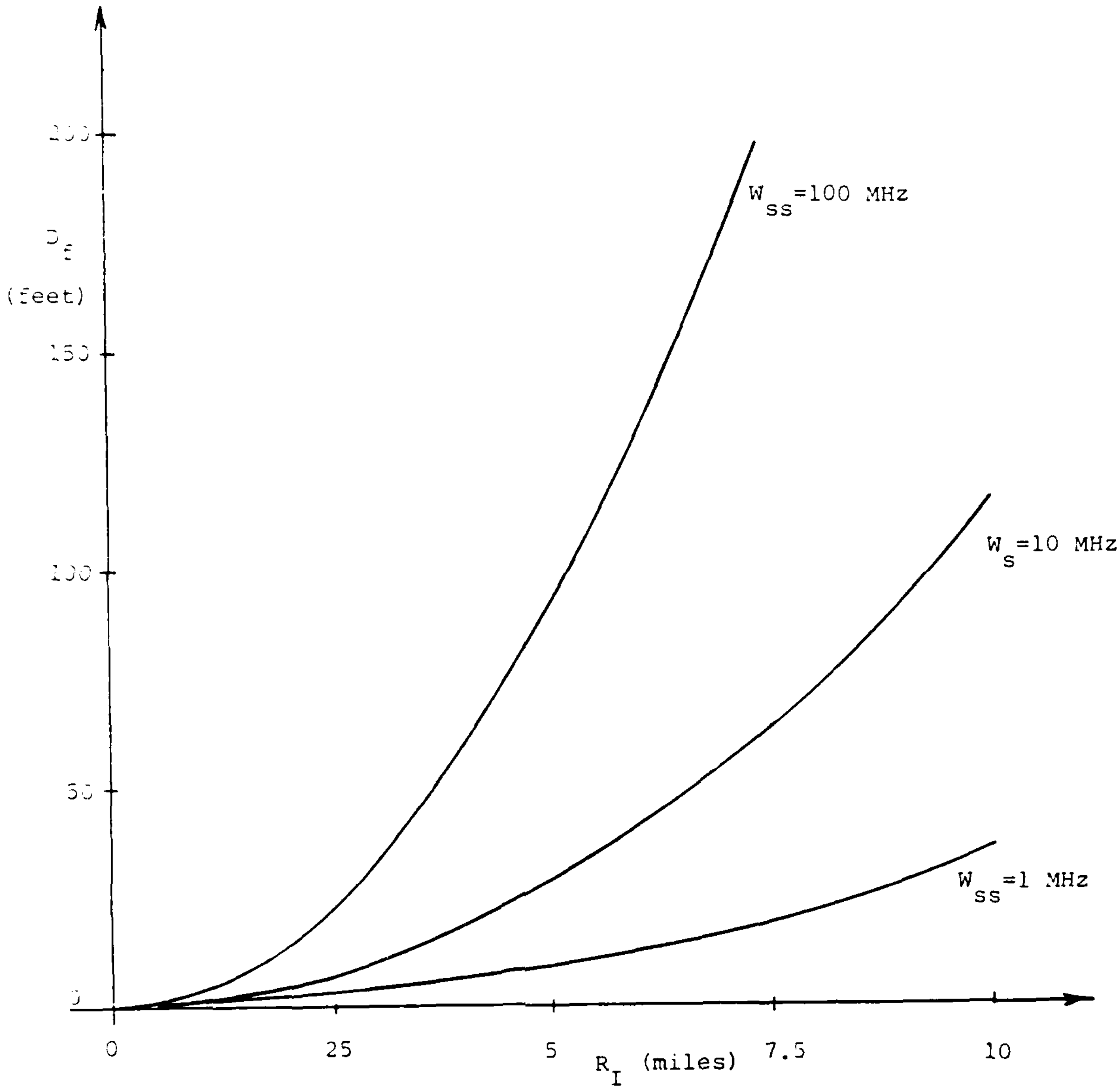

Figure 3-6. Antenna Diameter Required to Achieve Useful Intercept SNR Against Signal with Indicated Spread Spectrum Bandwidth ($1/R^4$ Propagation Assumed).

Based on Figure 3-6, $1/R^2$ propagation will be assumed for the intercept path. From Figure 3-5, a 25 foot antenna will provide an intercepted signal power well above the thermal noise floor when the intercept propagation path is $1/R^2$. Using Equation (3.10) and solving for the communication range with a 25 foot antenna yields the following condition under which the communications emitters are not resolved

$$R_C < \left[\frac{C_f}{25}\right] R_I \tag{3.20}$$

Equation (20) yields Figure 3-7, which plots the minimum resolvable emitter separation using a 25 foot antenna as a function of intercept range. The figure suggests that many emitters will be within the 3 dB beamwidth of an intercept antenna, particularly at 400 MHz. For instance, at an intercept range of 40 miles, the minimum resolvable separation is about 5 miles at 400 MHz. A circle with a diameter of 5 miles has an area of almost 20 square miles. Using Equation (3.7), the value of M such that the average communications range, $\langle d_o \rangle$, equals one-half mile is 101. Hence many emitters are expected to be in the 3 dB beamwidth and potentially mask the presence of one another.

The ability to extract a feature which could allow the individual emitters to be identified is discussed in the next section.

3.3 EMITTER DETECTION AND ISOLATION USING NON-LINEAR RECEIVER

3.3.1 Background to Non-Linear Intercept

It may be somewhat surprising that DS signals which are expected to have such low spectral density do in fact arrive at receivers well above the noise power spectral density. At friendly receivers, to which the DS signal is not being transmitted, this causes network interference. At unfriendly intercept receivers, the DS signal is well above the noise and provides an appreciable intercept SNR. These issues will now be investigated as preliminary to determining when in fact non-linear receivers are needed because the signal is below the receiver noise.

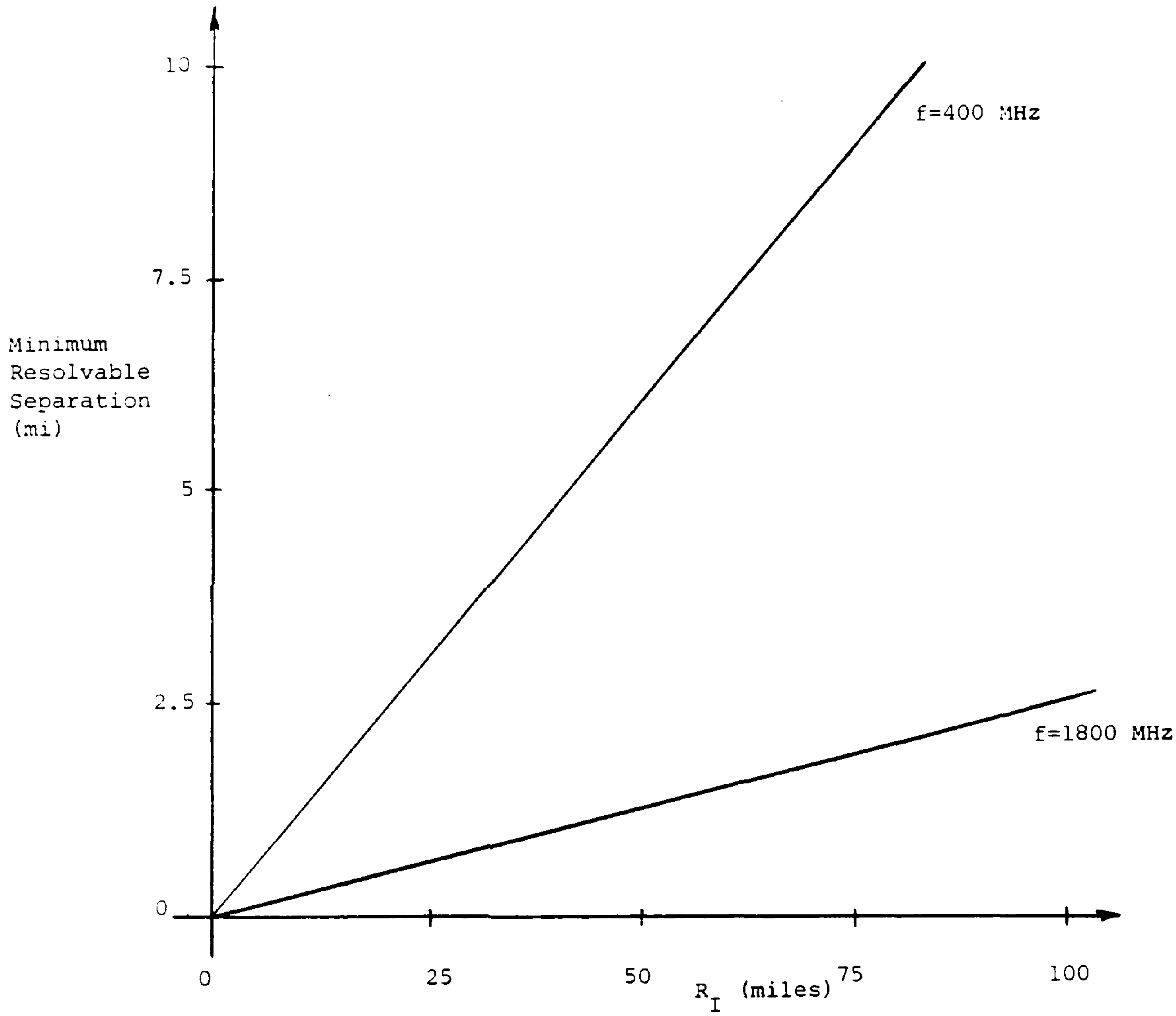

Figure 3-7. Minimum Resolvable (Cross Beam) Separation for a 25 foot Antenna Versus the Intercept Range.

It would not be unusual for a UHF ground-to-ground ($1/R^4$) communications system to transmit on ERP_T of 10 to 20 dBW. This power, when spread uniformly over the spread spectrum bandwidth W_{ss}, yields an intercepted power spectral density given by

$$Q_o = \frac{P_T G_{TI} G_{IT}}{\left(\frac{4\pi R_I}{\lambda}\right)^2 L_I W_{ss}} \tag{3.21}$$

$$= \frac{ERP_T \ [G_{TI}/G_{TR}] G_{TT}}{\left(\frac{4\pi R_I}{\lambda}\right)^2 L_I W_{ss}}$$

where $1/R^2$ intercept propagation is assumed and the variables are as defined in the previous section. Assuming the intercept thermal noise density is N_{oI}, the ratio Q_o/N_{oI} in dB may be written as follows:

$$(Q_o/N_{oI})_{dB} = (ERP_T)_{dBW} + [G_{TR}/G_{TI}]_{dB} + (G_{IT})_{dB} \tag{3.22}$$

$$= \left(\frac{4\pi R_I}{\lambda}\right)_{dB} \quad -(L_I)_{dB} - (W_{ss})_{dBHz} - (N_{oI})_{dBW/Hz}$$

Equation (3.2) can be used to calculate $(G_{IT})_{dB}$ and Equation (3.17) yields the free-space attenuation. Assuming a loss of 6 dB and an 8 dB noise figure Equation (3.22) becomes

$$(Q_o/N_{oI})_{dB} = 100.8 + (ERP_T)_{dBW} + 2(D_{ft})_{dBft} - [G_{TR}/G_{TI}]_{dB}$$

$$-(W_{ss})_{dBHz} - 2(R_{I,mi})_{dBmi} \tag{3.23}$$

As an example, suppose the ERP_T is 10 dBW, the intercept antenna has an 8 foot diameter, and the mainlobe-to-sidelobe ratio is 15 dB. Then Equation (3.23) becomes

$$(Q_o/N_{oI})_{dB} = 113.8 - (W_{ss})_{dBHz} - 2(R_{I,mi})_{dBmi} \tag{3.24}$$

The signal power spectral density is 10 dB or more greater than the noise spectral density whenever

$$(W_{ss})_{dBHz} + 2(R_{I,mi})_{dBmi} \leq 103.8 \qquad (3.25)$$

Even with a spread spectrum bandwidth of 100 MHz (80 dBHz), this means that at intercept ranges less than 15.5 miles the signal is well above the intercept thermal noise. The noise floor of a friendly receiver to which the propagation path is free space, but to which the signal is not intended, would likewise be dominated by the DS signal rather than the thermal noise.

To determine the impact of the anticipated $1/R^4$ propagation path between friendly receivers, Equation (3.21) is rewritten to replace the free-space attenuation with $\alpha(R_I)$ given by Equation (3.16). In this case R_I would represent the range to the interfering communications transmitter. At 400 MHz, and using $C(f,f_o)$ as 35 dB at one mile, we obtain

$$(Q_o/N_{oI})_{dB} = 65.8 + (ERP_T)_{dBW} + 2(D_{ft})_{dBft} - [G_{TR}/G_{TI}]_{dB}$$

$$- (W_{ss})_{dBHz} - 4(R_{I,mi})_{dBmi} \qquad (3.26)$$

Using the same values as follow Equation (3.23), Equation (3.26) becomes

$$(Q_o/N_{oI})_{dB} = 78.8 - (W_{ss})_{dBHz} - 4(R_{I,mi})_{dBmi} \qquad (3.27)$$

It follows that the noise floor would be increased 3 dB or more because of the addition of the signal power density whenever

$$(W_{ss})_{dB} + 4(R_{I,mi})_{dBmi} \leq 78.8 \qquad (3.28)$$

With a spread spectrum bandwidth of 80 dBHz, this occurs for an interference range of 0.93 miles or less. Hence friendly transmitters closer than about a mile are potential sources of significant self-interference for ground-to-ground $1/R^4$ communications at 400 MHz. Many transmitters simply increase the potential for self-interference. Interference effects could apparently be improved by increasing frequency to 1800 MHz thus achieving greater attenuation, higher mainlobe-to-sidelobe ratios and larger spreading bandwidth. However, as shown earlier, intercept at 1800 MHz requires a significantly smaller intercept antenna to achieve isolation of communication emitters. Multiple mainlobe emitters may well be needed to complicate the operations at unintended interceptors.

From Equation (3.25), it is apparent that the spread spectrum signal power in an appropriate intercept bandwidth may well be substantially above the thermal noise power in a variety of intercept situations. This being the case, the remainder of this section will assume that the intercepted power is well above the thermal noise. From the Low Probability of Detection (LPD) viewpoint, this is conservative since whatever contribution the noise makes will be to degrade the performance of detection and feature extraction receivers.

3.2.2 Detection Using a Dual Channel Cross Correlation Receiver

The dual channel cross correlation receiver is one type of non-linear receiver which in theory is capable of detecting signals even when the signal power spectral density is below the thermal noise power spectral density at all frequencies. A functional block diagram of a cross correlation receiver is shown in Figure 3-8. The signals from channels A and B provide a multiplicative reference for each other. When the signal is much stronger than the noise, the performance is similar to a matched-filter receiver with a noisy, rather than perfect, local replica of the incoming signal to be detected. When the intercepted signal power, Q, is well below the intercept power, N_I, the output signal to noise ratio, $(SNR)_o$, is given by

$$(SNR)_o = 2(Q/N)_I^2 \, TW \qquad (3.29)$$

This expression is typical of the output SNR of squaring or correlation receivers. In other receivers, the factor of two is replaced by another number less than two and typically between 1 and 1/4. The factor is two in Equation (3.29) because of the two antennas used by the cross correlation

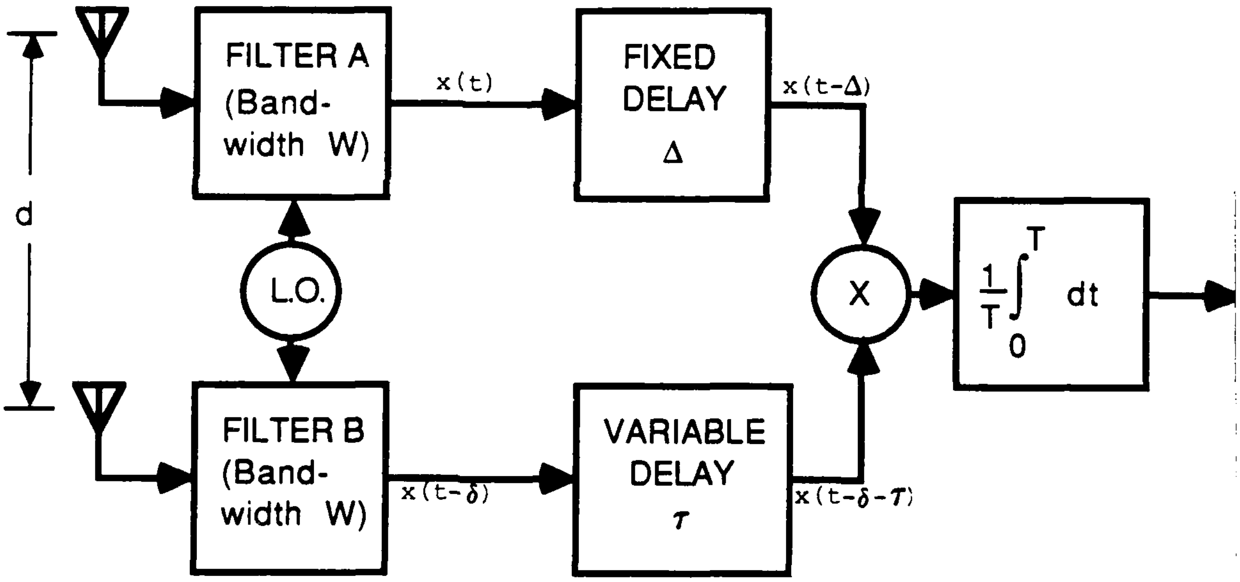

Figure 3-8. Functional Block Diagram of Cross Correlation Receiver

receiver. Equation (3.29) suggests that provided the input bandwidth W contains some signal power Q that integration over a sufficiently long interval T will result in a useful output SNR regardless of how small the input SNR denoted by (Q/N_I) becomes.

In practice the processing time T is limited by a number of issues including receiver mismatch, gain fluctuations, signal variations, and receiver precision and dynamic range. The ability of the cross correlation receiver to detect signals below the interference level is very much dependent on the strength, amplitude variation, number, and dynamic behavior of these nonwhite sources of interference. Correlated sources of interference entering both channels also degrade receiver detection performance.

The antenna beamwidth of the correlation viewer is assumed to be quite broad so that special antenna tracking is not required. Hence the signals from many emitters in the DS network are expected to enter the receiver. These DS signals are expressed in the from

$$s_m(t) = \sqrt{2S_m}\, b_m(t)u_m(t) \cos [2\pi f_c t + \theta_m] \tag{3.30}$$

where $b_m(t)$ is the bit phase of the m^{th} emitter at time t; $u_m(t)$ is the chip stream of the m^{th} emitter (which is assumed to be statistically independent from emitter to emitter); f_c is the center frequency assumed to be essentially the same for all emitters in the network; and θ_m is the carrier phase of the m^{th} carrier relative to θ_o, which is assumed to be zero. This means that the signal component of the composite waveform entering the multiplier in Figure 3.8 from channel A is given by

$$s_{mA}(t-\Delta) = \sqrt{2S_m}\, b_m(t-\Delta)u_m(t-\Delta)\cos [2\pi f_c(t-\Delta)+\theta_m] \tag{3.31}$$

The signal component from channel B is given by

$$\begin{aligned} s_m(t-\tau-\delta_m) = \sqrt{2S_m}\, & b_m(t-\tau-\delta_m)u_m(t-\tau-\delta_m) \\ & \cos [2\pi f_c(t-\tau-\delta_m)+ \theta_m] \end{aligned} \tag{3.32}$$

where δ_m is the differential propagation delay of the m^{th} signal between the two antennas.

The threat posed by the cross correlator is that by proper selection of the variable delay τ in channel B to a particular value, τ_m*, the m^{th} signal in channels A and B will be coherent resulting in an output of the integrator equal to S_m plus distortion. This particular value of τ_m* which brings the m^{th} signal into coincidence at the multiplier is equal to $\Delta - \delta_m$, where Δ is the maximum differential delay equal to at least the separation between antenna phase centers divided by the speed of light. The most negative propagation delay occurs when the signal arrives end-fire from antenna B to antenna A. Hence, the maximum required variable signal delay equal 2Δ.

Looking at Equations (31) and (32) it is clear that the mean shape of the integrator output near τ_m* is determined by te autocorrelation function of $u_m(t)$. Since this function is triangular spike band-limited to the receiver bandwidth W, the duration of the spike is approximately 1/W. However, since W is very nearly the spread spectrum bandwidth, W_{ss}, this spike is very narrow having a duration about equal to the chip interval. The sharpness of the autocorrelation spike also dictates the increment by which the variable delay should be changed. Assuming a delay increment which is a small fraction, say 1/5 or 1/10, of the chip interval the output of the integrator as a function of the delay τ is a sequence of autocorrelation spikes. The delays τ_m* at which they occur defines a Line of Bearing (LOB) on which the m^{th} emitter is located. If an identifying feature of the signal transmitted by the m^{th} emitter an be extracted by which LOB's can be exchanged and combined among intercept receivers, then the m^{th} emitter can be located. One such tag or identifying feature is the precise chip rate of the m^{th} emitter. Other tags include the exact center frequency, corrected for doppler if necessary, received power level in some situations, signal timing as the transmitter is tuned off and on, and perhaps certain patterns that the autocorrelation spikes produce. Tags of this type may pose a very severe threat to DS emitters when used in conjunction with LOB information derived from a cross correlation receiver. Various tags will be discussed later in this section, particularly the chip rate and the center or carrier frequency of a DS signal.

The critical issue is if a tag exists how can it be unambiguously associated with a certain autocorrelation spike and hence a certain LOB. It appears that once τ_m* is carefully determined based on the location of the autocorrelation spike, then additional feature detectors can be switched into the receiver. For instance an addition delay in one channel of approximately half-a-chip interval could yield the input to a chip rate detector. The square of the m^{th} signal achieved when τ_m* is used could provide information on the carrier center frequency.

The correlation spike of height S_m is distorted by the effects of noise, the other DS signals, and other interfering signals. When taking these sources into account, the output SNR for signal $s_o(t)$ as the square of the expected value divided by the variance of the integrator output, can be written in the form

$$(SNR)_o = \frac{S_o^2}{D_{SS} + D_{SP} + D_{NS} + D_{NP} + D_{NN} + D_{PP}} \tag{3.33}$$

where the particular delay τ_o* is assumed to exist in the cross correlation receiver. Th term D_{ss} is the distortion power due to the multiple signals interacting with one another, D_{SP} is the distortion power of the signals interacting with narrowband interferers, D_{NS} is the result of noise interacting with the signals, D_{NP} is the power caused by the interaction of noise and the narrowband interferers and D_{NN} and D_{PP} are the powers caused by the interaction of noise with itself and narrowband inteference with itself respectively.

The mathematical expressions for each of the distortion power terms are given below:

$$D_{SS} = \frac{1}{1.36\ TW_{ss}} \sum_{\substack{m=0 \\ m=q\neq 0}}^{M} \sum_{q=0}^{M} S_m S_q \tag{3.34}$$

where the value 1.36 arises from the matching spectral taper of the interfering DS signals and L is the number of signals which interfere with signal $s_o(t)$.

$$D_{SP} = \frac{2}{TW_{ss}} \sum_{m=0}^{M} \sum_{k=1}^{K} S_m P_k \left| \frac{\sin x k}{x k} \right|^2 \tag{3.35}$$

where M is the number of narrowband inteferers with powers P_m and the $[(\sin x)/x]^2$ factor accounts for the offset of the narrowband interferers from the center DS frequency.

$$D_{NS} = \frac{N_{OI}}{T} \sum_{m=0}^{M} S_m = \frac{(N_{oI} W_{ss})}{TW_{ss}} \sum_{m=0}^{M} S_m \tag{3.36}$$

where N_{oI} is the thermal noise power spectral density of the cross correlation receiver, assumed the same in both channels.

$$D_{NP} = \frac{N_{oI}}{T} \sum_{k=1}^{K} P_k = \frac{N_{oI} W_{ss}}{TW_{ss}} \sum_{k=1}^{K} P_k \tag{3.37}$$

$$= \frac{N_I}{TW_{ss}} \sum_{k=1}^{K} P_k$$

where N_I equals the intercept thermal noise power in the intercept bandwidth W_{ss}.

$$D_{NN} = \frac{N_{oI}{}^2 W_{ss}}{2T} = \frac{N_I{}^2}{2TW_{ss}} \tag{3.38}$$

and

$$D_{PP} = \frac{1}{2} \sum_{k=1}^{K} P_k^2 \tag{3.39}$$

Of special interest in a test case is the situation when P_k equals zero for all k and there is only one signal, $s_o(t)$. In this case Equations (3.33) to (3.39) yield

$$(SNR)_o = \frac{S_o^{\;2}}{\frac{N_I}{TW_{ss}} S_o + \frac{N_I^2}{2TW_{ss}}} = \frac{2\,(S_o/N_I)^2 TW}{1 + 2\,(S_o/N_I)} \qquad (3.40)$$

which is a known result and agrees with Equation (3.29) when the input SNR, denoted by (Q/N_I), is much smaller than unity.

As indicated earlier, of particular interest is the case when the signal power is well above the thermal noise power. In this case, the contributions of D_{NS} and D_{NN} can be ignored and the output SNR becomes

$$(SNR)_o = \frac{S_o^2}{D_{SS} + D_{SP} + D_{NP} + D_{PP}} \qquad (3.41)$$

where the D_{NP} term is retained because the narrowband interferers can be so strong compared to the signals.

Two cases related to Equation (3.41) will be considered. First, is the case of no narrowband interference for which

$$(SNR)_o = \frac{S_o^{\;2}}{D_{SS}} = \frac{1.36\, S_o^{\;2}\, TW_{ss}}{\sum\limits_{m=0}^{M} \sum\limits_{\substack{q=0 \\ m=q\neq 0}}^{M} S_m S_q} \qquad (3.42)$$

When all powers are the same Equation (3.42) yields

$$(SNR)_o = \frac{1.36\, TW_{ss}}{M^2 - M} \cong \frac{1.36\, TW_{ss}}{M^2} \qquad (3.43)$$

which generally speaking is expected to be large. However, if S_o is small compared to some S_m, m not equal to zero, there is an opportunity for self masking even in the cross correlator. Assume, for instance, that S_1 is much stronger than all other signals. Then Equation (3.42) yields

$$(SNR)_o = \frac{1.36\, S_o^2\, TW_{ss}}{S_1^2 + 2S_1 \sum_{\substack{m=0 \\ m\neq 1}}^{M} S_m} = \frac{1.36(S_o/S_1)^2 TW_{ss}}{1 + \frac{2}{S_1} \sum_{\substack{m=0 \\ m=1}}^{M} S_m} \tag{3.44}$$

$$\cong 1.36(S_o/S_1)^2 TW_{ss}$$

which shows how one strong signal can mask a much weaker one. However, the output SNR for emitter number "1" would be very large. This could result in emitter number "1" either lowering its power or perhaps being destroyed. This would then allow the TW_{ss} factor in the output SNR to yield an appreciable output SNR. It appears that strong signals, and their emitters, could be systematically eliminated allowing the subsequent exposure of weaker signals and their emitters. To avoid this, the communications might have to use bursts, such that the useful integration time T is limited, in accordance with increasing the number of emitters in the network, such that

$$\frac{TW_{ss}}{M^2} \cong 1 \tag{3.45}$$

This also implies that the emitter transmit duty cycle would need to be increased, perhaps using dummy traffic, to nearly unity. This could have operational consequences as well as shorten battery recharge intervals significantly.

Since the output of the cross correlator at τ_m* is the power of $s_m(t)$, it is not possible to avoid the cross correlation spike without reducing transmitted power once antenna, propagation and masking issues are fixed. However, it may be possible to significantly degrade the operation of a network of cross correlators by using repeated short codes in the DS signal. This would cause a number of minor cross correlation spikes with increasing amplitude until the spike of height S_m is achieved at variable τ_m*. The many minor spikes, however, could make it very difficult to pass reliable emitter Line of Bearing (LOB) information between intercept receivers to achieve emitter location. Alternately, all emitters could share a certain code segment or segments which would generate many false spikes and make the τ_m* values very difficult to determine. Sorting on only the largest spikes would allow the emitters with lower power to remain masked. Again, however, destruction of the emitters with the strongest power would have to be avoided by perhaps using power control and rapidly moving the emitters with the largest power.

Ultimately, however, the masking techniques which most capitalizes on the inherent weakness of the non-linear recievers is to locate DS signals where many interferers also operate. Of course, the environment cannot be so dense that the communicators cannot synchronize and exchange data. This leads to the second case of interest in which the total distortion power at the delay τ_o* is increased by the sum of D_{SP}, D_{NP} and D_{PP}. This yields the output SNR as given by Equation (3.41), which may be rewritten in the form

$$(SNR)_o = \frac{S_o^2 \, TW_{ss}}{\frac{1}{1.36} \sum_{m=0}^{M} \sum_{\substack{q=0 \\ m=q\neq 0}}^{M} S_m S_q + 2 \sum_{m=0}^{M} \sum_{k=1}^{K} S_m P_k X_k + N_I \sum_{k=1}^{K} P_k + \frac{TW_{ss}}{2} \sum_{k=1}^{K} P_k^2}$$

where X_k is defined to equal the spectral taper factor

$$X_k = \left[\frac{\sin x_k}{x_k} \right]^2 = \left[\frac{\sin \pi \, (f_c - f_k) T_c}{\pi (f_c - f_k) \, T_c} \right]^2 \qquad (3.47)$$

where f_m is the center frequency of the narrowband interferer and T_c is the chip duration of the DS communications. The average value of X_k is approximately 1/2.22 which will be used to simplify Equation (3.46).

Note from Equation (3.46) that the interferers have a dramatic impact on the output SNR. For instance, neglecting the contributions from D_{SS}, D_{SP} and D_{NP} yields an output SNR equal to

$$(SNR)_o = \frac{2S_o^2}{\sum_{k=1}^{K} P_k^2} \qquad (3.48)$$

which is expected to be low for reasonable values of K and P_k.

With N_I much less than the typical signal power, S_m, Equation (3.46) becomes

$$(SNR)_o = \frac{2S_o^2\, TW_{ss}}{1.47 \sum_{\substack{m=0\\ m=q\neq 0}}^{M} \sum_{q=0}^{M} S_m S_q + 1.80 \sum_{m=0}^{M} \sum_{k=1}^{K} S_m P_k + TW_{ss} \sum_{k=1}^{K} P_k^2} \quad (3.49)$$

Clearly, the cross correlation receiver must try to eliminate or excise the narrowband interference in the input before multiplication or after integration or both. However, in a dynamic environment, the integration time T may be long compared to the average time interval in which the number and total power of the interferers changes significantly. This makes excision at the integrator output more difficult.

The following definitions simplify the evaluation of Equation (3.49)

$$\alpha_m \quad = S_m/S_o \quad (3.50a)$$

and

$$\beta_k \quad = P_k/S_o \quad (3.50b)$$

Using Equation (3.50), Equation (3.49) becomes

$$(SNR)_o = \frac{2TW_{ss}}{1.47 \sum_{\substack{m=0\\ m=q\neq 0}}^{M} \sum_{q=0}^{M} \alpha_m \alpha_q + 1.80 \sum_{m=0}^{M} \sum_{k=1}^{K} \alpha_m \beta_k + TW_{ss} \sum_{k=1}^{K} \beta_k^2} \quad (3.51)$$

Generally, if the output SNR for a DS is several dB, say 8 to 18, then the presence of the autocorrelation spike can be detected and the setting of the variable delay at detection provides LOB information. As mentioned earlier, one means of complicating this operation, and thus degrading performance, is to create compound signals with multiple autocorrelation and cross correlation spikes.

For approximately equal powers of spread and unspread (narrowband) signals α_m equals about β_k which equals about unity for all values of m and k. In this case, Equation (3.51) becomes

$$(SNR)_o = \frac{2TW}{1.47\ (M^2 - M) + 1.80\ MK + KTW_{ss}} \tag{3.52}$$

$$\cong \frac{2}{K} \left[\frac{1}{1 + \frac{1}{TW_{ss}} [1.47\ \frac{M^2}{K} + 1.80M]} \right] \leq \frac{2}{K}$$

This expression confirms that narrowband interference needs to be excised from the input or appropriately filtered or ignored at the output of a cross correlation receiver in order for it to achieve reliable performance.

3.3.3 Detection Using a Chip Rate Detector

As indicated earlier, the potential exists for the cross correlation receiver to develop a LOB on each DS emitter for which the differential propagation between antennas is more than about $(W_{ss}\sqrt{2(SNR)_o})^{-1}$ seconds. This timing difference would typically correspond to a few feet with W_{ss} equal to 100 MHz or a few tens of feet when W_{ss} equals 10 MHz. If a feature of the m^{th} LOB is based, then multiple receivers and feature extractors could isolate individual DS emitters unless they were very close together. In terms of targeting, such a cluster could be a high value target. One feature which might possibly be used as a tag to identify a LOB is the emitter chip rate. However, the chip rates are expected to be very nearly identical. The issue then is how well can a chip rate detector distinguish between the very nearly chip rates used by the emitters in a DS network. This issue is discussed below and a detailed analysis of the performance of a chip rate detector is provided in Appendix A, which was prepared by Edgar German of GT-Tech, Inc.

A functional block diagram of a chip rate detector is shown in Figure 3-9. The basic goal of the receiver is to multiply the receiver input by a delayed version of the input and then bandpass filter. Note this could be achieved using two channels after τ_m* has been determined by placing an additional delay in one channel below multiplication and bandpass filtering.

The principle of operation for the chip rate detector is as follows. Given a chip sequence $u_o(t)$ the product $u_o(t)u_o(t-\tau)$ is random. However, the expected value of $u_o(t)u_o(t-\tau)$ is a deterministic square-wave function with a period equal to the chip duration. Since the expected value of $u_o(t)u_o(t-\tau)$ in the autocorrelation function, the power spectrum of the product $u_o(t)u_o(t-\tau)$ has harmonics at multiples of the reciprocal of the interval. The fundamental frequency of the discrete power spectrum is the chipping rate. Hence, extraction of this spectral line and the measurement of its frequency provides a measure of the chip rate transmitted by a DS emitter. Stochastic signals which have periodic statistics, such as the autocorrelation function, are called cyclostationary signals.

Three factors dominate the distinguishing capability of the chip rate detector. One is the narrowband interference whose dramatic effect was discussed for the cross correlator. Narrowband interference has similar effects on the output SNR of the chip rate detector as it did for the cross correlator. The second factor is the filter resolution of the chip rate detector. The processing time T must be such that the bandwidth of the bandpass filter 1/T is less than or equal to the difference is the chip rates to be distinguished. For instance a rate difference of one chip per second requires a filter with one Hertz of bandwidth or more. The third factor is the extent of self-masking interference the several chip sequences have on each other. These last two factors are treated in detail in Appendix A and the self-masking factor is discussed below.

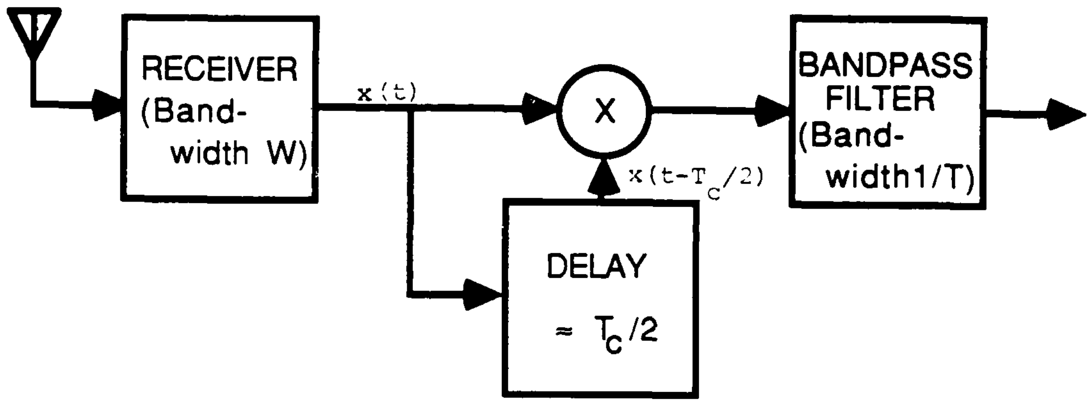

Figure 3-9. Functional Block Diagram of Chip Rate Detector

From Appendix A, the output SNR for the m^{th} DS signal is given by

$$(SNR)_{o,m} = \frac{S_m^{\;2} TW}{\sum_{\ell=0}^{M} S_\ell^2 + \frac{3}{2} \sum_{\substack{j=0 \\ j \neq k}}^{M} \sum_{k=0}^{M} S_j S_k} \tag{53}$$

where it is assumed that the signal power of the DS signals is well above the thermal noise level, N_I. From Equation (3.53), it is clear that with only one DS signal present the output SNR is bounded at the value TW. The reason why the term S_o^2 appears in the denominator is that even when the DS signal is very strong it is still random and this random behavior generates self noise which has a power of S_o^2/TW in the output bandwidth of 1/T Hertz centered on the frequency W Hz.

When all the M+1 signal powers are the same, the output SNR is the same for all signals at the value of

$$(SNR)_o = \frac{TW}{(M+1) + \frac{3}{2}\left[(M+1)^2 - (M+1)\right]} \cong \frac{2TW}{3M^2} \tag{3.54}$$

Since the signal of interest is a sinusoid in essentially Gaussian noise, an envelop detector at the output of the bandpass filter will reliably detect the chip rate line when $(SNR)_o$ is greater than about 10 dB. The probabilities of detection and false alarm are conveniently related to the value of the output SNR in Appendix VII of the report included here as Appendix A. For the output SNR to be less than 10, Equation (3.54) shows that the number of masking emitters, M, must satisfy

$$M > \sqrt{\frac{TW}{15}} \tag{3.55}$$

For values of TW greater than 10^7, the number of masking emitters must exceed 817. Hence, it would appear that emitters are not able to mask each other from a chip rate detector unless the chip rates are very close to one another. Certainly the rates should differ by no more than about 1/10 of a chip per second. This means that for moving emitters or receiver the time dilation, the source of doppler shift, will often provide more differences in the apparent chip rate than the transmitter timing sources. Such timing sources are extremely stable. If the chip rates differ by more than a fraction of a chip per second, then filtering may be able to isolate the individual chip rate lines in bandwidths where the SNR is quite large for even relatively large networks. As in the case of the cross correlator, it appears that narrowband interference is the key to whether the chip rate detector will achieve the necessary values of output SNR.

One possibility to lower the risk of being isolated by a chip rate detector is to jitter the chip rate. However the amount of jittered required is significant and therefore the structure of the despreading correlation in the friendly receiver is complex, unless a convolver implementation is used. A second possibility is to limit the integration time T to a maximum usable value of about $1/2R_H$ by hopping at a rate of R_H hops per second. This has significant potential as just a few tens of hops per second will dramatically reduce the usable integration times or increase the usable filter bandwidths. Hence, a hybrid or jittered DS system or both should be considered when the goal is to avoid a persistent, high technology, non-linear intercept receiver threat.

Alternately, the chip shape may be selected to radically reduce or eliminate the chip rate line. Theoretically this happens for sin x/x time-shaped pulser, which have a uniform bandlimited Fourier spectrum[2]. While those pulses are not realizable, the theoretical null for uniform spectrum can be approached with realizable pulse shapes. In this way, the chip rate line can be very much reduced. As a practical matter, chip shapes which are bandlimited have excessive temporal content at times well outside the "chip" interval. However, compromises and partial response techniques may exist allowing significant reduction in the performance of a chip rate detector.

---

[2] Reed, D.E., and Wickert, M.A., "Minimization of Detection of Symbol-Rate Spectral lines by Delay and Multiply Receivers," IEEE Trans. on Comm., Vol. 36, No.1, January, 1988, pp. 118-120.

Of course, placing the DS signals in a dense signal environment will dramatically degrade the performance of the chip rate detector and the cross correlation receiver. In this case, however, some of the "TW" product of DS signal must be used to overcome the power of the in-band interference. Hence the signal power spectral density can not be as low compared to the thermal noise.

CHAPTER 4

CONCLUSIONS

The technical analyses of the report began with consideration of angle sorting or isolation using directional antennas. The conclusion of the antenna analyses is that at 400 MHz it is very unlikely that intercept antennas will be large enough to resolve individual emitters. In fact, from an intercept range of about 15 miles, emitters within 2 miles of one another are likely to be unresolved. For a given aperture size, the beamwidth of an antenna at 1800 MHz is about 0.22 times narrower than at 400 MHz. Hence, for a 15 mile intercept range, the resolution is about 0.44 miles. These numbers assume a 25 foot azimuth aperture which is large for an airborne antenna anticipated when the intercepted range is 15 miles or more. Airborne arrays using multiple aircraft are a potential means of achieving the required effective aperture and this intercept threat should be considered if there is any evidence of its existence.

The second part of the antenna analysis reveals that with imminently usable antenna sizes the intercepted power for DS signals may be well above the thermal noise floor for free-space, $1/R^2$ propagation. Hence while antennas large enough to resolve emitters in angle are unrealistically large, antennas of realistic dimensions provide enough gain over $1/R^2$ paths to achieve large values of Signal-to-Noise Ratio (SNR). However, over $1/R^4$ propagation typical of UHF ground-to-ground intercept paths, the antennas again becomes very large. Being on the ground, however, such antennas could be built. But it appears, that as intercept range increases to protect the receiver antenna from hostilities near the tactical emitter, the required antenna size remains too large to survive in wartime. Collection sites may exist in peacetime which pose threats to DS signals over $1/R^4$ paths.

The typical intercept receiver for tactical DS signals is expected to have many DS signals present, each one being large compared to the thermal noise but comparable in power to each other. The intercept receiver, likely to be airborne, is also expected to find a dense environment of narrowband signals which result in a significant level of interference power. It is in this intercept context that the majority of the effort documented in this report was focused.

In this intercept context it is clear that the power of any one signal is typically well below the sum of the powers of the several other signals present in the receiver as a result of their emitters lying within the mainbeam of the intercept antenna. Hence, Fourier analysis or linear filtering by any method are not expected to perform well. The emitters are said to mask each other as the expected intercept SNR is on the order of 1/M where M is the total number of DS emitters in the antenna beamwidth. Therefore, non-linear receivers are required which have the ability to perform when the power of the Signal of Interest (SOI) is well below the sum of the powers of the Signals Not of Interest (SNOI). Conclusions regarding performance of such receivers are given below.

Non-linear receivers are able to detect periodic and certain other aspects of a signal even when the signal power is less than the noise power. This includes the energy of the signal at zero or twice the frequency, the Angle of Arrival (AOA) of the signal, the carrier frequency by measurements at twice the carrier frequency for BPSK spreading, the chip rate or its harmonies, and the hop rate or its harmonics. Baseband symbol rates can also be useful in distinguishing between the SOI and SNOI. Non-linear receivers include the total power radiometer, the frequency doubler, the auto and cross correlation receivers, and a variety of receiver subsystems called feature detectors.

Since non-linear receivers extract signal power their performance is expected to be good when there is only one signal plus thermal noise. Furthermore, the cross correlation receiver is able to adjust the relative signal delay such that a spike corresponding to the power of each signal may be extracted and perhaps isolated. Emitters whose differential delay between the antennas of a dual channel cross correlator is a nanosecond (foot) or more may be resolved and a Line of Bearing (LOB) determined. Hence the number of DS emitters in the mainbeam may be known and hence emitter masking is not complete. Without a dense signal environment or attention to signal design, emitters within networks are not expected to be closely spaced enough that the self masking of DS emitters is sufficient to overcome the ability of a cross correlator to isolate them. Repeated short codes for a given emitter and common code segments among emitters produce a number of off-peak autocorrelation spikes and cross correlation spikes. While the largest autocorrelation spikes are still as large with sub-coding as without, the many off-peak spikes greatly complicate the detection process. More importantly, the correlation functions with many spikes complicate the fundamental problem of tagging LOB's so they can be coordinated between receiver sites to provide emitter location. Hence, it would not be unexpected for a dedicated, highly computational intensive interceptor operating in a noise-only environment to derive a LOB for each DS emitter in a network of DS emitters. However, signal design may vastly complicate the problem of usefully coordinating this information between receiver sites by assigning identifying feature tags to each LOB. In fact, further signal design, can dramatically reduce the threat that useful features can be extracted at all.

While LOB detection can be made complicated through design of signals with command and composite codes, dramatic loss of receiver capability is not expected until further degradation is caused by a dense environment of unwanted, narrowband SNOI. The combination of signal design to avoid single spike autocorrelation functions, design to produce spikes in the cross correlation functions, design to avoid feature extraction, and the presence of a dense environment of SNOI should provide protection of the emitters in a very wide variety of tactical and surveillance situations.

A key element in the design of Low Probability of Intercept (LPI) signals is to avoid putting features into signals which can be extracted using nonlinear methods. For instance, the performance of chip rate detectors can be limited by jittering the chip rate and limited much more by Frequency Hopping (FH) since this limits the useful bandwidth of the bandpass filter searching for the chip rate "line." The chip rate "line" is broadened by the hopping to a null-to-null bandwidth equal to twice the hopping rate. Furthermore, the Fourier spectrum of the chip can be tailored to lower the harmonic content at the chip rate or any other frequency. The more bandlimited the chip shape is the less harmonic content at the chip rate. Such signals, however, do have "time-tails" which complicate friendly reception and increase the drop in network performance and capacity due to multipath and intersymbol interference. Again, a dense environment of narrowband SNOI has a dramatic and significant impact on the complexity, computer/processing content, and performance of the non-linear chip rate detector. Without specific design against chip rate detectors and in the absence of narrowband interference, it appears that a bank of bandpass filters with individual bandwidths of W Hertz could differentiate and isolate emitters whose chipping rates differ by W chips/second. There are no "sum and difference" chip rate lines as might be initially expected.

Another key emitter feature is the exact center frequency of an emitter. If this frequency can be repeatably differentiated among emitters it can be used as an LOB tag like the chip rate could. However, signal design can be used to complicate the task of useful carrier recovery by a noncooperative receiver. Such methods include nonuniform envelope and uniform envelope spreading sequences derived by digitizing bandlimited noise, various forms of QPSK spreading FH to avoid narrowband filtering (long integration time), Time Hopping (TH) to avoid long integration times, and jitter of the center carrier.

As an overall result, it appears that against conventional Fourier receivers that DS emitters within a DS network do in fact mask each other. Against a cross correlation or cross power spectrum analyzer the emitters with the beamwidth may be counted. Common and compound short codes complicate the required detection and a dense electromagnetic environment plus appropriate signal design should make LOB's very difficult to extract except for emitters with very large received SNR. Tagging these LOB's with useful and reliable features can be made very unlikely when signal design procedures are used and the operational environment is dense with dynamically varying SNOI.

APPENDIX A

Final Report

Performance of a Chip Rate Detecior with a Multiplicity of Pseudonoise Inputs

10 December 1987

Principal Investigator

Edgar H. German, Jr.

This is the final report on:

Subcontract No. SEC-TOA-88-0010
for:

M/A-COM Government Systems Inc.
Systems Engineering Center
8619 Westwood Center Drive
Vienna, Virginia 22180

By:

GT-Tech, Inc.
5 Meadow Mist Court
Reisterstown, Maryland 21136

Table of Contents

		Page
1.0	Introduction	1-1
2.0	Summary of Results	2-1
2.1	Chip Rate Detector Output Signal-to-Noise Ratio for Two Chip Streams and Noise	2-2
2.1.1	Small Input Signal-to-Noise Ratio	2-4
2.1.2	Large Input Signal-to-Noise Ratio	2-5
2.2	Generalization to N Chip Stream Inputs	2-7
3.0	Basics of the Analytical Method	3-1
4.0	Probability of Detection of the Chip Rate Detector Output	4-1
5.0	Simulation	5-1
5.1	Summary of the Method	5-1
5.2	Interpretation of the Plots	5-4
5.3	Statistical Stability	5-5
5.4	Summary of Results	5-5
6.0	Details of the Analysis	6-1
6.1	Modeling	6-1
6.2	Evaluation of the Expected Output Products	6-4
6.3	Calculation of the Chip Rate Detector Output Spectra	6-7
6.3.1	Identification of the Output Autocorrelation Terms (Types)	6-8
6.3.2	Evaluation Of the Individual Autocorrelation Terms	6-11
6.3.3	Compilation of Terms	6-18
6.3.4	Calculation of the Chip Rate Detector Output Signal-to-Noise Ratio	6-19

Appendices:

1. Unit Square Wave Autocorrelation
2. Random Square Wave Autocorrelation
3. Expansion of Periodic Summations
4. DC & Chip Mixing Terms
5. Chip/Noise Mixing Terms
6. Analysis of the Chip Rate Detector Output Signal-to-Noise Ratio
7. Probability Of Detection Nomogram

ANALYSIS AND SIMULATION OF A CHIP RATE DETECTOR

WITH A

MULTIPLICITY OF PSEUDONOISE INPUTS

1.0 INTRODUCTION

A standard method of detecting the presence of a pseudorandom (PN), spread spectrum, waveform is through the use of a chip rate detector. However, multiple chip stream inputs at slightly differing chip rates may conceal each other, or at best, generate "masking" noise for each other. The analyses, and the simulation performed, address and resolve the following issues:

1. Effects of multiple chip streams upon each other in terms of the signal-to-noise ratios of the various streams in the detector output.

2. Resolution between chip streams at different rates, but with the same encoding.

3. Masking effects of multiple chip stream interference upon the detectability of an individual chip stream.

4. Effect of receiver noise upon the detectability of multiple chip streams.

Simulation has been used to support the analyses by verifying the analytical results. Analyses to resolve these issues has involved:

1. Identification of the chip rate spectral lines of the detector output for a single chip stream as a reference case.

2. Identification of the continuous spectrum of the detector output for a single chip stream as a reference case.

3. Identification of the chip rate spectral lines of the detector output for multiple chip streams, including any "mixing" harmonics (if present).

4. Identification of the continuous spectra of the detector output for multiple chip streams, including any "mixing" harmonics.

5. Calculation of the ratios of the continuous and discrete spectral components.

6. Calculation of the output signal-to-interference ratio of the detector output filter as a function of the bandwidth (integration time) of that filter. This calculation considers both multiple chip streams and receiver noise as components of the interference.

Modeling of the chip rate detector has been performed at baseband to simplify the analysis. In block diagram form, the model appears in Figure 1-1.

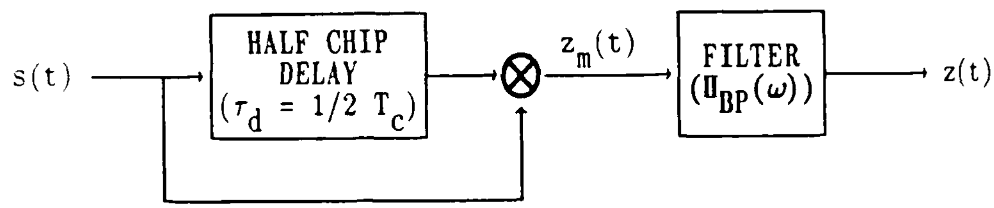

Figure 1-1 Chip Rate Detector

Derivation of the chip rate detector output characteristics will involve computation of the multiplier output ensemble mean frequency content and power spectrum. To this end the mean and autocorrelation function of the output will be computed and Fourier transformed as a simpler means of calculation.

2.0 SUMMARY OF RESULTS

While the analyses to determine the chip rate detector output signal-to-noise ratio(s) are quite lengthy, the basic results are simple to write and to interpret. Sections 1 to 5 describe the results and interpretation of the investigations of those results and form a self-standing document. Section 6 and the Appendices detail the derivation of the basic results.

Output spectra (chip rate lines and noise) of the chip rate detector are of three basic types:

I. Individual Spectral Components

Each chip stream, or noise, has a pair of components in the detector output that are the components that would be present for that individual input alone. Components for the individual inputs are:

Chip Streams

a. A periodic square wave at the component chip rate, which produces the desired chip rate spectral lines.

b. A continuous spectrum that is uncorrelated with the periodic square wave, and has a width of twice the chip rate at the first nulls. This spectral component causes "self" noise in the detector output.

There are no mixing chip rate lines; lines that could possibly occur due to, say, the sum and difference of the different chip rates.

Noise

a. An uninteresting DC component that is the value of the noise autocorrelation function at the half chip delay.

b. A continuous spectrum that is basically the convolution of the noise spectrum with itself. It has a width of approximately twice the chip rate. Two input spectra were used in the analyses: a rectangular spectrum and a sin(x)/x spectrum. Use of simulation verified the results for both noise spectra. In practice, the chip rate rectangular spectrum is the recommended filter as it will not reduce the desired chip rate lines as much. For simplicity in the analytical calculations, the sin(x)/x spectra was chosen for the complete output spectrum calculations. But, at the important chip rate line, the rectangular filter noise contribution was also calculated exactly.

For N chip streams at differing chip rates, there are N discrete line sets at the various chip rates and N sets of self noise, plus the noise DC and continuous spectrum. Assuming the chip rates of all the chip streams are similar, a narrowband output filter that is tuned to a particular chip rate will have only that chip rate line as its output (given sufficient resolution). All the continuous spectral components (within the filter bandwidth) will also appear as "noise" in the filter output.

Resolution between two different chip rate lines requires a filter whose bandwidth is less than the separation between the chip rates. Additionally, the filter must have enough of a roll-off to reject neighboring chip lines over a meaningful dynamic range.

II. Intermodulation Components

Each chip stream interacts with every other chip stream and the noise. These interactions occur pairwise. They are approximately twice the chip rate in bandwidth and appear as "noise" in the narrowband filter output.

The number of pairwise components are the the number of pairs that can be formed from N + 1 (N chip streams plus noise) things:

$$N_2 = \frac{N!}{2!(N-2)!} \text{ (chip/chip)} + N \text{ (chip/noise)}$$

$$= \frac{N(N+1)}{2}$$

which increases as the square of the number of chip streams.

III. DC Intermodulation Components

DC components representing the energy of the interchip modulation are present in the output of the multiplier. They are uninteresting as they do not appear in the chip rate detector output filter.

2.1 Chip Rate Detector Output Signal-to-Noise Ratio for Two Chip Streams and Noise

By collecting the aforementioned terms (Section 6 and the Appendices) the chip rate detector output signal-to-noise ratio can be calculated. Basic assumptions for the relationship are:

1. The narrowband filter has a noise-bandwidth $B = 1/T$ that is sufficiently narrow to reject other (different) chip rate lines.

2. Chip rates of the different streams are close to one another (say, within 10%) so that output noise spectra are relatively the same for pairwise intermodulation products.

The signal-to-noise ratio for a particular chip stream output with a pair of chip stream inputs and noise is:

$$\left[\frac{S}{N}\right]_{o,1} = \frac{S_1^2\ TW}{S_1^2 + S_2^2 + \alpha\ \pi^2/4\ N_I^2 + 3[S_1S_2 + \beta\ S_1N_I + \beta S_2N_I]}.$$

with

$$S_{1(2)} = \text{input power of chip stream } 1(2),$$

and

$$N_i = \text{input noise power.}$$

and is the basic result of this report!

The constants α and β are highly dependent upon the modeling of the noise spectrum used. A low-pass rectangular input filter, prior to the chip rate detector, with a bandwidth equal to the chip rate requires $\alpha = 1$, and agrees with textbook analyses for a single chip stream and noise. More conveniently, for analytical purposes and as another case for verifying the basic methodology by simulation, is filtering of only the noise with a filter having the chip shape as an impulse response requires $\alpha = 6/\pi^2$. This choice for α results in

$$\alpha\frac{\pi^2}{4} = \frac{3}{2},$$

and

$$\beta = 1.$$

In tabular form:

	Rectangular Filter	Chip Filter
$\alpha\frac{\pi^2}{4}$	$\frac{\pi^2}{4}$	$\frac{3}{2}$
β	$\frac{\pi^2}{6}$	3

Both noise spectra were included in the simulation and verified within 1 dB.

Results can also be written in terms of signal-to-noise ratios of the input signals, but interpretation in that form will be deferred for the moment. The other chip stream has the same expression for the output signal-to-noise ratio; but with the numerator identifying that chip amplitude (denominators are identical).

For interpretation of the result, two cases are of interest; large and small input signal-to-noise ratios.

2.1.1 Small Input Signal-to-Noise Ratio

Given the input signal-to-noise ratio for the reference chip stream

$$\left[\frac{S}{N}\right]_{i,1} \triangleq \frac{S_1}{N_I},$$

$$<< 1,$$

then:

$$\left[\frac{S}{N}\right]_{o,1} \cong \frac{TW}{S_2^2/S_1^2 + \alpha\ \pi^2/4\ N_I^2/S_1^2 + 3[S_2/S_1 + \beta S_2 N_I/S_1^2]},$$

and the result depends upon the ratio of the two chip stream powers.

Case I: The Chip Stream S_1 Dominates:

$$S_1 >> S_2$$

and

$$\left[\frac{S}{N}\right]_{o,1} \cong \frac{TW}{\alpha\ \pi^2/4\ N_I^2/S_1^2},$$

$$= \frac{1}{\alpha}\frac{4}{\pi^2}\ TW \left[\frac{S}{N}\right]_{i,1}^2,$$

which is the well known result for a chip rate detector with only a single chip stream and noise in the input ($\alpha = 1$).

Case II: <u>The Chip Stream S_2 Dominates:</u>

$$S_2 >> S_1$$

and

$$\left[\frac{S}{N}\right]_{o,1} \cong \frac{\frac{1}{\alpha}\left[\frac{2}{\pi}\right]^2\left[\frac{S}{N}\right]_{i,1}^2 TW}{1 + \frac{1}{\alpha}\left[\frac{2}{\pi}\right]^2\left[\frac{S}{N}\right]_{i,2}^2 + 3\,\frac{\beta}{\alpha}\left[\frac{2}{\pi}\right]^2 \left[\frac{S}{N}\right]_{i,2}},$$

where:

$$\left[\frac{S}{N}\right]_{i,2} \triangleq \frac{S_2}{N_I},$$

and, the results are written in terms of the signal-to-noise ratios of the input chip streams.

Two subcases present themselves according to whether the signal-to-noise of the second chip stream is small or large. If the second chip stream has a small signal-to-noise then the output signal-to-noise ratio reduces to simply the single chip stream case as expected.

For a large signal-to-noise of the second chip stream, the output signal-to-noise ratio becomes:

$$\left[\frac{S}{N}\right]_{o,1} \cong \left[\frac{S_1}{S_2}\right]^2 TW$$

which is worse than simply noise by the factor of $\alpha\, \pi^2/4$.

2.1.2 <u>Large Input Signal-to-Noise Ratio</u>

For a large input signal-to-noise ratio

$$\left[\frac{S}{N}\right]_{i,1} \triangleq \frac{S_1}{N_{I}},$$

$$\gg 1,$$

rewrite the expression above as:

$$\left[\frac{S}{N}\right]_{o,1} = \frac{TW}{1 + S_2^2/S_1^2 + 3S_2/S_1 + S_2/S_1\beta[N/S]_{i,1}},$$

which depends upon the ratio of the power in the two chip streams. Again, two cases present themselves.

Case I: <u>The Chip Stream S_1 Dominates:</u>

In this instance the apparent output is that of the reference chip stream by itself. Only the self-noise of the reference chip stream is present. And,

$$S_1 \gg S_2$$

and

$$\left[\frac{S}{N}\right]_{o,1} = TW,$$

The output is simply the "processing gain" of the detector.

Case II: <u>The Chip Stream S_2 Dominates:</u>

With

$$S_2 >> S_1$$

then

$$\left[\frac{S}{N}\right]_{o,1} = \frac{S_1^2}{S_2^2}TW.$$

The output signal-to-noise ratio depends only upon the ratio of the chip stream powers, as might be expected.

2.2 Generalization to N Chip Stream Inputs

Calculation of the signal and noise power for N chip streams in the chip rate detector input is a relatively simple generalization of the two chip stream case. From Appendix VI, the total "noise" out of the chip rate detector is:

$$TN = \sum_j \;{}^2_j + \alpha\,\pi^2/4\; N_I^2 + \frac{3}{2}\sum_j \sum_{\substack{k \\ j \neq k}} S_j S_k + 3\beta \sum_j S_j N_I,$$

where the sums are over the N chip streams.

By making reasonable assumptions about the distribution of the powers (signal-to-noise ratios) of the chip stream inputs an average output noise can be calculated. This average is:

$$E[TN] = N_I^2 \left[N\; E[SNR^2] + \alpha\,\pi^2/4 + \frac{3}{2}\,N(N-1)\; E[SNR]^2 + 3\beta N\; E[SNR]\right]$$

The output chip line power (normalized to the input noise power) for the j^{th} chip stream is

$$S = S_j^2/N_I^2\; TW$$

with the average output equal to:

$$E[S] = E[SNR^2].$$

With these quantities, the average output signal-to-noise ratio, over all chip streams is:

$$SNR_{av} = \frac{1}{N} \frac{TW}{\left[1 + \alpha\, \pi^2/(4N) + \frac{3}{2}\,(N-1)\; E[SNR]^2/E[SNR^2] + 3\beta E[SNR]/E[SNR^2]\right]}.$$

Further evaluation of the average signal-to-noise ratio requires specification of the distribution function of the chip stream signal-to-noise ratios.

Two cases will be considered. One will be a uniform distribution over dB of the signal-to-noise ratios of the chip stream transmitters. The other will be a uniform distribution over transmitter ranges, with all transmitted powers equal.

Case I:

Uniform Distribution of Signal-to-Noise Ratios (in dB).

Assume the distribution is given between zero and dB_{max}, then

$$p_{dB}(dB) = \frac{1}{dB_{max}} \begin{cases} 1, & 0 \le dB \le dB_{max}, \\ 0, & \text{otherwise.} \end{cases}$$

and obtaining the distribution of S through the relation

$$dB = 10 \log_{10}(S):$$

$$p_S(S) = \frac{1}{\ln S_{max}} \frac{1}{S},\; 1 \le S \le S_{max}.$$

With these relations, the average chip rate detector output signal-to-noise ratio is (for $S_{max} >> 1$):

$$SNR_{av} = \frac{1}{N} \frac{TW}{\left[1 + \alpha\, \pi^2/(4N) + 3(N-1)/\ln S_{max} + 6\beta/S_{max}\right]}.$$

For a large number of emitters ($N >> 1$) and high input maximum signal-to-noise ratios ($S_{max} >> 100$ (20 d B)), the the formula may be approximated by:

$$SNR_{av} = \frac{1}{N} \frac{TW}{\left[1 + 3(N-1)/\ln S_{max}\right]}.$$

A conclusion can be reached. The average signal-to-noise ratio decreases at least as fast as N for emitters spread over extremely wide dynamic ranges. For a 60 dB dynamic range:

$$SNR_{av} \cong \frac{1}{N} \frac{TW}{\left[1 + .22\ (N-1)\right]}.$$

Case II:

Uniform Distribution of Ranges

Assume the distribution is given between R_{min} and R_{max}, then

$$p_{dB}(dB) = \frac{1}{R_{max} - R_{min}} \begin{cases} 1, & R_{min} \le R \le R_{max}, \\ 0, & \text{otherwise}, \end{cases}$$

and obtain the distribution of S through the relation

$$S = \frac{A}{R^2}.$$

As in case I, for large max to min range range ratios:

$$SNR_{av} = \frac{1}{N} \frac{TW}{\left[1 + \alpha\ \pi^2/(4N) + \frac{9}{2}\ (N-1)\ R_{min}/R_{max} + 9\beta/SNR_{min\ range}\right]}.$$

Again, assuming the minimum range signal-to-noise ratio is large, and N also:

$$SNR_{av} = \frac{1}{N} \frac{TW}{\left[1 + \frac{9}{2}\ (N-1)\ R_{min}/R_{max}\right]}.$$

A similar conclusion to the uniform distribution in dB case can be reached. The average signal-to-noise ratio decreases as the number of emitters (N). A choice of maximum-to-minimum range of 1000 (60 dB dispersion) gives, in this instance:

$$SNR_{av} = \frac{1}{N} \frac{TW}{\left[1 + .0045(N-1)\right]}.$$

<u>Conclusion</u>

A large number of emitters tends to obscure each emitter's chip rate line. The obscuration increases as 10 log(N) in dB when the emitter signal-to-noise ratios are distributed over a wide range of values.!

3.0 BASICS OF THE ANALYTICAL METHOD

Analytical techniques used within this report derive two basic quantities; even though the derivations are extensive. These two quantities are the amplitude of the chip rate lines and the noise variance (both receiver noise and interchip mixing noise) out of a bandpass filter placed about the chip rate lines. Both quantities are obtained by calculating the time averaged autocorrelation function and its Fourier transform, the spectrum, of the chip rate detector output. The autocorrelation is the primary quantity calculated, as it reveals the cyclostationarity of pseudonoise chip streams (and, therefore, the chip rate lines) much more readily than a direct (but equivalent) spectrum calculation.

These quantities are not random variables; they represent the mean (amplitude) of the chip rate sine wave and the noise standard deviation. Assuming a Gaussian probability density for the total noise, the probability of detection of the chip stream can be calculated (See Section 4.).

The spectrum of the chip rate detector output (computed via the Fourier transform of the time averaged autocorrelation function) allows the signal amplitude and noise variance to be calculated by virtue of integrating the spectrum over the frequency range of interest.

Given an output spectrum $S_z(\omega)$ (a noise power density which will be calculated) of the delay and multiply circuit, the output power of the narrowband filter $H(\omega)$ (of bandwidth B) is:

$$N_0 = \frac{1}{2\pi} \int_{-\infty}^{\infty} |H(\omega)|^2 \, S_z(\omega) \, d\omega$$

If the filter is chosen to be rectangular and have a narrow bandwidth of $\tilde{B}$, about some frequency ω_0, then the output noise power is:

$$N_0 = \frac{1}{2\pi} \int_{-(\omega_0 - \tilde{B}/2)}^{(\omega_0 + \tilde{B}/2)} S_z(\omega) \, d\omega$$

+ the negative frequency contribution.

As both chip rate sine waves and noise have the same contributions for negative frequencies (spectra are even functions), the negative frequency contributions will be ignored hereafter as only ratios are of interest.

Assuming that the spectrum is reasonably smooth within the confines of the filter, then the noise power output is:

$$N_0 = \frac{\tilde{B}}{2\pi} S_z(\omega_0)$$

Now, $\tilde{B}$ is in radians per second. Rewriting the expression in Hertz ($B = \tilde{B}/2\pi$):

$$N_0 = B\, S_z(\omega_0) \ ,$$

$$= \frac{1}{T}\, S_z(\omega_0) \ ,$$

as $T = 1/B$ is the integration time of the filter.

If the spectrum includes a delta function at the frequency ω_0, then the filter output will also include a constant signal term independent of the filter bandwidth (as long as the signal term falls anywhere within the filter bandwidth). Let the sine wave spectrum be represented by:

$$S_A(\omega_0) = 2\pi\, A\ \delta(\omega - \omega_0),$$

then, the output is

$$S_A = A,$$

if $\omega_0 - \tilde{B}/2 < \omega < \omega_0 + \tilde{B}/2$ zero otherwise.

These relationships are used to interpret the results for the spectra computed subsequently.

<u>Actual Filtering</u>

While the perfectly rectangular filter gives a quick means of interpreting the results, actual filters differ in detail. The simulation, used in developing this report, uses a Fourier transform as the output filter bank. A straight-forward Fourier transform over N chips is identical to using an integrate and dump circuit with an integration time of NT_c. Or, as M consecutive transforms are taken with their magnitude squared output average over the M transforms, the integrate and dump can be looked upon as a sliding window.

The noise bandwidth of the sliding window integrator is exactly equal to $B = 1/T$, the ideal filter bandwidth. However, the discrete Fourier transform acts (with the equivalent sliding window) as though it has a sin(x)/x transfer function with consiuerable leakage into adjacent channels (Fourier coefficients). It is also difficult to read between the "cracks" when an input sine wave falls between the discrete transform frequencies.

By using a bell-shaped weighting over each span of chip detector output of T seconds, the effect is a bell-shaped impulse response of T seconds duration. The well-known cosine-squared weighting was used for the weighting. It effectively increases the noise bandwidth over the constant amplitude window by a factor of 3/2. The signal-to-noise ratio of each transform channel (filter) is decreased by 3/2. Leakage of the adjacent channels is still present; but the outputs are more readable due to the wider bandwidth and lack of perturbation from distant channels.

4.0 PROBABILITY OF DETECTION OF THE CHIP RATE DETECTOR OUTPUT

Efforts described in this report are devoted to computation, and verification, of the basic signal-to-noise output of the chip rate detector under various conditions. This quantity is not a random variable. It is the ratio of the mean output (squared) to the noise variance. These quantities specify two moments of the probability density of the chip rate detector output. If the output is assumed to be the sum of a sine wave plus a Gaussian random variable (the noise) then the signal-to-noise ratio calculated in this report specifies the random process in its entirety.

As the noise (chip mixing plus receiver noise) is narrowband filtered; the Central Limit Theorem allows us to infer that the chip rate detector output is, in fact, composed of Gaussian noise. The correlated delta function is the sine wave output. An envelope detector (placed at the chip rate detector) output will be the optimum estimator of the sine wave presence.

Each integration time of the bandpass filter (T) produces a statistically independent sample of the sine wave plus noise process. By placing a threshold at the envelope detector output the presence (or absence) of a chip line can be estimated. Two quantities express the effectiveness of the detector: (1.) the probability of detection (P_d), and (2.) the probability of a false alarm (β). These quantities are derived from Marcum's Q function using the signal-to-noise ratio out of the bandpass filter as the argument. A nomogram is given in Appendix VII for computing the probabilities, given the signal-to-noise ratio; or any quantity given the other two. As an example from the nomogram:

$$P_D = .99,$$

$$\beta = 10^{-2},$$

then

$$SNR \cong 11.4 \text{ dB}$$

out of the detector. The TW product and the signal-to-noise ratio into the detector must be sufficient to provide this SNR out of the chip rate detector output filter into the envelop detector.!

5.0 SIMULATION

5.1 Summary of Method

Verification of the analyses was performed through a complete simulation of the operation of the chip rate detector. Simulated inputs included single and double (at differing rates) chip streams with Gaussian random noise. When two chip streams were used as the input they had identical encoding, but were adjusted so that the slowest always started behind the higher rate stream to avoid corrupting results by the peaking at coincidence . A block diagram of the simulated processing, using digital signal processing techniques, is given in Figure 5-1.

Simulation results verified the analytical conclusions within less than 1 dB over a wide range of cases. Signal-to-noise ratios for single and double chip streams, and single and double chip streams with noise found by simulation agreed with the predicted ones.

Input Filtering

The input filter to the chip rate detector was varied over a wide range of bandwidths before settling on the method used in this report. Simulated and theoretical results agreed for a wide range of bandwidths (greater than the chip rate) as long as the noise-bandwidth of the filter was used to calculate the noise input power. A typical filtered waveform is shown in Figure 5-2. In that plot, two chip streams and noise are present. The chip streams and noise all have equal powers; namely 0 dB. signal-to-noise ratios for both chip streams. As can be seen, the chip streams are firmly embedded in the noise.

For the purposes of the spectrum plots in this report, and reasonable analytical calculations, where a complete demonstration of the output artifacts of the chip rate detector and a verification of the accuracy of the theoretical analyses is desired, a particular arrangement of input filtering was used. The chip streams were unfiltered, and the noise was filtered with a chip shaped impulse response filter to give a noise spectrum identical to that of the chip streams. With this choice of filtering, both the predicted artifacts (chip rate lines at higher harmonics) and the effect of noise filtering at the chip rate bandwidth can be demonstrated. It should be emphasized that the basic results of output signal-to-noise ratios are not affected by this choice (as verified by many simulation runs), only the details of the presentation.

Output Filtering

A Fourier transformer offers the opportunity to have both an output filter at the chip rate lines and a spectrum measuring device in one package. An integration time of 64 chips (TW = 64) was used and a transform length of 1024. By choosing 16 samples per chip, a chip rate of 1/16 of the sampling rate was obtained with minimal aliasing due to fold-over. Further, the choice of the transform length of 1024 was equivalent to a resolution of 1/1024 of the chip rate.

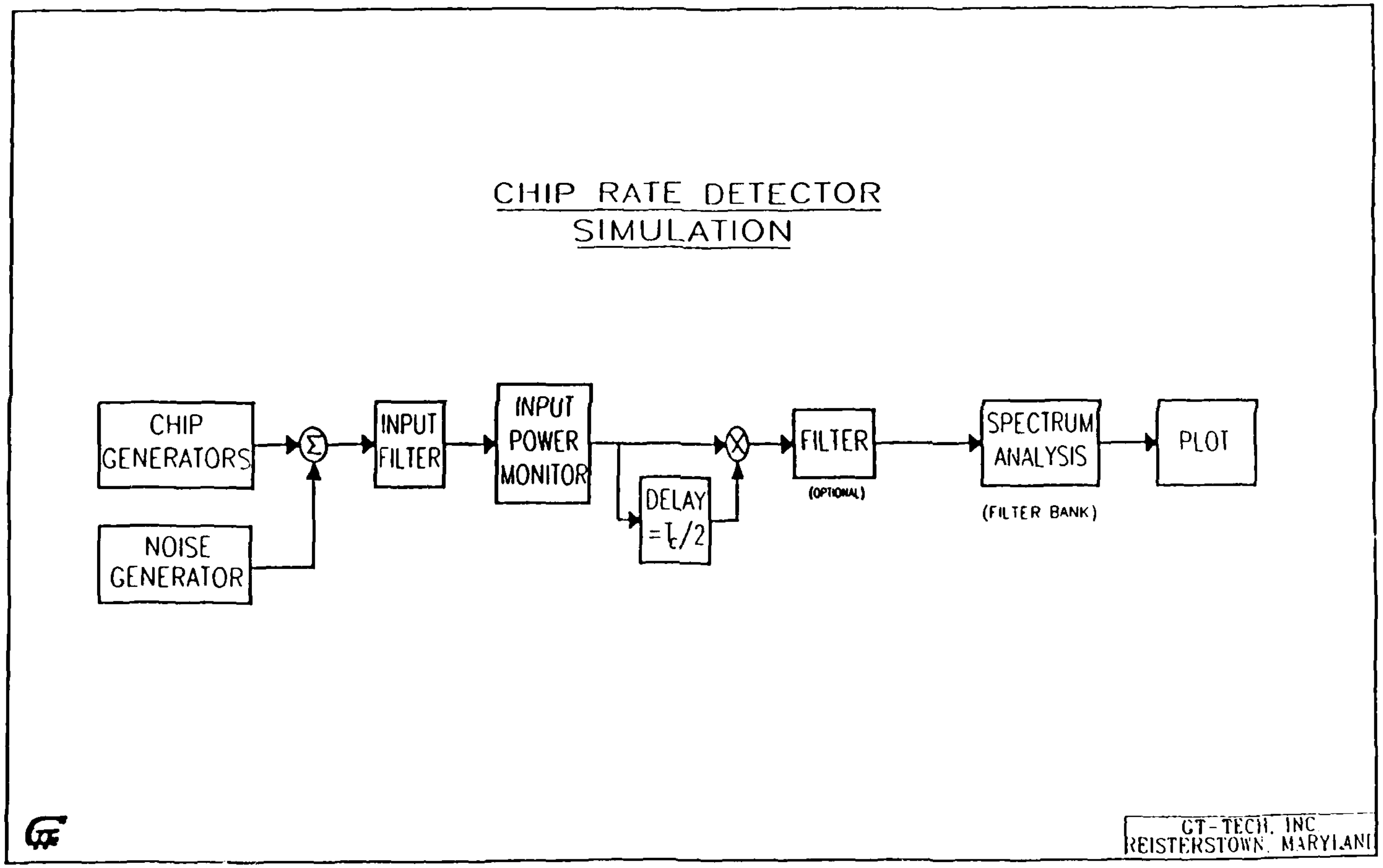
CHIP RATE DETECTOR
SIMULATION
CHIP GENERATORS
NOISE GENERATOR
INPUT FILTER
INPUT POWER MONITOR
DELAY $=T_c/2$
FILTER
(OPTIONAL)
SPECTRUM ANALYSIS
(FILTER BANK)
PLOT
GT-TECH, INC
REISTERSTOWN, MARYLAND

Figure 5 – 1

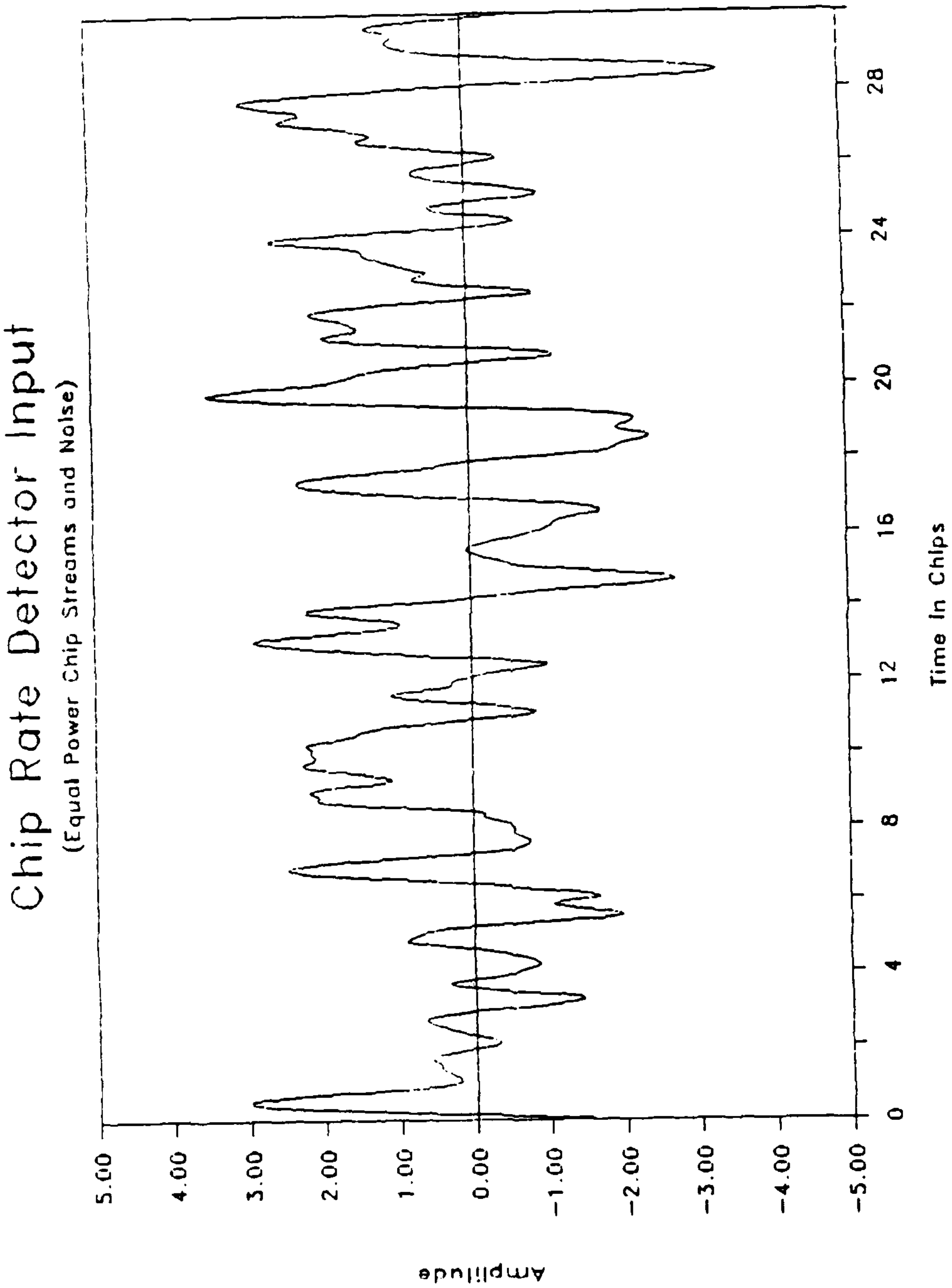
Chip Rate Detector Input
(Equal Power Chip Streams and Noise)
Amplitude
5.00
4.00
3.00
2.00
1.00
0.00
-1.00
-2.00
-3.00
-4.00
-5.00
0
4
8
12
16
20
24
28
Time In Chips

Figure 5 - 2

To obtain smoother plots at the chip rate line, and alleviate the sidelobe leakage from transform channels at frequencies that did not fall exactly upon one of the transform frequencies, cosine-squared weighting of the input data to the transform was used in the double chip stream cases. With the cosine-squared windowing, the effective TW product is decreased by a factor of 2/3^{rds} corresponding to the increase (3/2) in noise-bandwidth of the cosine-squared filtering. The windowing also decreased the resolution by 2/3^{rds}.

As the discrete transform of of a real function is redundant in its second half, only the first 512 values (channels) were used in the output plots.

5.2 Interpretation of the Plots

For simplicity of interpretation, the chip rate was called 100 Hz. A value of 100 kHz, or 100 mHz. could be assigned as well. The Fourier transform interval between frequencies was 1600 Hz./1024 = 1.5625 Hz. With the cosine squared windowing, the leakage from the discrete lines extended only into adjacent cells at a meaningful level. The second chip stream was chosen as 110 Hz. to ensure a good separation (resolution) between the expected chip rate lines. A 10% separation was well within the analytical tolerance for verifying results.

In fact, this relatively wide separation, compared to expected emitter rates. resulted in an interesting artifact that was also predicted by the analyses. As the chip rate detector has a half chip delay only for the reference (100 Hz) chip stream, the 110 Hz stream does not have a half chip delay. The output square wave for this stream is, therefore, asymmetrical and results in (small) even harmonic (200 Hz, 400 Hz, etc.) chip rate lines. This effect decreases with the square of the percentage of asymmetry; in practical situations the artifacts would be undetectable.

Plots presented in the following pages were made by transferring the output files of the simulator (written in Turbo Pascal) to Lotus 123 worksheets. Use of Lotus 123 also allowed rapid and precise analysis of the data. Signal-to-noise ratios of the chip rate lines were calculated by comparing the chip rate channel outputs to channels displaced by two where only noise was present. As the continuous spectrum of the noise is relatively constant within this small interval, this assumption is certainly valid.

Additional checking of the analytical results was performed to validate the general calculations. Dc-to-chip rate line ratios ($\pi^2/4$ for a single chip stream) were compared to the theoretical predictions and found to agree within less than 1 dB. Also, the ratio of 1st to 3rd chip rate harmonics (9) was checked; again the results were well within 1 dB.

To increase the dynamic range of the accompanying plots, continuous noise spectra were extracted from the results of the simulation by simply replacing the discrete line values by the adjacent channel values. The discrete spectrum plots also include the continuous noise spectrum. DC components were remove from the discrete spectrum plots by the same method to increase their dynamic range as well.

5.3 Statistical Stability

Obtaining good spectral estimates, and meaningful signal-to-noise ratios requires many runs of the simulation program. The magnitude squared out of each transform channel was averaged over 400 runs to obtain good (stable) power spectrum and signal-to-noise ratio estimates. At best, for relatively independent transform channel outputs, the standard deviation of a given channel would be $\sqrt{1/400} = 1/20^{th}$ of the expected value of the channel output. The two sigma value gives an error of less than ± 10% about 90% of the time (and greater the other 10% of the time). An inspection of the plots shows that the graphing adheres well to these criteria.

5.4 Summary of Results:

The object of the simulation was verification of the basic input-output signal-to-noise equation (See Section 2 and Appendix VI):

$$\left[\frac{S}{N}\right]_{o,1} = \frac{S_1^2 \, TW}{S_1^2 + S_2^2 + (\alpha\, \pi^2/4)\, N_I^2 + 3[S_1S_2 + \beta\, S_1N_I + \beta S_2N_I]} \, .$$

with

$$S_{1(2)} = \text{power of chip stream } 1(2),$$

and

$$N_I = \text{noise power.}$$

α and β are chosen, as discussed in Section 6.1.4, according to the noise spectrum chosen.

For the chip shaped noise filter, the values of the constants are:

$$\alpha\,\frac{\pi^2}{4} = \frac{3}{2},$$

$$\beta = 1.$$

And for the rectangular filter (a 3 pole Butterworth), the values are:

$$\alpha\,\frac{\pi^2}{4} = \frac{\pi^2}{4},$$

$$\beta = \pi^2/6.$$

Verification of the equation was performed by using numerous signal-to-noise ratios for the input quantities. After a number of trial runs demonstrated the correctness of the simulation, worst case runs were made within the limits of the transform size. These runs are given in Figures 5-3 through 5-10.

Discussion of the Simulation Runs:

Single Chip Stream, Infinite Signal-to-Noise Ratio (Fig. 5-3,4)

Input values:

$$S_1 = 1,$$

$$S_2 = 0,$$

$$N_I = 0, \text{ (infinite input signal-to-noise ratio).}$$

$$\alpha \frac{\pi^2}{4} = \frac{3}{2},$$

$$\beta = 1.$$

From the output signal-to-noise ratio equation above, the theoretical value is:

$$\left[\frac{S}{N}\right]_{o,1} = TW_a,$$

$$= \frac{2}{3} 64,$$

$$= 42.67.$$

TW_a is the product obtained after windowing (filtering) of the data prior to transformation with the factor of 2/3 (due to the noise-bandwidth increase) used for the cosine-squared weighting.

From the data which was used to make the plots of Figure 5-3,4, the measured value was found to be:

$$\left[\frac{S}{N}\right]_{o,1}^{M} = 42.27,$$

which agrees remarkably well with the theoretical value!

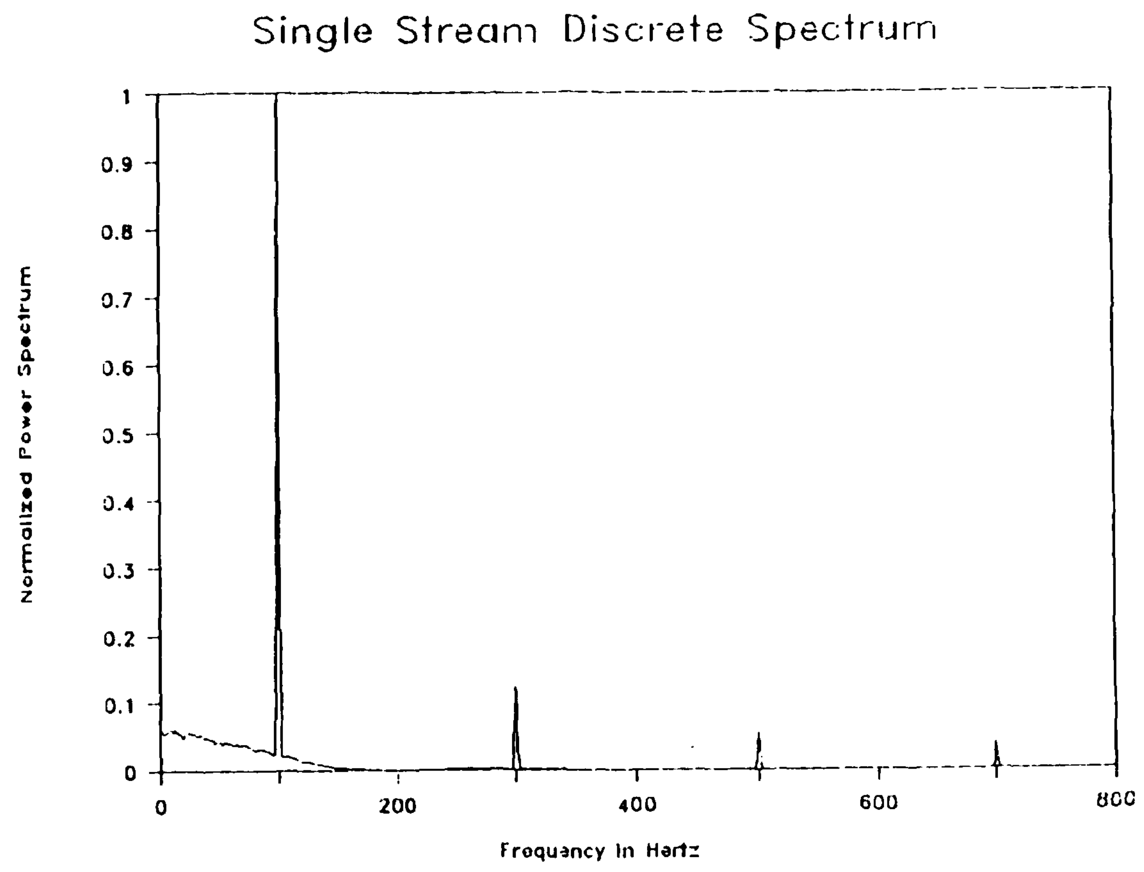
Single Stream Discrete Spectrum
Normalized Power Spectrum
0
0.1
0.2
0.3
0.4
0.5
0.6
0.7
0.8
0.9
1
0
200
400
600
800
Frequency in Hertz

Figure 5 – 3

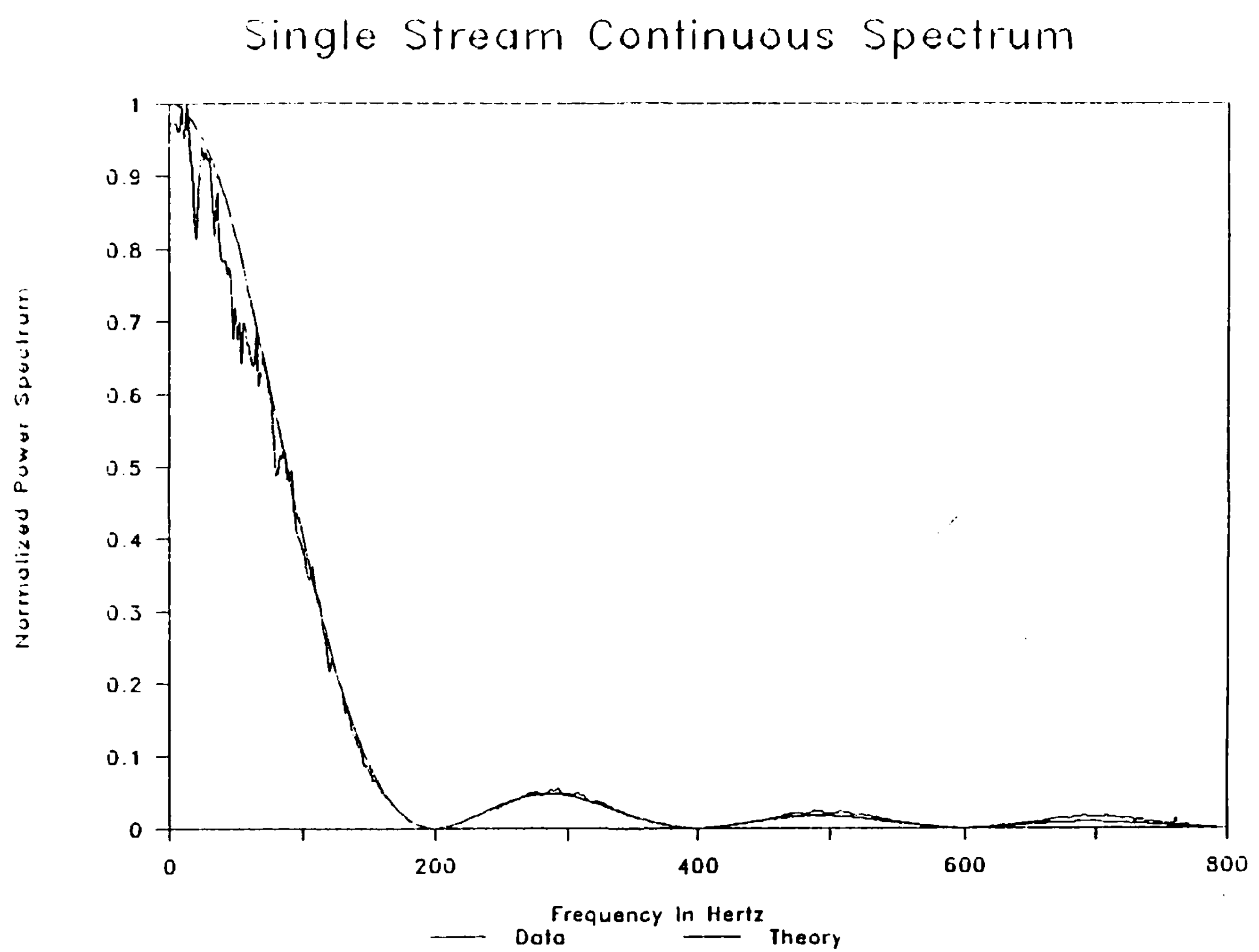
Single Stream Continuous Spectrum
Normalized Power Spectrum
1
0.9
0.8
0.7
0.6
0.5
0.4
0.3
0.2
0.1
0
0
200
400
600
800
Frequency In Hertz
Data
Theory

Figure 5 – 4

Single Chip Stream and Noise, 0 dB. Signal-to-Noise Ratios (Fig. 5-5,6)

Input values:

$$S_1 = 1,$$

$$S_2 = 0,$$

$$N_I = 2, \text{ (-3 dB. input signal-to-noise ratios).}$$

$$\alpha \frac{\pi^2}{4} = \frac{3}{2},$$

$$\beta = 1.$$

From the output signal-to-noise ratio equation above, the theoretical value is:

$$\left[\frac{S}{N}\right]_{o,1} = \frac{1}{13} TW_a,$$

$$= 3.28$$

From the data which was used to make the plots of Figure 5-9,10, the measured values for the two chip streams were found to be:

$$\left[\frac{S}{N}\right]_{o,1}^{M} = 3.22, \text{ (100 Hz. chip rate).}$$

which is within .1 db of the theoretical value.

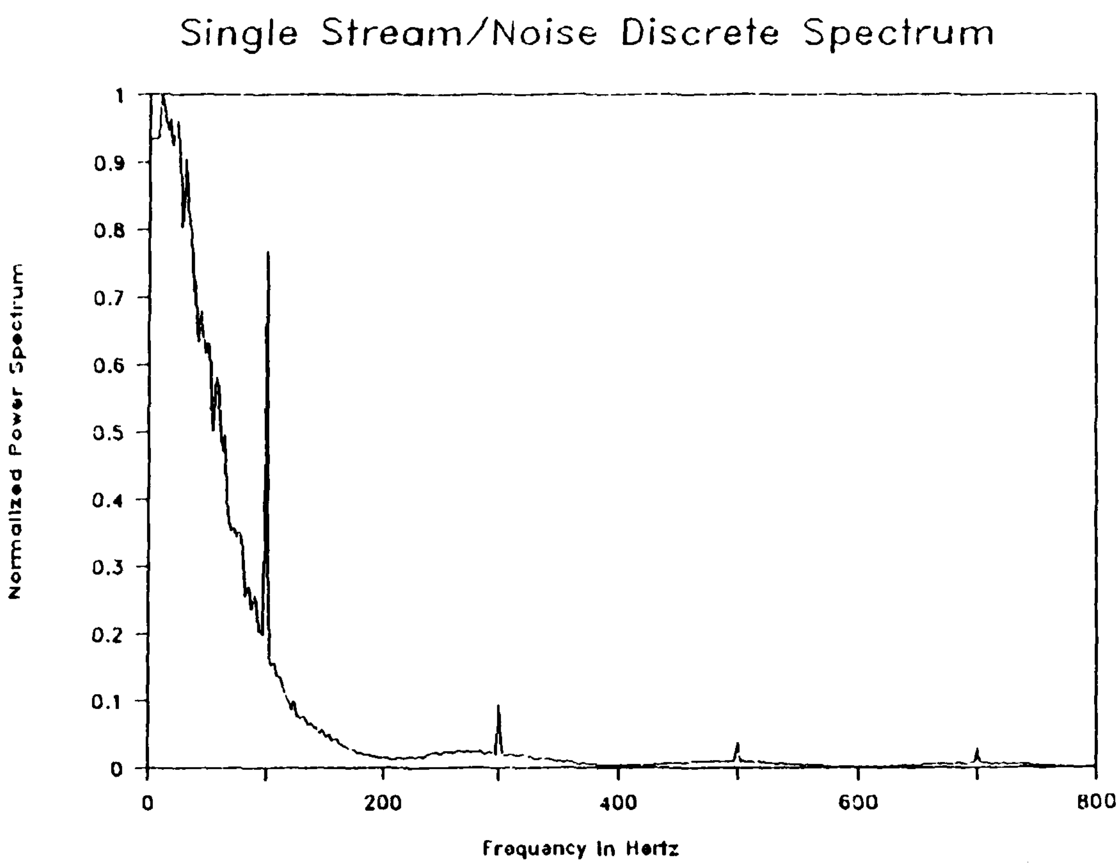
Single Stream/Noise Discrete Spectrum
Normalized Power Spectrum
1
0.9
0.8
0.7
0.6
0.5
0.4
0.3
0.2
0.1
0
0
200
400
600
800
Frequancy In Hertz

Figure 5 – 5

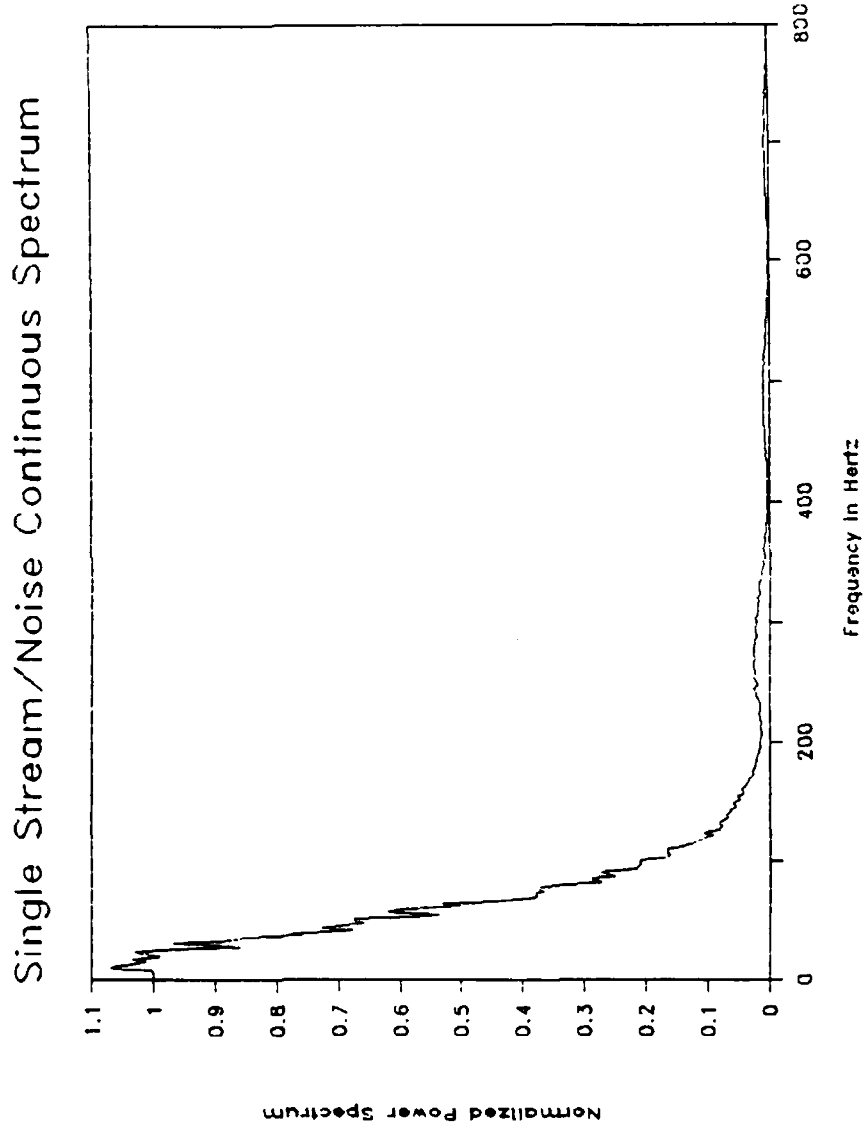
Single Stream/Noise Continuous Spectrum
Normalized Power Spectrum
Frequency in Hertz
0
0.1
0.2
0.3
0.4
0.5
0.6
0.7
0.8
0.9
1
1.1
0
200
400
600
800

Figure 5 – 6

Double Chip Streams, Infinite Signal-to-Noise Ratios (Fig. 5-7,8)

Input values:

$$S_1 = 1,$$

$$S_2 = 1, \text{ (0 dB with respect to reference chip stream)}$$

$$N_I = 0, \text{ (infinite input signal-to-noise ratios).}$$

$$\alpha \frac{\pi^2}{4} = \frac{3}{2},$$

$$\beta = 1.$$

From the output signal-to-noise ratio equation above, the theoretical value is:

$$\left[\frac{S}{N}\right]_{o,1} = \frac{TW_a}{5},$$

$$= 8.53,$$

$$\left[\frac{S}{N}\right]_{o,2} = \frac{TW_a}{5},$$

$$=8.53.$$

From the data which was used to make the plots of Figure 5-5,6, the measured values for the two chip streams were found to be:

$$\left[\frac{S}{N}\right]^M_{o,1} = 8.27, \text{ (100 Hz. chip rate).}$$

$$\left[\frac{S}{N}\right]^M_{o,2} = 7.76, \text{ (110 Hz. chip rate).}$$

Both are within .41 db of the theoretical value, which is quite good considering the 10% difference in the chip rates.

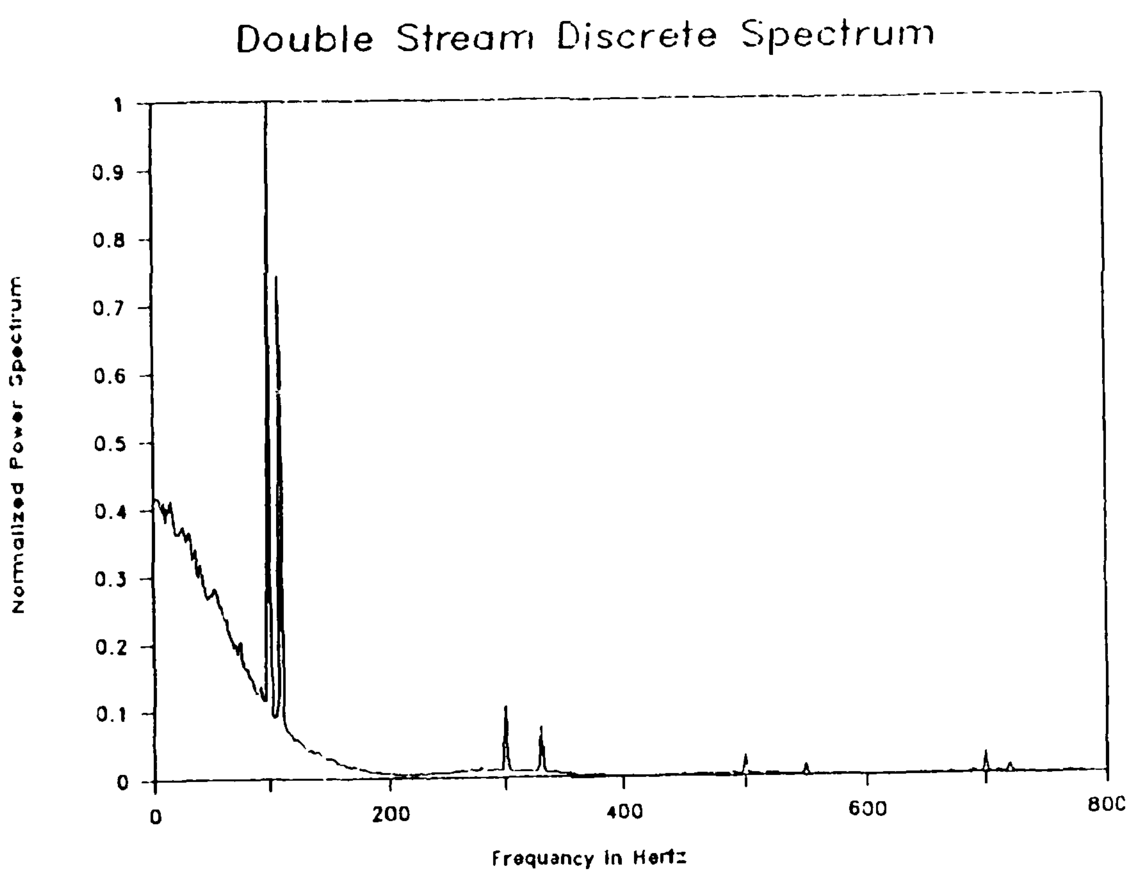
Double Stream Discrete Spectrum
Normalized Power Spectrum
1
0.9
0.8
0.7
0.6
0.5
0.4
0.3
0.2
0.1
0
0
200
400
600
80C
Frequancy in Hertz

Figure 5 – 7

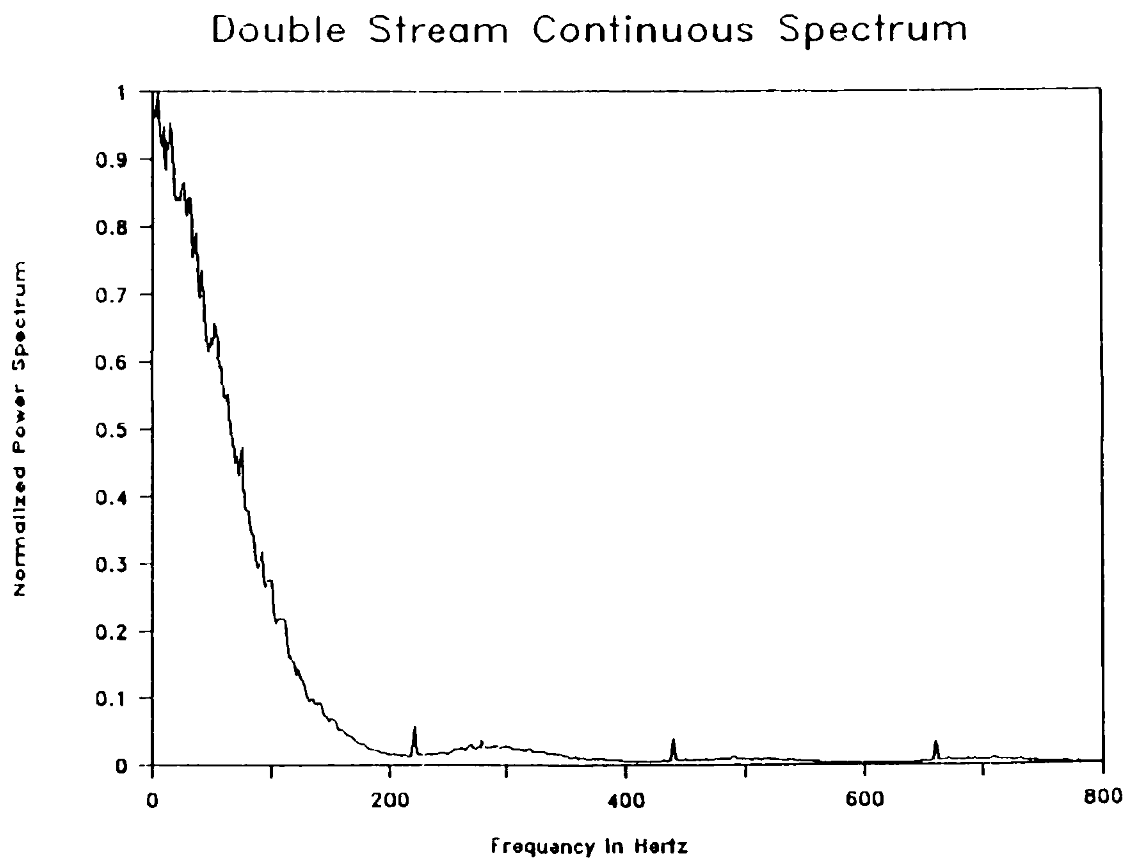

Double Stream Continuous Spectrum
Normalized Power Spectrum
1
0.9
0.8
0.7
0.6
0.5
0.4
0.3
0.2
0.1
0
0
200
400
600
800
Frequancy In Hertz

Figure 5 - 8

Double Chip Streams and Noise, 0 dB. Signal-to-Noise Ratios (Fig. 5-9,10)

Input values:

$$S_1 = 1,$$

$$S_2 = 1, \text{ (0 dB. with respect to reference chip stream)}$$

$$N_I = 1, \text{ (0 dB. input signal-to-noise ratios).}$$

$$\alpha \frac{\pi^2}{4} = \frac{3}{2},$$

$$\beta = 1.$$

From the output signal-to-noise ratio equation above, the theoretical value is:

$$\left[\frac{S}{N}\right]_{o,1} = \frac{1}{12.5} TW_a,$$

$$= 3.41$$

From the data which was used to make the plots of Figure 5-9,10, the measured values for the two chip streams were found to be:

$$\left[\frac{S}{N}\right]^M_{o,1} = 3.36, \text{ (100 Hz. chip rate).}$$

$$\left[\frac{S}{N}\right]^M_{o,2} = 3.53, \text{ (110 Hz. chip rate).}$$

Both are within .1 db of the theoretical value, which is quite good considering the 10% difference in the chip rates.

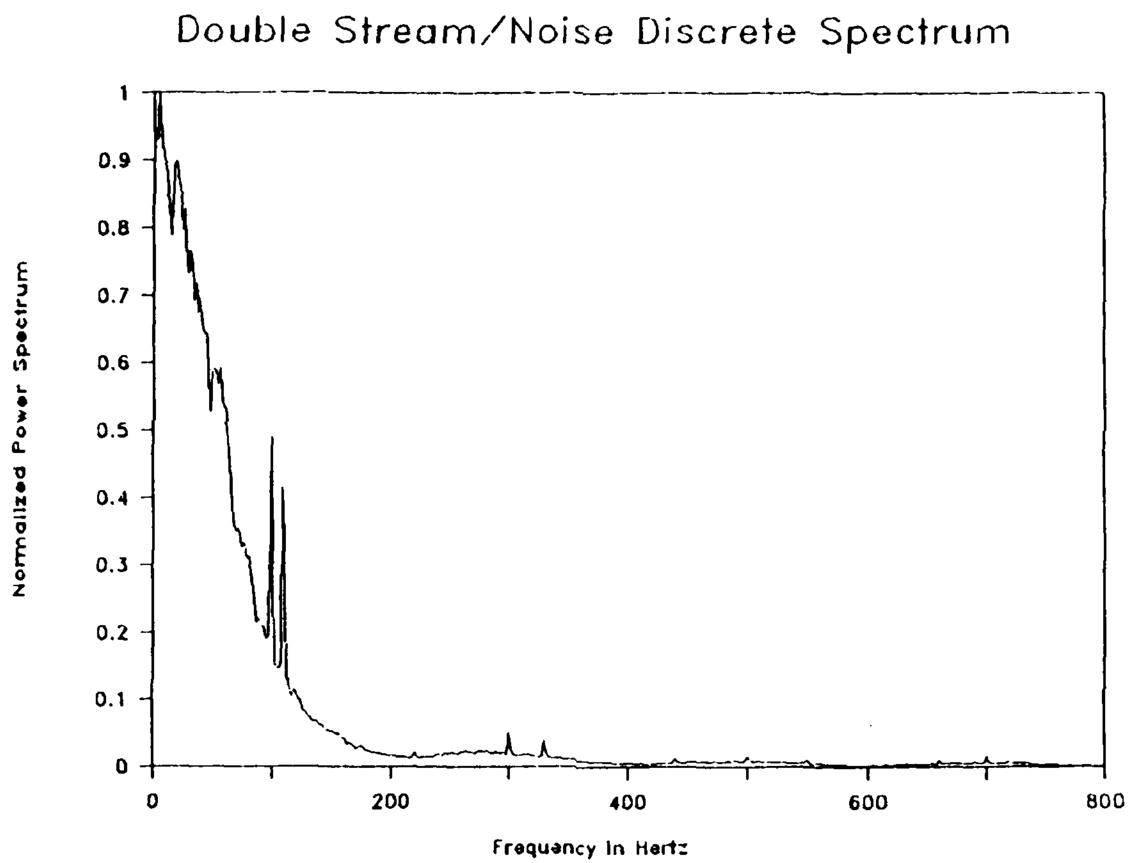
Double Stream/Noise Discrete Spectrum
Normalized Power Spectrum
1
0.9
0.8
0.7
0.6
0.5
0.4
0.3
0.2
0.1
0
0
200
400
600
800
Frequency In Hertz

Figure 5 - 9

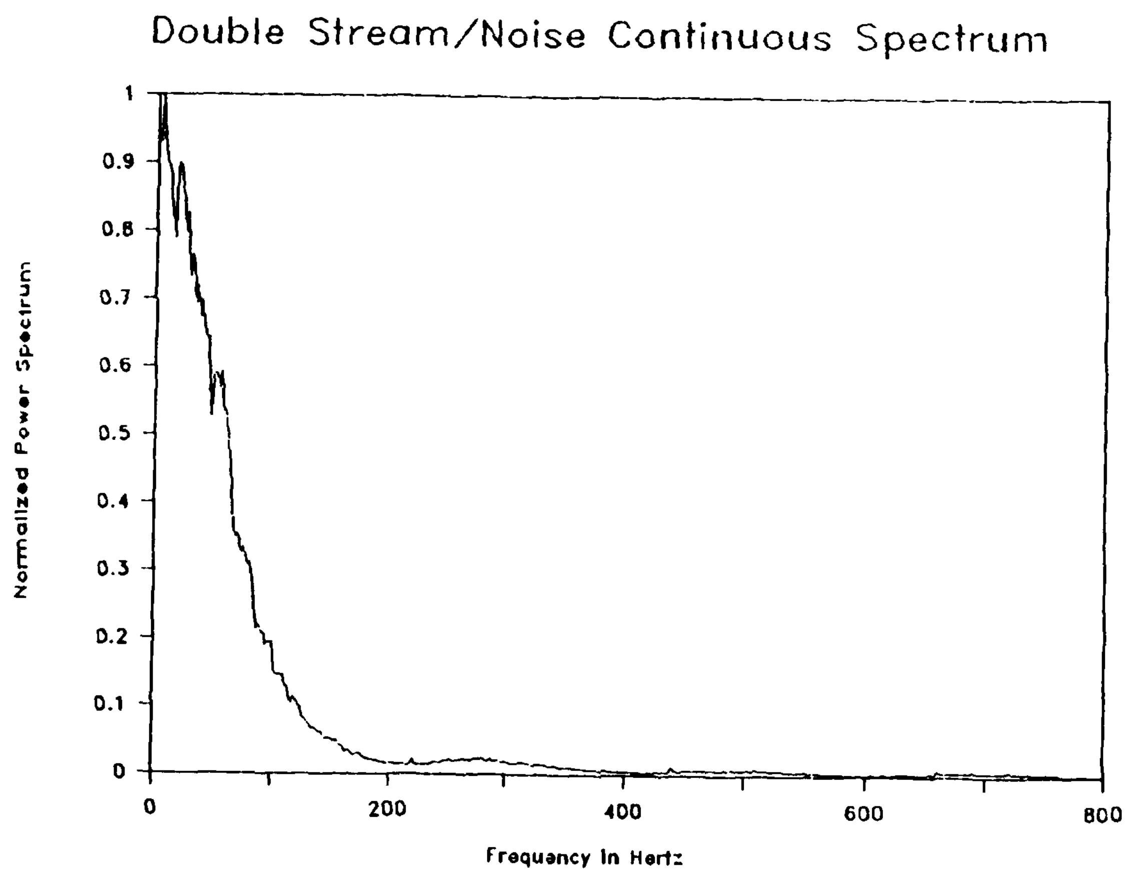
Double Stream/Noise Continuous Spectrum
Normalized Power Spectrum
1
0.9
0.8
0.7
0.6
0.5
0.4
0.3
0.2
0.1
0
0
200
400
600
800
Frequency In Hertz

Figure 5 – 10

Single Chip Stream and Noise, 0 dB. Signal-to-Noise Ratio, Rectangular Filter (Fig. 5-11,12)

Input values:

$$S_1 = 1,$$

$$S_2 = 0,$$

$$N_I = 1, \text{ (0 dB. input signal-to-noise ratio).}$$

$$\alpha \frac{\pi^2}{4} = \frac{\pi^2}{4},$$

$$\beta = \frac{\pi^2}{6}.$$

From the output signal-to-noise ratio equation above, the theoretical value is:

$$\left[\frac{S}{N}\right]_{o,1} = \frac{1}{8.4} TW_a,$$

$$= 5.08.$$

From the data which was used to make the plots of Figure 5-11,12, the measured value was found to be:

$$\left[\frac{S}{N}\right]_{o,1}^{M} = 4.98, \text{ (100 Hz. chip rate).}$$

The value is within .1 db of the theoretical value, which is quite good.

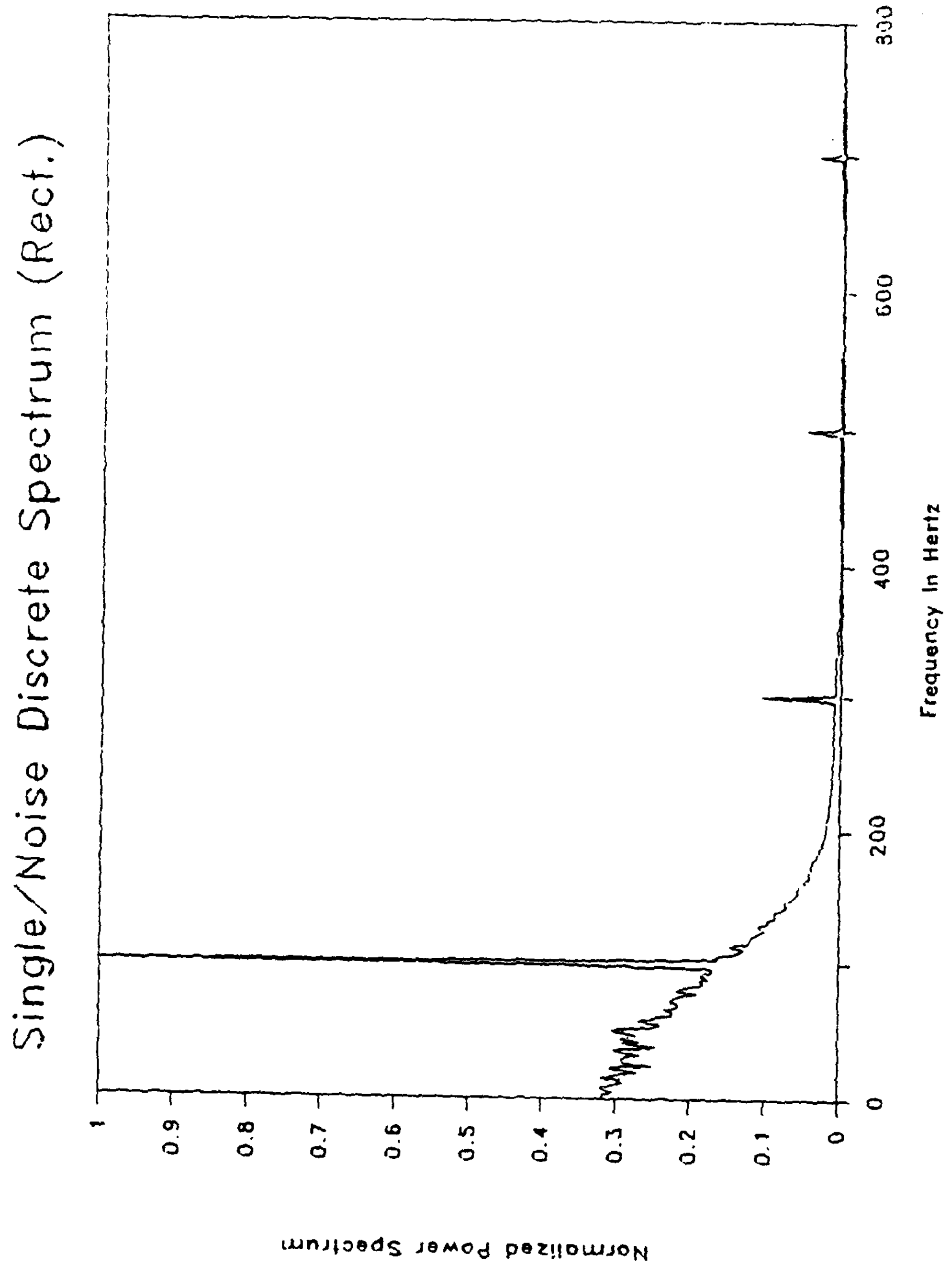
Single/Noise Discrete Spectrum (Rect.)
Normalized Power Spectrum
Frequency In Hertz
0
0.1
0.2
0.3
0.4
0.5
0.6
0.7
0.8
0.9
1
0
200
400
600

Figure 5 - 11

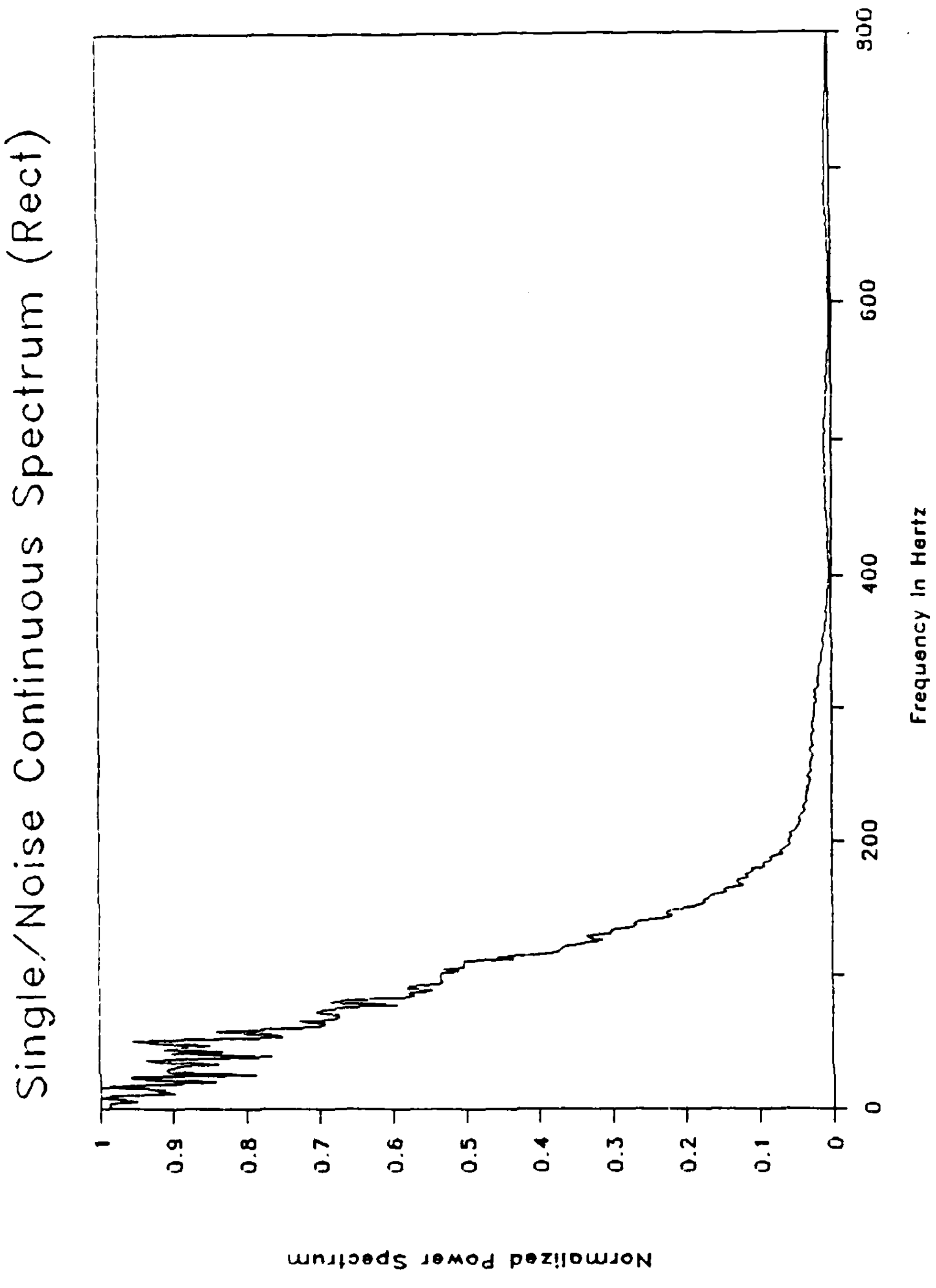
Single/Noise Continuous Spectrum (Rect)
Normalized Power Spectrum
Frequency In Hertz
0
0.1
0.2
0.3
0.4
0.5
0.6
0.7
0.8
0.9
1
0
200
400
600
800

Figure 5 - 12

5.4 Conclusions

Results of the simulation of the chip rate detector confirmed the analyses and validated the basic output signal-to-noise ratio formula given in Section 1 of this report within 1 db.

6.0 DETAILS OF THE ANALYSIS

Within this section the details of the chip stream and noise modeling will be described. Next, the output of the chip rate detector will be calculated for two chip streams and noise. Then, the autocorrelation of the detector, and concomitantly, the power spectrum of the the detector output will be found. The periodic chip rate components of the output are identified and separated from the continuous (noise) components. The value of the continuous spectrum is found at the chip rate line as it is the noise component of the signal-to-noise ratio. Lastly, the signal-to-noise ratio is calculated as the ratio of the chip rate line (at a particular chip rate) to the sum of the total noise contribution from chip and noise sources at the chip rate line.

At best, the aforementioned calculation is long and tedious. Fortunately, the result quoted in the (Section II) is short and simple to interpret. The basics of the calculation will be presented in this section with repetitive calculations of partial autocorrelations (and spectra) relegated to the Appendices.

6.1 Modeling

Definition of a Pseudonoise Chip Stream

A pseudonoise chip stream x(t) is defined by

$$x_1(t) = \sum c_k w_1(t - kT_1),$$

where:

c_k = pseudorandom encoding sequence,

$w_1(t)$ = reference chip shape,

T_1 = reference chip spacing,

$$f_1 = \frac{1}{T_1},$$
$$= \text{chip rate.}$$

A rectangular chip shape will be used in the final results, but it is unnecessary to restrict the calculations at this point to particulars.

To obtain other chip rates it is only necessary to rescale the chip shape:

$$w_2(t) = w_1\left[\frac{T_1}{T_2}\, t\right];$$

and the chip stream at another rate is

$$x_2(t) = \sum c_k \, w_2(t - kT_2),$$

$$= \sum c_k \, w_1\left[\frac{T_1}{T_2}(t - kT_2)\right],$$

is another chip stream at a chip rate of $f_2 = 1/T_2$. The factor of T_1/T_2 also scales the chip shape, if desired, to allow for the chip production by a clocked D/A converter.

Properties of the PN Encoding Sequence

Statistical properties of the PN encoding sequence will be limited to constant, unity amplitude, zero mean sequences typical of spread spectrum systems. Computations to be encountered will require knowledge of the second and forth moments:

Second Moments:

$$E[c_j c_k] = \delta_{jk}$$

$$\triangleq \begin{cases} 1, & j = k, \\ 0, & j \neq k. \end{cases}$$

Fourth Moments:

$$E[c_k c_j c_m c_n] = \delta_{jk}\delta_{mn} + \delta_{jm}\delta_{kn} + \delta_{jn}\delta_{km} - 2\delta_{jkmn}$$

with $\delta_{jkmn} = 0$ unless all the indices are equal ($j = k = m = n$).

For rectangular chips, the fourth moments can be ignored as the delay and multiply output can be decomposed into constituent streams that avoids their use.

Multiple Input Definition:

Input to the chip rate detector will be assumed to be the linear combination of two different chip streams that have the same encoding (but different rates) and receiver noise. Subsequently, the results for two chip streams will be found to be easily generalized to many chip streams. And as the chip stream will be assumed to have independent encoding values from chip-to-chip, the results will also hold for chip streams with different encoding sequences (except when the delay between the identically encoded chip streams is less than one chip time).

The linear combination is given by:

$$s(t) = A_1x_1(t) + A_2x_2(t + \tau_2) + n(t)$$

where $x_1(t)$ and $x_2(t)$ are the chip streams defined above, τ_2 is the offset of the second chip stream, and $n(t)$ is the receiver noise. Receiver noise will be assumed to have mean zero and an autocorrelation function defined by $R_{nn}(\tau)$ (and a spectrum given by the Fourier transform of $R_{nn}(\tau)$).

<u>Output of the Chip Rate Detector:</u>

From Figure 1, the output of the multiplier is given by:

$$z_m(t) = s^*(t)s(t + \tau_d), \quad * \Rightarrow \text{complex conjugation},$$

with $\tau_d = .5T_1$; namely the chip rate detector is designed to have a half chip delay upon the reference chip stream $x_1(t)$. The complex conjugation simplifies later work.

In terms of the constituent inputs the multiplier output is given by:

$$\begin{aligned} z_m(t) = {} & A_1^2\, x_1^*(t)x_1(t + \tau_d) + A_2^2\, x_2^*(t + \tau_2)x_2(t + \tau_2 + \tau_d) \\ & + n^*(t)n(t + \tau_d) \\ & + A_1A_2\, x_1^*(t)x_2(t + \tau_2 + \tau_d) + A_1\, x_1^*(t)n(t + \tau_d) \\ & + A_2A_1\, x_2^*(t + \tau_2)x_1(t + \tau_d) + A_2\, x_2^*(t + \tau_2)n(t + \tau_d) \\ & + A_1\, n^*(t)x_1(t + \tau_d) + A_2\, n^*(t)x_2(t + \tau_2 + \tau_d). \end{aligned}$$

And only four types of cross-product terms are present; and this would be true regardless of the number of chip streams. Therefore, detailed consideration of these four types of terms is sufficient to determine the properties of the expected output of the chip rate detector.

In obvious notation, these terms are:

I. <u>Single Chip Stream Output Product:</u>

$$z_{xx}(0,\tau) = A_x^2\, x^*(t)x(t + \tau)$$

II. Chip Stream Pair Output Product

$$z_{xy}(0,\tau) = A_x A_y \; x^*(t)y(t+\tau)$$

III. Chip Stream/Noise Product

$$z_{xn}(0,\tau) = A_x \; x^*(t)n(t+\tau)$$

IV. Noise Output Product

$$z_{nn}(0,\tau) = n^*(t)n(t+\tau)$$

with, for example,

$$z_{xy}(\tau_1,\tau_2) \triangleq A_x A_y \; x^*(t+\tau_1)y(t+\tau_2).$$

6.2 Evaluation of Expected Output Products:

Types I and II

First, the output chip stream product Type II will be evaluated as Type I is a special case of this product ($x = y$). For evaluation, the chip stream representation is inserted and the expectation over the PN encoding sequence is taken to find the average value. Performing these operations:

$$z_{xy}(0,\tau) = A_x A_y \; x^*(t)y(t+\tau)$$

$$= A_x A_y \sum_k \sum_j c_k c_j \; w_1^*(t - jT_1) \; w_2(t - kT_2 + \tau),$$

and taking the expectation:

$$E[z_{xy}(0,\tau)] = A_x A_y \sum_k \sum_j \delta_{kj} \; w_1(t - jT_1) \; w_2(t - kT_2 + \tau),$$

$$= A_x A_y \sum_j w_1(t - jT_1) \; w_2(t - jT_2 + \tau).$$

If the chip rates of the two streams are identical ($T_1 = T_2$), then the expectation is a periodic function in t with a period of the chip time T_1. Letting $t \Rightarrow t + T_1$ and replacing the dummy summation index with $\tilde{j} = j - 1$, demonstrates the periodicity. Otherwise, the function is aperiodic if one chip rate is a fraction, close to unity, of the other. Therefore, the only chip rate lines are the individual lines that would come out of the chip rate detector had only single chip streams been present.

The cross product terms will only contribute when they line up at some time given by solving the simultaneous equations (found by equating the arguments of a particular chip to zero):

$$t - jT_1 = 0,$$

$$t - jT_2 + \tau = 0$$

or,

$$j(T_1 - T_2) = -\tau,$$

$$j = \frac{-\tau}{T_1 - T_2}.$$

At this chip time the two different chip streams will overlap and produce a "blip" that lasts for a time depending on the difference in their rates. "Blip" time can be found by similar equations at the leading and trailing edges of chip line up. According to their range (τ), and chip rates, this coincidence can have occurred in the past or will occur in the future.

Frequency Content of the Type I Terms

By simple examination of the expectation of the expression above, for equal chip times, the frequency content of the discrete lines may be found. A general Fourier transform is not necessary to see the result for rectangular chips. Consider the expression above for x = y:

$$E[z_{xx}(0,\tau)] = A_x^2 \sum_j w_1(t - jT_1)\, w_1(t - jT_1 + \tau).$$

With $\tau = T_1/2$, a half-chip overlap, the summation can be seen , graphically, to be equivalent to a simple square wave at the chip rate as in the following Figure 6-1. Of course, this was the reason for use of a chip rate detector in the first place.

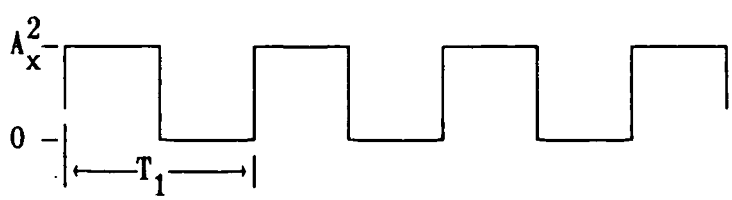

Figure 6-1 Chip rate Detector Output

AD-A194 425 DETECTABILITY OF A DIRECT SEQUENCE EMITTER WITHIN A NETWORK OF DIRECT SEQ (U) M/A-COM SYSTEMS ENGINEERING CENTER VIENNA VA D L NICHOLSON ET AL JAN 88 2/2

UNCLASSIFIED ARO-25331 EL DAAL03-87-C-0020 F/G 17/4 NL

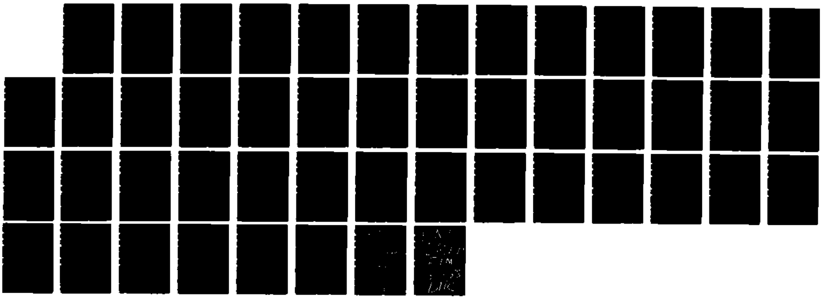

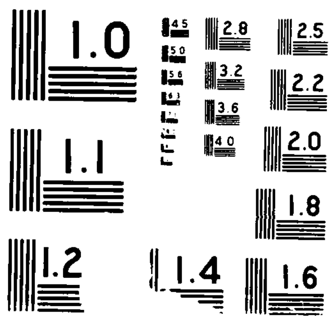
1.0
2.8
2.5
3.2
2.2
3.6
4.0
2.0
1.1
1.8
1.2
1.4
1.6

Chip rate lines will appear at odd harmonics of the chip rate plus a DC term of $.5A_x^2$ as expected of chip rate detectors. A transform of the general expression above can be performed to provide the line amplitude for arbitrary chip shapes; but this operation will be deferred until after the autocorrelation function of the output is calculated to find both the discrete and continuous spectra.

For a chip stream other than the reference stream, the square wave is asymmetrical due to the fact that the reference half-chip delay is not half a chip in this instance. The spectrum will then include both odd and even chip rate harmonics terms at the chip rate of the particular stream under discussion.

The increasing separation of higher harmonic lines from the reference chip stream may be a possible identifier at a sufficient signal-to-noise ratio.

Type III

As the noise is independent of the chip stream, and has zero mean, this type of term also has a zero mean, and therefore, does not contribute to the mean output.

Type IV

The expectation of this term is straight forward and easy to interpret. Taking the expectation of $z_{nn}(t,\tau)$:

$$E[z_{nn}(0,\tau)] = E[n^*(t)n(t + \tau)],$$

$$= R_{nn}(\tau).$$

for stationary noise. The expected mean value of the noise is a DC term which is merely the input noise autocorrelation evaluated at one-half chip time offset from the peak. And this is to be expected; a zero delay ($\tau = 0$) would simply be a power measurement of the noise.

Summary of the Chip Rate Detector Output Expectations (Means)

Expected outputs of the chip rate detector are what might be expected. Discrete spectral lines of each chip stream are present and depend upon the chip shape. For a rectangular chip stream, the reference chip stream has a symmetrical square wave as its output; precisely what would be obtained if it were the only input. Other chip streams, with differing chip rates, have asymmetrical square waves (as the half-chip delay is not half a chip for rates differing from the reference chip stream) at their own chip rates. As these waves are asymmetrical, they also have even harmonics present. However, these will be quite small for chip rates close to that of the reference.

Mixing of chip streams produces a "blip" in the output when the chip streams overlap; this output can be in the present, past, or future depending upon range and chip rates and start of the observation time.

Mixing of chips and noise produces a mean zero output with no periodic content.

And as expected, the noise output expectation, a DC voltage, is no more than the noise autocorrelation function evaluated at a half-chip time.

6.3 Calculation of the Chip Rate Detector Output Spectra

Expected values of the detector output have given insight into the operation of the chip rate detector. The output spectrum allows the output signal-to-noise ratios to be developed. Evaluation of the output spectrum of the chip rate detector is straightforward, but arduous. The simplest approach is the calculation of the time averaged autocorrelation as the detector chip stream outputs are not stationary. This generalized quantity also allows a generalized spectrum to be calculated as in the stationary case (which is a specialization). They are, however, cyclostationary which allows the generalized spectrum to identify both the discrete and continuous spectral components.

Calculation of the Chip Rate Detector Autocorrelation Function

First the output of the delay and multiply will be evaluated. The time averaged autocorrelation function is defined by:

$$R_{zz}^{m}(\tau) = \lim_{T\to\infty} \frac{1}{2T} \int_{-T}^{T} E[z_m^*(t) z_m(t+\tau)]\, dt.$$

For future use the time averaged autocorrelation function will be hereafter simply called the "autocorrelation function; and the operation will be identified by:

$$\left\langle E[\cdot] \right\rangle \triangleq \lim_{T\to\infty} \frac{1}{2T} \int_{-T}^{T} E[\cdot]\, dt.$$

And using the multiplier output from above:

$$R_{zz}^{m}(\tau) = \left\langle E[s(t)s^*(t+\tau_d)s^*(t+\tau)s(t+\tau_d+\tau)] \right\rangle$$

with s(t) given again by:

$$s(t) = A_1\, x_1(t) + A_2\, x_2(t+\tau_2) + n(t).$$

In the previous notation, where the four types of cross products were identified, the delay and multiply output can be written a little more simply:

$$z_m(t) = s^*(t)s(t + \tau_d)$$

$$= z_{11}(0,\tau_d) + z_{22}(\tau_2,\tau_2 + \tau_d) + z_{nn}(0,\tau_d) \quad \text{(a)}$$

$$+ z_{12}(0,\tau_2 + \tau_d) + z_{21}(\tau_2,\tau_d) \quad \text{(b)}$$

$$+ z_{1n}(0,\tau_d) + z_{n1}(0,\tau_d) \quad \text{(c)}$$

$$+ z_{2n}(\tau_2,\tau_d) + z_{n2}(0,\tau_2 + \tau_d). \quad \text{(d)}$$

Next, the correlation products must be formed, which is tedious at best. To reduce the number of terms, a simplifying assumption will be made. It will be assumed that the two input streams never line up during the period of observation; the "blips" identified in the multiplier output above are not present. In this case, the codes may be considered as independent. In the analysis, the code $x_2(t)$ will have a code sequence b_k, rather than c_k; otherwise, the code properties will remain the same.

6.3.1 Identification of the Output Autocorrelation Terms (Types)

Fortunately, by virtue of taking expectations, many of the cross-product correlation terms will vanish. For example, the expectation of the product

$$E[z_{11}(0,\tau_d)z_{12}(0,\tau_d + \tau)] =$$

$$A_1^3A_2\sum_k\sum_j\sum_m\sum_n E[c_kc_jc_mb_n]$$

$$\cdot w_1(t - jT_1)\ w_1^*(t - kT_1 + \tau_d)$$

$$\cdot w_1^*(t - jT_1 + \tau)\ w_2(t - kT_2 + \tau_d + \tau),$$

is zero as

$$E[c_kc_jc_mb_n] = E[c_kc_jc_m]\ E[b_n]$$

$$= 0$$

for the independent, mean zero coding. Any correlation product containing only single members of the coding streams, or noise, must vanish in a similar manner. No cross-products between members of lines (a) through (d) will be retained!

The remaining terms are:

$$z_m(t) = s^*(t)s(t + \tau_d)$$

$$= z_{11}^*(0,\tau_d)z_{11}(\tau,\tau_d + \tau)$$

$$+ z_{22}^*(\tau_2,\tau_2 + \tau_d)z_{22}(\tau_2 + \tau,\tau_2 + \tau_d + \tau)$$

$$+ z_{nn}^*(0,\tau_d)z_{nn}(\tau,\tau_d + \tau)$$

$$+ z_{11}^*(0,\tau_d)z_{22}(\tau_2 + \tau,\tau_2 + \tau_d + \tau)$$

$$+ z_{22}^*(\tau_2,\tau_2 + \tau_d)z_{11}(\tau,\tau_d + \tau)$$

$$+ z_{11}^*(0,\tau_d)z_{nn}(\tau,\tau_d + \tau)$$

$$+ z_{nn}^*(0,\tau_d)z_{11}(\tau,\tau_d + \tau)$$

$$+ z_{22}^*(\tau_2,\tau_2 + \tau_d)\ z_{nn}(\tau,\tau_d + \tau)$$

$$+ z_{nn}^*(0,\tau_d)z_{22}(\tau_2 + \tau,\tau_2 + \tau_d + \tau)$$

$$+ z_{12}^*(0,\tau_2 + \tau_d)z_{12}(\tau,\tau_2 + \tau_d + \tau)$$

$$+ z_{12}^*(0,\tau_2 + \tau_d)z_{21}(\tau_2 + \tau,\tau_d + \tau)$$

$$+ z_{21}^*(\tau_2,\tau_d)z_{12}(\tau,\tau_2 + \tau_d + \tau)$$

$$+ z_{21}^*(\tau_2,\tau_d)z_{21}(\tau_2 + \tau,\tau_d + \tau)$$

$$+ z_{1n}^*(0,\tau_d)z_{1n}(\tau,\tau_d + \tau)$$

$$+ z_{1n}^{*}(0,\tau_d) z_{n1}(\tau,\tau_d + \tau)$$

$$+ z_{n1}^{*}(0,\tau_d) z_{1n}(\tau,\tau_d + \tau)$$

$$+ z_{n1}^{*}(0,\tau_d) z_{n1}(\tau,\tau_d + \tau)$$

$$+ z_{2n}^{*}(\tau_2,\tau_d)\ z_{2n}(\tau_2 + \tau,\tau_d + \tau)$$

$$+ z_{2n}^{*}(\tau_2,\tau_d) z_{n2}(\tau,\tau_2 + \tau_d + \tau)$$

$$+ z_{n2}^{*}(0,\tau_2 + \tau_d) z_{2n}(\tau_2 + \tau,\tau_d + \tau)$$

$$+ z_{n2}^{*}(0,\tau_2 + \tau_d) z_{n2}(\tau,\tau_2 + \tau_d + \tau)$$

Notation for the individual terms may again be simplified by writing:

$$z_{xyuv}(\tau_1,\tau_2,\tau_3,\tau_4) = z_{xy}^{*}(\tau_1,\tau_2)\ z_{uv}(\tau_3,\tau_4)$$

$$\triangleq A_x A_y A_u A_v\ x(t + \tau_1) y^{*}(t + \tau_2) u^{*}(t + \tau_3) v(t + \tau_4)$$

with the partial autocorrelations of each term denoted by a similar notation ($1 \leftrightarrow x$, $2 \leftrightarrow y$, $n \leftrightarrow n$):

$$R_{xyuv}(\tau_1,\tau_2,\tau_3,\tau_4) \triangleq \left\langle E\ [z_{xy}^{*}(\tau_1,\tau_2)\ z_{uv}(\tau_3,\tau_4)]\right\rangle.$$

Using this notation, the delay and multiply output autocorrelation is:

$$R_{zz}^{m}(\tau) = \left\langle E\ [z_m^{*}(t)\ z_m(t + \tau)]\right\rangle$$

$$= R_{1111}(0,\tau_d,\tau,\tau_d + \tau) \qquad \text{(Individual Input Terms)}$$

$$+ R_{2222}(\tau_2,\tau_2 + \tau_d,\tau_2 + \tau,\tau_2 + \tau_d + \tau)$$

$$+ R_{nnnn}(0,\tau_d,\tau,\tau_d + \tau)$$

$$+ R_{1122}(0,\tau_d,\tau_2 + \tau,\tau_2 + \tau_d + \tau) \qquad \text{(DC Terms)}$$

$$+ R_{2211}(\tau_2,\tau_2 + \tau_d,\tau,\tau_d + \tau)$$

$$+ R_{11nn}(0, \tau_d, \tau, \tau_d + \tau)$$

$$+ R_{nn11}(0, \tau_d, \tau, \tau_d + \tau)$$

$$+ R_{22nn}(\tau_2, \tau_2 + \tau_d, \tau, \tau_d + \tau)$$

$$+ R_{nn22}(0, \tau_d, \tau_2 + \tau, \tau_2 + \tau_d + \tau)$$

$$+ R_{1212}(0, \tau_2 + \tau_d, \tau, \tau_2 + \tau_d + \tau) \qquad \text{(Chip Mixing Terms)}$$

$$+ R_{1221}(0, \tau_2 + \tau_d, \tau_2 + \tau, \tau_d + \tau)$$

$$+ R_{2112}(\tau_2, \tau_d, \tau, \tau_2 + \tau_d + \tau)$$

$$+ R_{2121}(\tau_2, \tau_d, \tau_2 + \tau, \tau_d + \tau)$$

$$+ R_{1n1n}(0, \tau_d, \tau, \tau_d + \tau) \qquad \text{(Noise/Chip 1 Mixing Terms)}$$

$$+ R_{1nn1}(0, \tau_d, \tau, \tau_d + \tau)$$

$$+ R_{n11n}(0, \tau_d, \tau, \tau_d + \tau)$$

$$+ R_{n1n1}(0, \tau_d, \tau, \tau_d + \tau)$$

$$+ R_{2nn2}(\tau_2, \tau_d, \tau, \tau_d + \tau) \qquad \text{(Noise/Chip 2 Mixing Terms)}$$

$$+ R_{2nn2}(\tau_2, \tau_d, \tau, \tau_2 + \tau_d + \tau)$$

$$+ R_{n22n}(0, \tau_2 + \tau_d, \tau_2 + \tau, \tau_d + \tau)$$

$$+ R_{n2n2}(0, \tau_d, \tau, \tau_2 + \tau_d + \tau)$$

6.3.2 Evaluation of the Individual Autocorrelation Terms

All the individual terms do not have to be evaluated separately; only the few classes identified above. Individual input terms, those that would be present if no other input be present, will be evaluated in detail as exemplar cases. Details of other terms will be relegated to Appendices.

Individual Input Terms

These terms are present with only a single input. Other types of terms deal with the interaction between terms.

(a.) <u>Chip Stream</u>

It is sufficient to compute the autocorrelation product $R_{2222}(\tau)$; $R_{1111}(\tau)$ is a special case with τ_2 set to zero. In detail, the product is:

$$R_{2222}(\tau_2, \tau_2 + \tau_d, \tau_2 + \tau, \tau_2 + \tau_d + \tau)$$

$$= \Big\langle A^4 \sum_k \sum_j \sum_m \sum_n E[c_k c_j c_m c_n]$$

$$\cdot w_2(t - jT_2 + \tau_2) w2t - kT_2 + \tau_2 + \tau_d)$$

$$\cdot w_2(t - jT_2 + \tau_2 + \tau) w_2^*(t - kT_2 + \tau_2 + \tau_d + \tau) \Big\rangle$$

Computation of this autocorrelation can be performed analytically using the fourth moments of the encoding sequence for an arbitrary chip shape; but it is simpler, and more intuitive, to use graphical methods with rectangular chipping.

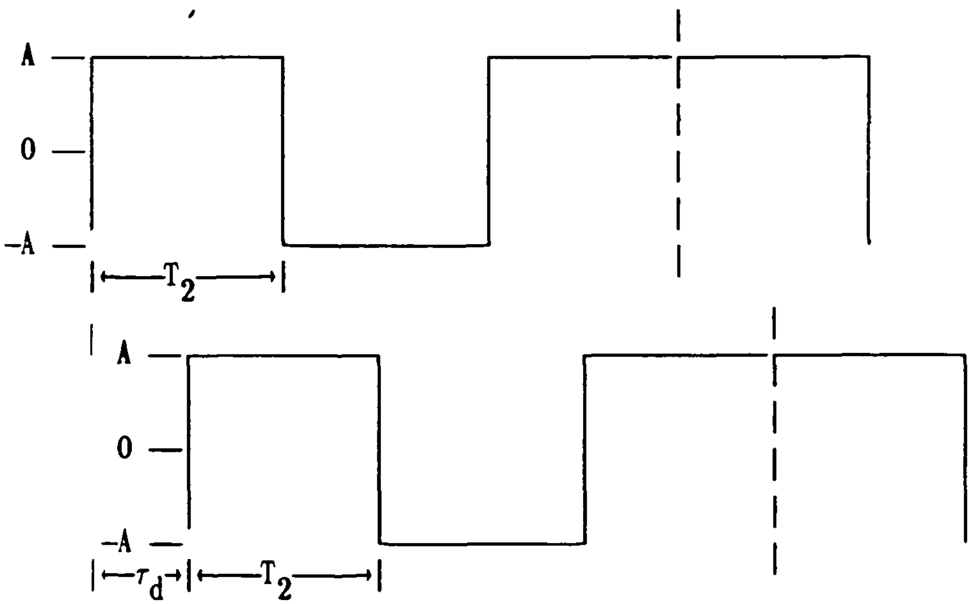

Figure 6-2a. Chip Sequence and Delayed Version

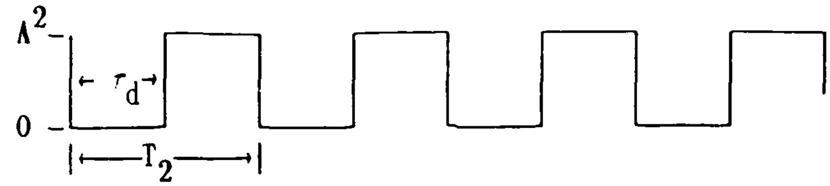

Figure 6-2b. Deterministic Product Chip Rate Waveform

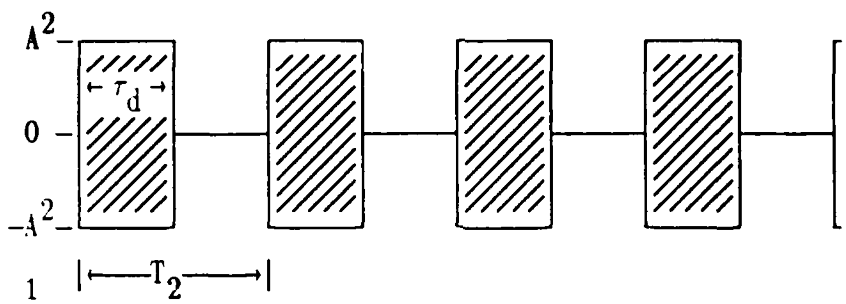

Figure 6-2c. Random Product Chip Waveform

From Figure 6-2 the output of the delay and multiply can be seen to be composed of two waveforms. A deterministic square wave, with a period of the chip rate, occurs due to the same chip being multiplied by itself for a time $\tau_{ov} = T_2 - \tau_d$ as in Figure 6-2b. A random waveform, as in Figure 6-2c, develops in the region between overlaps. The random waveform has equilikely $\pm A^2$ states which have a duration of τ_d. Also, the random waveform is completely uncorrelated with the deterministic waveform as each is zero where the other has a value.

Therefore, the autocorrelation of the composite waveform is the sum of the autocorrelations of the waveforms in Figure 6-2b and 6-2c, and is given by:

$$R_{xxxx}(\tau) = A^4 \,[R_{(\text{Unit Square Wave Autocorrelation})}(\tau)$$

$$+ R_{(\text{Random Biphase (Duration } \tau_d\text{, Interval } T_2))}(\tau)];$$

where from Appendix I:

$$R_{(\text{Unit Square Wave Autocorrelation})}(\tau)$$

$$= A^4 \sum_k f_j^2 \, e^{-ik\omega_2 \tau}$$

with the square wave coefficients

$$f_k = \begin{cases} 1/2, & k = 0, \\ (-1)^k \frac{1}{\pi k}, & k \text{ odd}, \\ 0, & \text{otherwise}. \end{cases}$$

and $\omega_1 = \omega_c = 2\pi/T_c$ is the chip rate.

As the spectrum is the transform of the autocorrelation function, it has only discrete lines at DC and the harmonics of the chip rate. The spectrum can be written in terms of impulse functions:

$$S_{SW}(\omega) = 2\pi \, A^4 \sum_k f_k^2 \, \delta(\omega - k\omega_c)$$

$$= A^4 \, [\tfrac{1}{4} \, \delta(0) + \sum_k{}' \left[\frac{1}{\pi k}\right]^2 \delta(\omega - k\omega_c), \quad ' \Rightarrow \text{exclude } k = 0.$$

The value of the 1st chip rate line, the signal output component of the chip rate detector is, therefore:

$$S_1 = A^4 \frac{1}{\pi^2},$$

And from Appendix II,

$$R_{(\text{Random Biphase (Duration } \tau_d, \text{ Interval } T_2))}(\tau)];$$

$$= A^4 \frac{1}{T_c} \int_{-\infty}^{\infty} w_d(t) w_d(t + \tau) \, dt,$$

where $w_d(t)$ is the rectangular chip of width τ_d (Figure 6–2c), and the autocorrelation is a simple triangle with a base of $2\tau_d$ and a height of τ_d/T_2. As the spectrum is the Fourier transform of the autocorrelation (Appendix II):

$$S_{RB}(\omega) = A^4 \frac{\tau_d^2}{T_2} \left| \frac{\sin(\omega\tau_d/2)}{\omega\tau_d/2} \right|^2,$$

$$= A^4 \frac{T_2}{4} \left| \frac{\sin(\omega T_2/4)}{\omega T_2/4} \right|^2, \text{ for } \tau_d \cong T_2/2,$$

which is a power spectrum that is twice as wide as the input chip stream spectrum.

At harmonics of the chip rate where a narrowband filter will be placed to detect the chip rate line the continuous spectrum will have the value:

$$S_{RB}(\omega_k) = A^4 \frac{T_2}{(\pi k)^2} \sin^2(\pi k/2).$$

(b.) Noise

Development of the delayed and multiplied noise autocorrelation requires assumptions about the statistics, and spectrum, of the noise. The bandwidth of the noise and it's spectrum do not change the basic physics; but they do change the exact form of the output signal-to-noise ratio constant and the difficulty of the calculations. The autocorrelation of the multiplier output was found to be:

$$R_{nnnn}(\tau) = \left\langle E[n(t)n^*(t + \tau_d)n^*(t + \tau)n(t + \tau_d + \tau)] \right\rangle,$$

$$= E[n(0)n^*(\tau_d)n^*(\tau)n(\tau_d + \tau)],$$

$$= E[X_1X_2X_3X_4]$$

assuming the noise process is stationary.

From J. H. Laning, Jr. and R. H. Battin, "Random Processes in Automatic Control", McGraw–Hill Book Company, Inc. 1956, the expectation can be found for Gaussian processes as

$$E[X_1X_2X_3X_4] = m_{12}m_{34} + m_{13}m_{24} + m_{14}m_{23},$$

where

$$m_{ij} = E[x(\tau_i)x(\tau_j)]$$
$$= R_{xx}(\tau_i - \tau_j).$$

In this instance the correlation $R_{nnnn}(\tau)$ is given by:

$$R_{nnnn}(\tau) = R_{nn}(\tau_d)^2 + R_{nn}(\tau)^2 + R_{nn}(\tau + \tau_d)R_{nn}(\tau - \tau_d),$$

where $R_{nn}(\tau)$ is the autocorrelation function of the input noise process.

The output noise spectrum is obtained through taking the transform of $R_{nnnn}(\tau)$:

and

$\delta(o)$

$$S_{nnnn}(\omega) = 2\pi\,\hat{}\,R_{nn}(\tau_d)^2 + \frac{1}{2\pi}\int d\omega_1\; S_{nn}(\omega_1)S_{nn}(\omega_1 - \omega)$$
$$+ \frac{1}{2\pi}\int d\omega_1\; S_{nn}(\omega_1)S_{nn}(\omega_1 - \omega)\; e^{i2\omega_1\tau_d}$$

where $S_{nn}(\omega)$ is the spectrum of the input noise given by:

$$S_{nn}(\omega) = \int R_{nn}(\tau)\; e^{-i\omega\tau}\, d\tau.$$

For computational purposes, two autocorrelation functions will be chosen for the noise, or equivalently, spectra.

I. <u>Noise Using Chip Spectra</u>

Noise spectra may be chosen to be identical to the chip spectra; namely, having the same basic bandwidth. In this case, the noise autocorrelation function is given by the usual triangle:

$$R_{nn}(\tau) = N_I \left\{ \begin{array}{ll} [1 - \frac{|t|}{T_1}, & |t| \le T_1, \\ 0, & \text{otherwise.} \end{array} \right\},$$

with a spectrum

$$S_{nn}(\omega) = N_I\ T_1 \left|\frac{\sin(\omega T_1/2)}{\omega T_1/2}\right|^2 .$$

As this is identical to the spectrum of a chip stream, the formula of Appendix IV for $S_{1nn1}(\omega)$ and $S_{1n1n}(\omega)$ may be used for the spectrum $S_{nnnn}(\omega)$. Therefore,

$$S_{nnnn}(\omega) = \frac{\pi}{4} N_I^2\ \delta(0)$$

$$+ T_1\ N_I^2\ \frac{2}{(\omega T_1)^2}\left[[2 - \cos(\omega T_1/2)]\left[1 + \frac{1}{2}\ \frac{\sin(\omega T_1/2)}{\omega T_1/2}\right]\right].$$

At $\omega = \omega_1 = 2\pi/T_1$, the chip rate, the multiplier output spectrum amplitude due to the noise component is:

$$S_{nnnn}(\omega_1) = \frac{1}{2}\ T_1\ N_I^2\ \frac{3}{\pi^2}$$

II. Rectangular Noise Spectrum

A rectangular noise spectrum, of a width of twice the chip rate, may be chosen. It, however, complicates later chip/noise calculations. The rectangular spectrum is given by:

$$S_{nn}(\omega) = \left\{\begin{array}{r} \frac{\pi}{\omega_c}\ N_I,\ \ |\omega| \le \omega_c, \\ 0,\ \text{otherwise.} \end{array}\right\},$$

From earlier work, the multiplier output spectrum is given by:

$$S_{nnnn}(\omega) = 2\pi\ \delta(0)\ R_{nn}(\tau_d)^2$$

$$+ \frac{1}{2\pi}\left[\frac{\pi}{\omega_1}\right]^2 N_I^2\ (2\omega_1 - \omega)\left[1 + \frac{\sin[(2\omega_1-\omega)\tau_d]}{(2\omega_1-\omega)\tau_d}\right],$$

for $|\omega| \le 2\omega_1$, and is zero otherwise.

At the chip rate the multiplier continuous noise spectrum output has the value:

$$S_{nnnn}(\omega_1) = T_1 \frac{1}{4} N_I^2.$$

This value will produce the classical results for the output of a chip rate detector for a single chip stream and noise. But, this spectrum makes the rest of the work in this paper extremely difficult. The triangular noise autocorrelation above, with the bell-shaped spectrum, allows the rest of the analysis to be much simpler.

And the difference in the output noise powers, of the two cases, is easily calculable. Taking the ratio of the cases I and II:

$$\frac{C_I}{C_{II}} = \frac{6}{\pi^2},$$

$$= .608,$$

$$= -2.12 \text{ dB},$$

Hereafter, the noise autocorrelation of case I, the triangular form, will be used in the analytical calculations with the results verified by simulation.

In the final results the noise contribution constant will be identified as

$$C_n = \alpha \frac{\pi^2}{4},$$

with

$$\alpha = \frac{6}{\pi^2}.$$

Then, for comparison with other chip rate detector work, α can be chosen as unity or the value given above for simplified formulae ($C_n = 3/2$).

6.3.3 Compilation of Terms

From the efforts of the previous section and the Appendices, the total discrete and continuous contributions to the chip rate detector output can be collected. Work in this section has identified four types of output terms from the chip rate detector. These types and the pages upon which they may be found within the derivations are:

I. Chip Rate Sine Waves:

An individual chip rate line power:

$$P_j = \frac{S_j^2}{\pi^2}, \qquad \text{(Page 6 – 14)}$$

with

$$S_j = A_j^2, \text{ the input power of the } j^{th} \text{ chip stream (at baseband).}$$

II. Chip and Noise Independent "Noise" Spectra Outputs

Individual chip stream continuous spectrum value at the chip rate:

$$P_j^C = S_j^2 \frac{T_j}{\pi^2}, \qquad \text{(Page 6 – 15)}$$

with

$$1/T_j = \text{chip rate of the } j^{th} \text{ chip stream.}$$

Noise continuous spectrum value at the chip rate:

Chip shaped impulse response filter:

$$S_{nnnn}(\omega_1) = \frac{1}{2} T_1 N_I^2 \frac{3}{\pi^2}. \qquad \text{(Page 6 – 17)}$$

Rectangular noise spectrum:

$$S_{nnnn}(\omega_1) = T_1 \frac{1}{4} N_{ij_I}^2 \qquad \text{(Page 6 – 18)}$$

III. Chip/Chip and Chip/Noise Intermodulation Spectra

Chip/chip mixing continuous spectrum value at the chip rate:

$$P_{jk}^{CM} = T_1 S_j S_k \frac{3}{\pi^2}, \qquad \text{(Appendix – 14)}$$

with

$1/T_1$ = chip width of the chip streams all considered approximately equal.

Chip/Noise continuous spectrum value at the chip rate:

Chip shaped impulse response filter:

$$S_{nnnn}(\omega_1) = T_1\ S_j N_I\ \frac{3}{\pi^2}. \qquad \text{(Appendix - 18)}$$

Rectangular noise spectrum:

$$S_{nnnn}(\omega_1) = \frac{1}{2}\ T_1\ S_j N_i. \qquad \text{(Appendix - 19)}$$

6.3.4 Calculation of the Chip Rate Detector Output Signal-to-Noise Ratio

By combining the various terms, above, the output signal-to-noise ratio may be found.

First, the chip rate sine wave power for the j^{th} chip stream (I) is identified as the signal power output. It is

$$S_o = P_j$$

$$= \frac{S_j^2}{\pi^2},$$

Then, the continuous chip stream spectrum powers (II and III), at the chip rate are summed together, multiplied by the narrow band chip detector output filter bandwidth ($B = 1/T$), to form the total noise output (for two chip streams):

Chip Shaped Noise Spectrum

$$N_o = B\ \frac{T_1}{\pi^2} \left[\ S_1^2 + S_2^2 + \frac{3}{2}\ N_I^2 + 3\ [S_1\ S_2 + S_1 N_I + S_2 N_I\ \right],$$

and the chip detector output output signal-to-noise ratio is:

$$\left[\frac{S}{N}\right]_{o,j} = \frac{S_o}{N_o},$$

$B = \frac{1}{T}$, $T_1 = \frac{1}{W}$ $\therefore$ $BT_1 = \frac{1}{TW}$

$$= \frac{S_j^2 \, TW}{\left[S_1^2 + S_2^2 + \frac{3}{2} N_I^2 + 3 \, [S_1 \, S_2 + S_1 N_I + S_2 N_I \right]},$$

with $W = 1/T_1$ as the chip rate in hertz, and T, the bandwidth (or integration time of) the output filter.

<u>Rectangular Noise Spectrum</u>

$$N_o = B \frac{T_1}{\pi^2} \left[S_1^2 + S_2^2 + \frac{\pi^2}{4} N_I^2 + 3 \, [S_1 S_2 + \frac{\pi^2}{6} \, [S_1 N_I + S_2 N_I] \right],$$

and the chip detector output ~~output~~ signal-to-noise ratio is:

$$\left[\frac{S}{N}\right]_{o,j} = \frac{S_o}{N_o},$$

$$= \frac{S_j^2 \, TW}{\left[S_1^2 + S_2^2 + \frac{\pi^2}{4} N_I^2 + 3 \, [S_1 S_2 + \frac{\pi^2}{6} \, [S_1 N_I + S_2 N_I] \right]},$$

<u>And we have the major result of this report!</u>

By defining two constants α and β, the two cases (chip shape and rectangular input noise spectra can be written in a single form for use in the rest of this report. Define:

<u>Chip Shaped Input Noise Spectrum:</u>

$$\alpha = \frac{6}{\pi^2},$$

and

$$\beta = 1;$$

<u>Rectangular Input Noise Spectrum:</u>

$$\alpha = 1,$$

$$\beta = \frac{\pi^2}{6}.$$

With these values, the signal-to-noise ratio for both cases both cases may be written in the form:

$$\left[\frac{S}{N}\right]_{o,j} = \frac{S_o}{N_o},$$

$$= \frac{S_j^2 \, TW}{\left[\; S_1^2 + S_2^2 + \alpha \frac{\pi^2}{4} N_I^2 + 3 \; [S_1 S_2 + \beta \; [S_1 N_I + S_2 N_I] \; \right]} \; .$$

which is the form used throughout this report.

APPENDICES

APPENDIX I

Unit Square Wave Autocorrelation

Expansion of the periodic chip function in a Fourier series is relatively simple. An expansion is given by:

$$f(t) = \sum f_k \, e^{i2\pi k\frac{t}{T_c}},$$

with coefficients

$$f_k = \frac{1}{T_c} \int_{-T_c/2}^{T_c/2} f(t) \, e^{-i2\pi k\frac{t}{T_c}} \, dt.$$

For the unit square wave of a width of half a period, the coefficients are:

$$f_k = \begin{cases} 1/2, & k = 0, \\ (-1)^k \frac{1}{\pi k}, & k \text{ odd}, \\ 0, & \text{otherwise.} \end{cases}$$

The autocorrelation function is

$$\begin{aligned} R_{ff}(\tau) &= \left\langle \sum \sum f_j^* f_k \, e^{i(\omega_k - \omega_j)t} \, e^{i\omega_k \tau} \right\rangle, \\ &= \sum |f_j|^2 \, e^{i\omega_j \tau}. \end{aligned}$$

where $\omega_j = 2\pi k/T_c$ is a harmonic of the chip rate.

As the spectrum is the transform of the autocorrelation function, it has only discrete lines at DC and the harmonics of the chip rate.

APPENDIX II

Random Square Wave Autocorrelation

A unit amplitude, binary, random square wave can be represented as

$$f(t) = \sum c_k \, w(t - kT_c).$$

The time averaged autocorrelation function is given by

$$R_{ff}(\tau) = \lim_{T\to\infty} \frac{1}{2T} \int_{-T}^{T} E[f(t)f(t+\tau)]\, dt,$$

$$= \lim_{T\to\infty} \frac{1}{2T} \int_{-T}^{T} \sum_{j,k} E[c_k c_j]\; w(t - kT_c)w(t - jT_c + \tau)\, dt,$$

$$= \lim_{T\to\infty} \frac{1}{2T} \int_{-T}^{T} \sum_{k} w(t - kT_c)w(t - kT_c + \tau)\, dt,$$

as $E[c_k c_j] = \delta_{jk}$ for uncorrelated binary sequences with values of ±1.

To evaluate the expression, change the variable of integration and the order of summation. The resulting expression is

$$R_{ff}(\tau) = \lim_{T\to\infty} \frac{1}{2T} \sum_{k} \int_{-T-kT_c}^{T-kT_c} w(t)w(t+\tau)\, dt,$$

$$= \frac{1}{T_c} \int_{-\infty}^{\infty} w(t)w(t+\tau)\, dt,$$

upon letting $T = NT_c$ and taking the limit on N, and assuming the chip shape falls of reasonably rapidly (which it, of course, does for rectangular chips).

For rectangular chips of width T_w, the autocorrelation is a simple triangle with a base of $2T_w$ and a height of T_w/T_c. As the spectrum is the Fourier transform of the autocorrelation, the simple relation for the spectrum is:

$$S_f(\omega) = \frac{1}{T_c} |W(\omega)|^2,$$

using simple transform relations, and

$$W(\omega) = \int_{-\infty}^{\infty} w(t)\, e^{-i\omega t}\, dt$$

is the Fourier transform of the chip shape.

For the rectangular chip of width T_w, the power spectrum is

$$S_f(\omega) = \frac{T_w^2}{T_c} \left| \frac{\sin(\omega T_w/2)}{\omega T_w/2} \right|^2 ,$$

which is the typical spectrum for rectangular chips. The spectral width to the first null is the radian frequency $\omega_{null} = 2\pi/T_w$. Therefore, a chip rate detector which has a delay of one-half chip has a continuous power spectral output component that is twice as wide as the input chip stream)as might be expected).

At the chip rate, the self-noise power spectrum out of the chip rate detector, of a single chip stream, has the value (assume $T_w = .5\ T_c$):

$$S_f(\omega_c) = T_c \frac{1}{\pi^2} ,$$

APPENDIX III

Expansion of Periodic Summations

Expansion of the periodic chip summations in a Fourier series is relatively simple. As before, an expansion is given by:

$$f(t) = \sum f_k \, e^{i2\pi k \frac{t}{T_c}},$$

with coefficients

$$f_k = \frac{1}{T_c} \int_{-T_c/2}^{T_c/2} f(t) \, e^{-i2\pi k \frac{t}{T_c}} \, dt.$$

and where

$$f(t) = \sum_k w(t - kT_c) w(t - kT_c + \tau).$$

Inserting the summation in the coefficient expression:

$$f_k = \frac{1}{T_c} \int_{-T_c/2}^{T_c/2} \sum_k w(t - kT_c) w(t - kT_c + \tau) \, e^{-i2\pi k \frac{t}{T_c}} \, dt,$$

$$= \frac{1}{T_c} \sum_k \int_{-T_c/2 - kT_c}^{T_c/2 - kT_c} w(t) w(t + \tau) \, e^{-i2\pi k \frac{t}{T_c}} \, dt.$$

And finally:

$$f_k = \frac{1}{T_c} \int_{-\infty}^{\infty} w(t) w(t + \tau) \, e^{-i2\pi k \frac{t}{T_c}} \, dt.$$

APPENDIX IV

DC & Chip Mixing Terms:

These terms only occur due to the interaction of chip streams with each other, or with noise, entering the chip rate detector.

Chip Streams

A typical chip mixing term is

$$R_{1122}(\tau_1,\tau_2,\tau_3,\tau_4) = \Big\langle A_1^2 A_2^2 \sum_k \sum_j \sum_m \sum_n E[c_k c_j] E[b_m b_n]$$

$$\cdot w_1(t - jT_1 + \tau_1)\, w_1^*(t - kT_1 + \tau_2)$$

$$\cdot w_2^*(t - jT_2 + \tau_3)\, w_2(t - kT_2 + \tau_4)\Big\rangle$$

$$= \Big\langle A_1^2 A_2^2 \sum_k w_1(t - jT_1 + \tau_1)\, w_1^*(t - jT_1 + \tau_2)$$

$$\cdot \sum_j w_2^*(t - kT_2 + \tau_3)\, w_2(t - kT_2 + \tau_4)\Big\rangle$$

Other chip mixing terms are merely changes of subscripts and times (τ_q's); they are different cases of the correlation product under consideration.

Now, the summations are periodic functions in the chip times and can be expanded in Fourier series. For example:

$$f_1(t) \triangleq \sum a_n\, e^{in\omega_1 t}, \quad \omega_1 = \frac{2\pi}{T_1},$$

$$= \sum_k w_1(t - jT_1 + \tau_1)\, w_1^*(t - jT_1 + \tau_2)$$

and from Appendix III:

$$a_n = e^{in\omega_1 \tau_1} \frac{1}{T_1} \int_{-\infty}^{\infty} w_1(t)\, w_1^*(t + \tau_2 - \tau_1)\, e^{-in\omega_1 t} dt.$$

As the chip shape is given in terms of its transform by

$$w_1(t) = \frac{1}{2\pi}\int_{-\infty}^{\infty} W_1(\omega)\, e^{i\omega t}\, d\omega$$

$$a_n = e^{in\omega_1\tau_1}\left[\frac{1}{2\pi}\right]^2 \frac{1}{T_1}\int_{-\infty}^{\infty} dt \int_{-\infty}^{\infty} d\omega'' \int_{-\infty}^{\infty} d\omega'\ W_1(\omega'') W_1^*(\omega')$$

$$\cdot e^{i(\omega''-\omega'-n\omega_1)t}\ e^{-i\omega'(\tau_2 - \tau_1)}\ dt.$$

$$a_n = e^{in\omega_1\tau_1}\ \frac{1}{2\pi}\frac{1}{T_1}\int_{-\infty}^{\infty} d\omega'\ W_1(\omega' + n\omega_1) W_1^*(\omega')\ e^{-i\omega'(\tau_2 - \tau_1)}.$$

Similarly, the other periodic function can be written as a Fourier series:

$$f_2(t) \triangleq \sum d_m\, e^{im\omega_2 t}, \quad \omega_2 = \frac{2\pi}{T_2},$$

$$= \sum_k w_2(t - kT_2 + \tau_3)\ w_2^*(t - jT_2 + \tau_4)$$

with

$$d_m = e^{im\omega_2\tau_3}\ \frac{1}{2\pi}\frac{1}{T_2}\int_{-\infty}^{\infty} d\omega''\ W_2(\omega'' + n\omega_2) W_2^*(\omega'')\ e^{-i\omega''(\tau_4 - \tau_3)}.$$

Finally, the time averaged expectation, using the Fourier series representations, is

$$R_{1122}(\tau_1,\tau_2,\tau_3,\tau_4) = A_1^2 A_2^2 \sum_m \sum_n a_n d_m^* \left\langle e^{i(n\omega_1 - im\omega_2)t} \right\rangle$$

Time averages of sine waves vanish. As ω_1/ω_2 is close to unity (clock rates are similar), the only contributor of interest is the zeroth. Higher order contributors will occur at $N\omega_1 = M\omega_2$ if $\omega_1/\omega_2 = M/N$. When M/N is close to one, these contributors occur at frequencies where the chip rate lines are too far down to be of interest. Therefore,

$$R_{1122}(\tau_1,\tau_2,\tau_3,\tau_4)$$

$$= A_1^2 A_2^2 \; a_0 d_0^*$$

$$= A_1^2 A_2^2 \; \frac{1}{2\pi} \frac{1}{T_1} \int_{-\infty}^{\infty} d\omega' \; |W_1(\omega')|^2 \; e^{-i\omega'(\tau_2 - \tau_1)} .$$

$$\cdot \; \frac{1}{2\pi} \frac{1}{T_2} \int_{-\infty}^{\infty} d\omega'' \; |W_2^*(\omega'')|^2 \; e^{\; i\omega''(\tau_4 - \tau_3)} .$$

Other pair products follow an identical development. They are simply rearrangements of the arguments τ_q. For example, the term

$$R_{1212}(\tau_1, \tau_2, \tau_3, \tau_4) = \Big\langle \; A_1^2 A_2^2 \sum_k \sum_j \sum_m \sum_n E[c_k c_m] E[b_j b_n]$$

$$\cdot w_1(t - kT_1 + \tau_1) \; w_2^*(t - jT_2 + \tau_2)$$

$$\cdot w_1^*(t - jT_1 + \tau_3) \; w_2(t - kT_2 + \tau_4) \Big\rangle$$

$$= \Big\langle \; A_1^2 A_2^2 \sum_k w_1(t - kT_1 + \tau_1) \; w_2^*(t - jT_2 + \tau_2)$$

$$\cdot \; \sum_j w_1^*(t - kT_1 + \tau_3) \; w_2(t - jT_2 + \tau_4) \Big\rangle$$

$$R_{1212}(\tau_1, \tau_2, \tau_3, \tau_4) = R_{1122}(\tau_1, \tau_3, \tau_2, \tau_4)$$

as the summation can be rearranged to have an identical appearance to R_{1122}; but with the ordering of the τ_q's changed. Conjugation can be adjusted to convenience as the chip functions are real. Continuing, the remaining correlation products are:

$$R_{1221}(\tau_1, \tau_2, \tau_3, \tau_4) = R_{1122}(\tau_1, \tau_4, \tau_3, \tau_2)$$

$$R_{2112}(\tau_1, \tau_2, \tau_3, \tau_4) = R_{1122}(\tau_3, \tau_2, \tau_1, \tau_4)$$

$$R_{2121}(\tau_1, \tau_2, \tau_3, \tau_4) = R_{1122}(\tau_4, \tau_2, \tau_3, \tau_1)$$

$$R_{2211}(\tau_1, \tau_2, \tau_3, \tau_4) = R_{1122}(\tau_3, \tau_4, \tau_1, \tau_2)$$

The interesting term in the expression for $R_{1122}(\tau_1,\tau_2,\tau_3,\tau_4)$ is the complex exponential:

$$D_\delta(\tau_1,\tau_2,\tau_3,\tau_4) = \frac{1}{2\pi}\, e^{-i\omega'(\tau_2 - \tau_1)}\, e^{i\omega''(\tau_4 - \tau_3)},$$

as the spectrum is obtained from the autocorrelation by the transform:

$$S(\omega) = \int_{-\infty}^{\infty} R(\tau)\, e^{-i\omega\tau}\, d\tau,$$

and only the complex exponentials depend upon τ. The different terms develop different δ functions that collapse the autocorrelation products into partial spectrums that may be easily interpreted.

Evaluation of the function D_δ is most easily performed by considering the integral:

$$S^{\delta}_{1234}(\omega) = \int_{-\infty}^{\infty} D_\delta(\tau_1,\tau_2,\tau_3,\tau_4)\, e^{-i\omega\tau}\, d\tau$$

$$= \frac{1}{2\pi} \int_{-\infty}^{\infty} e^{-i\omega'(\tau_2 - \tau_1)}\, e^{i\omega''(\tau_4 - \tau_3)}\, e^{-i\omega\tau}\, d\tau$$

For the various correlation products, the corresponding delay differences can be tabulated in terms of the ordering of the arguments for R_{1122}:

$$R_{1122} \Leftrightarrow (\tau_1,\tau_2,\tau_3,\tau_4) \Leftrightarrow (\tau_2 - \tau_1),\ (\tau_4 - \tau_3) \Leftrightarrow \tau_d,\ \tau_d$$

$$R_{2211} \Leftrightarrow (\tau_3,\tau_4,\tau_1,\tau_2) \Leftrightarrow (\tau_4 - \tau_3),\ (\tau_2 - \tau_1) \Leftrightarrow \tau_d,\ \tau_d$$

$$R_{1212} \Leftrightarrow (\tau_1,\tau_3,\tau_2,\tau_4) \Leftrightarrow (\tau_3 - \tau_1),\ (\tau_4 - \tau_2) \Leftrightarrow \tau,\ \tau$$

$$R_{1221} \Leftrightarrow (\tau_1,\tau_4,\tau_3,\tau_2) \Leftrightarrow (\tau_4 - \tau_1),\ (\tau_2 - \tau_3) \Leftrightarrow \tau_d + \tau,\ \tau_d - \tau$$

$$R_{2112} \Leftrightarrow (\tau_3,\tau_2,\tau_1,\tau_4) \Leftrightarrow (\tau_2 - \tau_3),\ (\tau_4 - \tau_1) \Leftrightarrow \tau_d - \tau,\ \tau_d + \tau$$

$$R_{2121} \Leftrightarrow (\tau_4,\tau_2,\tau_3,\tau_1) \Leftrightarrow (\tau_2 - \tau_4),\ (\tau_1 - \tau_3) \Leftrightarrow -\tau,\ -\tau$$

where the actual values of the arguments of the correlation products have been used on the right of the table.

With these pairs the integrals become:

$$S^{\delta}_{1122}(\omega) = \delta(\omega)\ e^{-i(\omega' - i\omega'')\tau_d}$$

$$S^{\delta}_{2211}(\omega) = S^{\delta}_{1122}(\omega)$$

$$S^{\delta}_{1212}(\omega) = \delta(\omega' - \omega'' + \omega)$$

$$S^{\delta}_{1221}(\omega) = \frac{1}{2\pi}\int_{-\infty}^{\infty} e^{-i\omega'(\tau_d + \tau)}\ e^{i\omega''(\tau_d - \tau)}\ e^{-i\omega\tau}\ d\tau$$

$$= e^{-i(\omega' - \omega'')\tau_d}\ \delta(\omega' + \omega'' + \omega)$$

$$= e^{i(2\omega'' + \omega)\tau_d}\ \delta(\omega' + \omega'' + \omega)$$

$$S^{\delta}_{2112}(\omega) = \frac{1}{2\pi}\int_{-\infty}^{\infty} e^{-i\omega'(\tau_d - \tau)}\ e^{i\omega''(\tau_d + \tau)}\ e^{-i\omega\tau}\ d\tau$$

$$= e^{-i(\omega' - \omega'')\tau_d}\ \delta(\omega' + \omega'' - \omega)$$

$$= e^{i(2\omega'' - \omega)\tau_d}\ \delta(\omega' + \omega'' - \omega)$$

$$S^{\delta}_{2121}(\omega) = \delta(\omega' + \omega'' + \omega)$$

Lastly, the autocorrelation product spectra can be calculated from these results. The delta functions are inserted and the integrals contracted, when possible. The partial spectra are:

DC Terms:

$$S_{1122}(\omega)$$

$$= 2\pi\ \delta(\omega)\ A_1^2 A_2^2\ \frac{1}{2\pi}\frac{1}{T_1}\int_{-\infty}^{\infty} d\omega'\ |W_1(\omega')|^2\ e^{-i\omega'\tau_d}$$

$$\cdot\ \frac{1}{2\pi}\frac{1}{T_2}\int_{-\infty}^{\infty} d\omega''\ |W_2^*(\omega'')|^2\ e^{\ i\omega''\tau_d}.$$

Now from Appendix II, each of the integrals is simply the convolution of the chip shape with itself evaluated at $\tau_d = T_c/2$. As this is a unit height triangle with a base of $2T_c$, the result is simply 1/2 if the chip durations are approximately equal.

Therefore,

$$S_{1122}(\omega) = 2\pi\ \delta(\omega)\ \frac{1}{4}\ A_1^2A_2^2$$
$$= S_{2211}(\omega).$$

Chip Mixing Terms:

I:

$$S_{1212}(\omega) = A_1^2A_2^2\ \frac{1}{2\pi}\ \frac{1}{T_1}\ \frac{1}{T_2} \int_{-\infty}^{\infty} d\omega''\ |W_1(\omega'' - \omega)|^2 |W_2^*(\omega'')|^2.$$

which will subsequently be evaluated.

II:

$$S_{2121}(\omega) = A_1^2A_2^2\ \frac{1}{2\pi}\ \frac{1}{T_1}\ \frac{1}{T_2} \int_{-\infty}^{\infty} d\omega''\ |W_1(-\ \omega'' - \omega)|^2\ |W_2^*(\omega'')|^2$$
$$= S_{1212}(\omega),$$

upon letting $\omega'' = \overline{\omega}''$ and using the fact that the chip shapes are real.

III:

$$S_{1221}(\omega) = e^{i\omega\tau_d}\ A_1^2A_2^2\ \frac{1}{2\pi}\ \frac{1}{T_1}\ \frac{1}{T_2} \int_{-\infty}^{\infty} d\omega''\ |W_1(\omega'' + \omega)|^2\ |W_2^*(\omega'')|^2\ e^{i2\omega''\tau_d}\ .$$

IV:

$$S_{2112}(\omega) = e^{-i\omega\tau_d}\ A_1^2A_2^2\ \frac{1}{2\pi}\ \frac{1}{T_1}\ \frac{1}{T_2} \int_{-\infty}^{\infty} d\omega''\ |W_1(\omega'' + \omega)|^2\ |W_2^*(\omega'')|^2\ e^{-i2\omega''\tau_d}$$
$$= S_{1221}^*(\omega),$$

and the sum $S_{1221}(\omega) + S_{2112}(\omega)$ is real.

Evaluation of the Integral:

All four terms involve the integral:

$$I(\omega,\tau) = \frac{1}{2\pi}\frac{1}{T_1}\frac{1}{T_2}\int_{-\infty}^{\infty} d\omega'' \ |W_1(\omega'' + \omega)|^2 \ |W_2^*(\omega'')|^2 \ e^{-i2\omega''\tau},$$

where τ is $(0,\tau_d)$. To evaluate the integral define:

$$F_p(\omega) \triangleq \frac{1}{T_p} |W_p^*(\omega'')|^2, \ p = 1,2.$$

Then $F_p(\omega)$ is the Fourier transform of the convolution

$$f_p(t) = \frac{1}{T_p}\int_{-\infty}^{\infty} du \ w_p^*(u) w_p(u + \tau)$$

which is the usual triangle of unit height for rectangular chips $w_p(u)$.

Rewriting the integral in terms of the F_p's:

$$I(\omega,\tau) = \frac{1}{2\pi}\int_{-\infty}^{\infty} d\omega'' \ F_1^*(\omega'' + \omega) \ F_2(\omega'') \ e^{-i2\omega''\tau},$$

$$= \frac{1}{2\pi}\int_{-\infty}^{\infty} d\omega'' \int_{-\infty}^{\infty} du \int_{-\infty}^{\infty} dv \ e^{i\omega''(u - v - 2\tau)} \ e^{i\omega u} \ f_1^*(u) \ f_2(v),$$

Using the delta function obtained by the integration over ω'':

$$I(\omega,\tau) = \int_{-\infty}^{\infty} du \ f_1^*(u) \ f_2(u - 2\tau) \ e^{i\omega u},$$

which is comparatively simple to evaluate in the cases of interest.

$\underline{\tau = 0}$:

$$I(\omega,0) = \int_{-\infty}^{\infty} du\ f_1^*(u)\ f_2(u)\ e^{i\omega u},$$

As the chips are approximately equal:

$$f_1^*(u)\ f_2(u) = \begin{cases} \left[1 - \frac{|u|}{T_1}\right]^2, & |u|| \le T_1, \\ 0, & \text{otherwise.} \end{cases}$$

and

$$I(\omega,0) = \int_{-\infty}^{\infty} du\ f_1^*(u)\ f_2(u)\ e^{i\omega u},$$

$$I(\omega,0) = T_1 \left[\int_0^1 du\ (1-u)^2\ e^{i\omega T_1 u} + \int_0^1 du\ (1-u)^2\ e^{-i\omega T_1 u}\right]$$

$$I(\omega,0) = T_1 \frac{4}{(\omega T_1)^2} \left[1 - \frac{\sin(\omega T_1)}{\omega T_1}\right]$$

which is always positive and has a value of $4T_1/6$ at DC. With this result the partial spectrums $S_{1212}(\omega)$ and $S_{2121}(\omega)$ are given by:

$$S_{1212}(\omega) = 4T_1\ A_1^2 A_2^2 \frac{1}{(\omega T_1)^2} \left[1 - \frac{\sin(\omega T_1)}{\omega T_1}\right]$$

$$= S_{2121}^*(\omega).$$

$\underline{\tau = 2\tau_d}$:

$$I(\omega,2\tau_d) = \int_{-\infty}^{\infty} du\ f_1^*(u)\ f_2(u - 2\tau_d\ )\ e^{i\omega u},$$

$$I(\omega,2\tau_d) = e^{i\omega\tau_d} \int_{-\infty}^{\infty} du\ f_1^*(u + \tau_d)\ f_2(u - \tau_d)\ e^{i\omega u},$$

As the chips are approximately equal, and only overlap in the region $-T_d \leq u \leq T_d$:

$$f_1^*(u + \tau_d)\ f_2(u - \tau_d) = \begin{cases} \left[\frac{1}{4} - \left[\frac{u}{T_1}\right]^2\right], & |u| \leq \tau_d, \\ 0, \text{ otherwise.} \end{cases}$$

and

$$I(\omega, 2\tau_d) = e^{i\omega\tau_d} \int_{-T_1/2}^{T_1/2} du \left[\frac{1}{4} - \left[\frac{u}{T_1}\right]^2\right] e^{i\omega u},$$

upon changing variables of integration. Evaluating the integral gives:

$$I(\omega, 2\tau_d) = T_1/2\ e^{i\omega\tau_d} \left[\frac{1}{\omega T_1/2}\right]^2 \left[\frac{\sin(\omega T_1/2)}{\omega T_1/2} - \cos(\omega T_1/2)\right]$$

and, therefore,

$$S_{2112}(\omega) = \frac{T_1}{2} A_1^2 A_2^2 \left[\frac{1}{\omega T_1/2}\right]^2 \left[\frac{\sin(\omega T_1/2)}{\omega T_1/2} - \cos(\omega T_1/2)\right]$$

<u>Combination of the Chip Mixing Terms:</u>

With the results in hand for the four chip mixing terms (I, II, III, and IV), the addition of them produces the total mixing spectrum. The partial spectrums $S_{2112}(\omega)$ and $S_{1221}(\omega)$ can be added to produce:

$$S_{2112}(\omega) + S_{1221}(\omega)$$

$$= S_{2112}(\omega) + S^*_{2112}(\omega)$$

$$= 4T_1\ A_1^2 A_2^2 \left[\frac{1}{\omega T_1}\right]^2 \left[\frac{\sin(\omega T_1/2)}{\omega T_1/2} - \cos(\omega T_1/2)\right]$$

and the other pair of mixing terms give:

$$S_{1212}(\omega) + S_{2121}(\omega)$$

$$= 8T_1\ A_1^2 A_2^2 \frac{1}{(\omega T_1)^2} \left[1 - \frac{\sin(\omega T_1)}{\omega T_1}\right]$$

Finally, the chip mixing spectrum is the relatively simple result:

$$S_{12}^{M}(\omega) \triangleq S_{2112}(\omega) + S_{1221}(\omega) + S_{1212}(\omega) + S_{2121}(\omega)$$

$$= 4T_1 \; A_1^2 A_2^2 \, \frac{1}{(\omega T_1)^2} \left[[2 - \cos(\omega T_1/2)] \left[1 + \frac{1}{2} \, \frac{\sin(\omega T_1/2)}{\omega T_1/2} \right] \right].$$

At the chip rate harmonics ($\omega = \omega_1 = 2\pi/T_1$), where a narrowband output filter can be placed to detect the chip rate line, the continuous chip mixing spectrum has the value:

$$S_{12}^{M}(\omega_k) = T_1 \; A_1^2 A_2^2 \, \frac{3}{\pi^2} \, ,$$

which is a major result!

APPENDIX V

Chip/Noise Mixing Terms:

DC Term

Mixing of noise with a chip stream is typified by the term:

$$R_{xxnn}(\tau) = \left\langle A^2 \sum_k \sum_j E[c_k c_j]\ w_1(t - jT_1)\ w_1^*(t - kT_1 + \tau_d) \right.$$
$$\left. \cdot E[n^*(t + \tau)n(t + \tau_d + \tau)] \right\rangle,$$
$$= \left\langle A^2 R_{nn}(\tau_d) \sum_k w_1(t - kT_1)\ w_1^*(t - kT_1 + \tau_d) \right\rangle,$$

which is simply a DC term as it is independent of τ. Stationarity of the noise process and the second moment of the chip stream were used to arrive at this result.

The chip summation is no more than the continuous spectrum of the input chip stream evaluated at τ_d (See Appendix II). For τ_d of one-half of a chip time, that autocorrelation is .5. Therefore, the DC noise/chip contributions are:

$$R_{11nn}(\tau) = \frac{A^2}{2} R_{nn}(\tau_d) \quad ,$$
$$= R_{22nn}(\tau_d),$$
$$= R_{nn11}(\tau_d),$$
$$= R_{nn22}(\tau_d),$$

As the output contains all four terms, the total DC contribution from the chip/noise mixing is:

$$S_{nc}^{DC}(\omega) = 2A^2 \int_{-\infty}^{\infty} R_{nn}(\tau_d)\ e^{-\omega\tau}\ d\tau$$

or

$$= 2A^2\ 2\pi\ R_{nn}(\tau_d)\ \delta(0).$$

Chip/Noise Continuous Spectral Terms:

Evaluation of these terms proceeds much like earlier work. Calculate a single term in general form and the other terms are special cases. Now, consider

$$R_{1n1n} = \left\langle A^2 \sum_k \sum_j E[c_k c_j]\ w_1(t - jT_1 + \tau_1)\ w_1^*(t - kT_1 + \tau_3) \cdot E[n^*(t + \tau_2) n(t + \tau_4)] \right\rangle,$$

$$R_{1n1n}(\tau) = R_{nn}(\tau_4 - \tau_2) \left\langle A^2 \sum_k w_1(t - kT_1 + \tau_1)\ w_1^*(t - kT_1 + \tau_3) \right\rangle,$$

$$\triangleq R_{1n1n}(\tau_1, \tau_2, \tau_3, \tau_4)$$

$$R_{1nn1}(\tau_1, \tau_2, \tau_3, \tau_4) = R_{1n1n}(\tau_1, \tau_2, \tau_4, \tau_3)$$

$$R_{n11n}(\tau_1, \tau_2, \tau_3, \tau_4) = R_{1n1n}(\tau_2, \tau_1, \tau_3, \tau_4)$$

$$R_{n1n1}(\tau_1, \tau_2, \tau_3, \tau_4) = R_{1n1n}(\tau_2, \tau_1, \tau_4, \tau_3)$$

From earlier work, the periodic chip stream time average is given by:

$$\left\langle A^2 \sum_k w_1(t - kT_1 + \tau_1)\ w_1^*(t - kT_1 + \tau_3) \right\rangle$$

$$= \left\langle A^2 \sum_k a_k\ e^{i\omega_1 kT_1} \right\rangle$$

$$= A^2\ a_0$$

with

$$a_0 = A^2 \frac{1}{T_1} \int_{-\infty}^{\infty} w_1^*(t) w_1(t + \tau_3 - \tau_1)\ dt,$$

$$\triangleq R_{ww}(\tau_3 - \tau_1).$$

Therefore, the general term can be written as

$$R_{1n1n}(\tau_1, \tau_2, \tau_3, \tau_4) = R_{nn}(\tau_4 - \tau_2)\ R_{ww}(\tau_3 - \tau_1),$$

and as

$$R_{1nn1}(\tau_1, \tau_2, \tau_3, \tau_4) = R_{1n1n}(\tau_1, \tau_2, \tau_4, \tau_3)$$

$$= R_{nn}(\tau_3 - \tau_2)\ R_{ww}(\tau_4 - \tau_1),$$

$$R_{n11n}(\tau_1, \tau_2, \tau_3, \tau_4) = R_{1n1n}(\tau_2, \tau_1, \tau_3, \tau_4)$$

$$= R_{nn}(\tau_4 - \tau_1)\ R_{ww}(\tau_3 - \tau_1),$$

$$R_{n1n1}(\tau_1, \tau_2, \tau_3, \tau_4) = R_{1n1n}(\tau_2, \tau_1, \tau_4, \tau_3)$$

$$= R_{nn}(\tau_3 - \tau_1)\ R_{ww}(\tau_4 - \tau_2).$$

With these general forms the actual values of the τ_q's may be inserted from the table:

$$R_{1n1n}(\tau_1, \tau_2, \tau_3, \tau_4) = R^*_{nn}(\tau)\ R_{ww}(\tau),$$

$$R_{1nn1}(\tau_1, \tau_2, \tau_3, \tau_4) = R^*_{nn}(\tau - \tau_d)\ R_{ww}(\tau + \tau_d),$$

$$R_{n11n}(\tau_1, \tau_2, \tau_3, \tau_4) = R^*_{nn}(\tau + \tau_d)\ R_{ww}(\tau - \tau_d),$$

$$R_{n1n1}(\tau_1, \tau_2, \tau_3, \tau_4) = R^*_{nn}(\tau)\ R_{ww}(\tau).$$

Conjugation of the real noise autocorrelation function has been performed to simplify subsequent spectrum calculations.

The spectrum of the term R_{1nn1} is given by the transform on τ:

$$S_{1nn1}(\omega) = \int_{-\infty}^{\infty} R^*_{nn}(\tau - \tau_d)\ R_{ww}(\tau + \tau_d)\ e^{i\omega\tau}\ d\tau,$$

The spectrum is easiest to evaluate in this form if assumptions are made about the about the autocorrelation (or spectrum) of the noise. If the noise spectrum is assumed to be a bell-shaped one, with a bandwidth equal to the chip rate, the the autocorrelation of the noise may be taken to be

$$R_{nn}(\tau) = N_{IP}\ u(\tau),$$

where $u(\tau)$ is a triangle of a base width of $2T_1$. If the noise is taken to have a wider bandwidth, then the triangle is more narrow. With this choice of the autocorrelation:

$$S_{1nn1}(\omega) = N_{IP}\, A^2 \int_{-\infty}^{\infty} u_n(\tau - \tau_d)\, u(\tau + \tau_d)\, e^{i\omega\tau}\, d\tau,$$

which is identical to integrals evaluated previously in terms of chip mixing $(I(\omega,\tau))$. The result for the sum of the four terms may be written immediately from the chip mixing results.

$$S_{1n}^{C}(\omega) \triangleq S_{1n1n}(\omega) + S_{n1n1}(\omega) + S_{1nn2}(\omega) + S_{n11n}(\omega)$$

$$= 4T_1\, A_1^2 N_{IP} \frac{1}{(\omega T_1)^2} \left[[2 - \cos(\omega T_1/2)] \left[1 + \frac{1}{2} \frac{\sin(\omega T_1/2)}{\omega T_1/2} \right] \right] .$$

At the chip rate harmonics ($\omega = \omega_1 = 2\pi/T_1$), where a narrowband output filter can be placed to detect the chip rate line, the continuous chip/noise mixing spectrum has the value:

$$S_{1n}^{C}(\omega_k) = T_1\, A_1^2 A_2^2 \frac{3}{\pi^2} ,$$

---

which is a major result!

Constant Input Spectrum to the Chip Rate

A similar calculation for the rectangular spectrum results in a very small value for the value of the chip/noise spectrum at the chip rate. By using the constant valued spectrum for the noise (to the chip rate) the value of the continuous chip/noise spectrum in this instance is:

$$S_{1n}^{C/C}(\omega_k) = T_1\, A_1^2\, N_I \frac{1}{\pi} \left[2\, Si(4\pi) - Si(8\pi) \right] ,$$

where the function Si(x) is given by

$$Si(x) = \int_0^x \frac{\sin(u)}{u}\, du.$$

To a good degree of approximation, the values of $Si(4\pi)$ and $Si(8\pi)$ can be replace by $2/\pi$, the asymptotic value of the function.

Therefore, the continuous spectrum has the value:

$$S_{1n}^{C/C}(\omega_k) = T_1 \, A_1^2 \, N_I \, \frac{1}{2},$$

for the rectangular input noise spectrum. This value is considerably smaller than that for the chip shaped input noise spectrum result, above, as the chip/noise products are less correlated due to the wider noise bandwidth.

APPENDIX VI

Analysis of the Chip Rate Detector Output Signal-to-Noise Ratio

The signal-to-noise ratio for a particular chip stream output with a pair of chip stream inputs and noise is (Section 6.1.4):

$$\left[\frac{S}{N}\right]_{o,1} = \frac{S_1^2\ TW}{S_1^2 + S_2^2 + \alpha\ \pi^2/4\ N_I^2 + 3[S_1S_2 + \beta S_1N_I + \beta S_2N_I]}.$$

with α and β constants depending upon the noise spectrum model chosen. The other chip stream has the same expression for the signal-to-noise ratio; but with the numerator identifying that chip amplitude (denominators are identical).

With a rectangular filter (with an upper cut-off of the chip rate) $\alpha = 1$ and $\beta = \pi^2/6$. For a chip shaped impulse response filter, $\alpha\ \pi^2/4 = 3/2$ and $\beta = 1$.

For interpretation of the result, two cases are of interest; large and small input signal-to-noise ratios.

Small Input Signal-to-Noise Ratio

Given the input signal-to-noise ratio

$$\left[\frac{S}{N}\right]_{i,1} \triangleq \frac{S_1}{N_I},$$

$$\ll 1,$$

rewrite the expression above as:

$$\left[\frac{S}{N}\right]_{o,1} = \frac{TW}{\dfrac{S_1^2 + S_2^2 + \alpha\ \pi^2/4\ N_I^2 + 3[S_1S_2 + \beta S_1N_I + \beta S_2N_I]}{S_1^2}},$$

$$\left[\frac{S}{N}\right]_{o,1} \cong \frac{TW}{S_2^2/S_1^2 + \alpha\ \pi^2/4\ N_I^2/S_1^2 + 3[S_2/S_1 + \beta S_2N_I/S_1^2]},$$

and the result depends upon the ratio of the two chip stream powers.

Case I: The Chip Stream S_1 Dominates:

$$S_1 \gg S_2$$

and

$$\left[\frac{S}{N}\right]_{o,1} \cong \frac{TW}{\alpha\ \pi^2/4\ N_I^2/S_1^2}\ .$$

$$= \frac{1}{\alpha}\ \frac{4}{\pi^2}\ TW\ \left[\frac{S}{N}\right]_{i,1}^2,$$

which is the well known result for a chip rate detector with only a single chip stream and noise in the input ($\alpha = 1$).

Case II: <u>The Chip Stream S_2 Dominates:</u>

$$S_2 >> S_1$$

and

$$\left[\frac{S}{N}\right]_{o,1} \cong \frac{TW}{S_2^2/S_1^2 + \alpha\ \pi^2/4\ N_I^2/S_1^2 + 3\beta S_2 N_I/S_1^2}\ ,$$

Now, things are a good deal more complicated. However, the results can also be written in terms of the signal-to-noise ratio of the second chip stream.

Letting the second chip stream signal-to-noise ratio be:

$$\left[\frac{S}{N}\right]_{i,2} \triangleq \frac{S_2}{N_I},$$

then,

$$\left[\frac{S}{N}\right]_{o,1} \cong \frac{\frac{1}{\alpha}\left[\frac{2}{\pi}\right]^2\left[\frac{S}{N}\right]_{i,1}^2\ TW}{1 + \frac{1}{\alpha}\left[\frac{2}{\pi}\right]^2\left[\frac{S}{N}\right]_{i,2}^2 + 3\ \frac{\beta}{\alpha}\left[\frac{2}{\pi}\right]^2\ \left[\frac{S}{N}\right]_{i,2}},$$

and two subcases present themselves according to whether the signal-to-noise of the second chip stream is small or large. If the second chip stream has a small signal-to-noise then the output signal-to-noise ratio reduces to simply the single chip stream case as expected.

For a large signal-to-noise of the second chip stream, the output signal-to-noise ratio becomes:

$$\left[\frac{S}{N}\right]_{o,1} \cong \left[\frac{S_1}{S_2}\right]^2$$

which is worse than simply noise by the factor of $\alpha\ \pi^2/4$.

Large Input Signal-to-Noise Ratio

For a large input signal-to-noise ratio

$$\left[\frac{S}{N}\right]_{i,1} \triangleq \frac{S_1}{N_I},$$

$$\gg 1,$$

rewrite the expression above as:

$$\left[\frac{S}{N}\right]_{o,1} = \frac{TW}{1 + S_2^2/S^2{}_1 + 3S_2/S_1 + 3\beta\, S_2/S_1\ [N/S]_{i,1}},$$

which depends upon the ratio of the power in the two chip streams. Again, two cases present themselves.

Case I: The Chip Stream S_1 Dominates:

In this instance the apparent output is that of the reference chip stream by itself. Only the self-noise of the reference chip stream is present. And,

$$S_1 \gg S_2$$

and

$$\left[\frac{S}{N}\right]_{o,1} = TW,$$

Case II: The Chip Stream S_2 Dominates:

With

$$S_2 \gg S_1$$

then

$$\left[\frac{S}{N}\right]_{o,1} = \frac{S_1^2}{S_2^1}\, TW.$$

The output signal-to-noise ratio depends only upon the ratio of the chip stream powers, as might be expected.

Generalization to N Chip Stream Inputs

Calculation of the signal and noise power for N chip streams in the chip rate detector input is a relatively simple generalization of the two chip stream case. From Section 6, an examination of the terms in the chip detector output reveals that there are only two types that contribute at the chip rate. One is the self-noise of the chip stream/noise, which is quadratic in the chip/noise powers. There are N chip terms and one noise term. The other type is the intermodulation noise of the chip streams/noise which results in the cross-power terms. There are N(N–1)/2 chip/chip terms and N chip/noise terms.

Therefore, the total "noise" out of the chip rate detector is:

$$TN = \sum_j S_j^2 + \alpha\, \pi^2/4\; N_I^2 + \frac{3}{2} \sum_j \sum_{\substack{k \\ j \neq k}} S_j S_k + 3\beta \sum_j S_j N_I,$$

where the sums are over the N chip streams. By making reasonable assumptions about the distribution of the powers (signal-to-noise ratios) of the chip stream inputs an average output noise can be calculated. This average over the powers is:

$$E[TN] = N_I^2 \left[N\, E[SNR^2] + \alpha\, \pi^2/4 + \frac{3}{2} N(N-1)\; E[SNR]^2 + 3\beta\, N\, E[SNR] \right]$$

The output chip line power (normalized to the input noise power) for the j^{th} chip stream is

$$S = S_j^2/N_I^2\; TW$$

with the average output equal to:

$$E[S] = E[SNR^2].$$

With these quantities, the average output signal-to-noise ratio, over all chip streams is:

$$SNR_{av} = \frac{E[SNR^2]\; TW}{\left[N\, E[SNR^2] + \alpha\, \pi^2/4 + \frac{3}{2} N(N-1)\; E[SNR]^2 + 3\beta N\, E[SNR] \right]}$$

$$= \frac{1}{N} \frac{TW}{\left[1 + \alpha\, \pi^2/(4N) + \frac{3}{2} (N-1)\; E[SNR]^2/E[SNR^2] + 3\beta\, E[SNR]/E[SNR^2] \right]}.$$

Further evaluation of the average signal-to-noise ratio requires specification of the distribution function of the chip stream signal-to-noise ratios.

Two,cases will be considered. One will be a uniform distribution over dB of the signal-to-noise ratios of the chip stream transmitters. The other will be a uniform distribution over transmitter ranges, with all transmitted powers equal.

Case I:

Uniform Distribution of Signal-to-Noise Ratios (in dB).

Assume the distribution is given between zero and dB_{max}, then

$$p_{dB}(dB) = \frac{1}{dB_{max}} \begin{cases} 1, & 0 \le dB \le dB_{max}, \\ 0, & \text{otherwise.} \end{cases}$$

and obtaining the distribution of S through the relation

$$dB = 10 \log_{10}(S):$$

$$p_S(S) = \frac{1}{\ln S_{max}} \frac{1}{S}, \; 1 \le S \le S_{max}.$$

The expectations follow:

$$E[S] = \frac{S_{max} - 1}{\ln S_{max}},$$

$$E[S] = \frac{1}{2} \frac{S_{max}^2 - 1}{\ln S_{max}},$$

and the desired ratios are (for $S_{max} >> 1$)

$$\frac{E[S]^2}{E[S^2]} = \frac{2}{\ln S_{max}},$$

$$\frac{E[S]}{E[S^2]} = \frac{2}{S_{max}}.$$

With these relations, the average chip rate detector output signal-to-noise ratio is:

$$SNR_{av} \equiv \frac{1}{N} \frac{TW}{\left[1 + \alpha \pi^2/(4N) + 3(N-1)/\ln S_{max} + 6\beta/S_{max}\right]}.$$

For a large number of emitters ($N >> 1$) and high input maximum signal-to-noise ratios ($S_{max} >> 100$ (20 d B)), the the formula may be approximated by:

$$SNR_{av} = \frac{1}{N} \frac{TW}{\left[1 + 3(N-1)/\ln S_{max}\right]}.$$

A conclusion can be reached. The average signal-to-noise ratio decreases at least as fast as N for emitters spread over extremely wide dynamic ranges. For a 60 dB dynamic range:

$$SNR_{av} = \frac{1}{N} \frac{TW}{\left[1 + .22\ (N-1)\right]}.$$

Case II:

Uniform Distribution of Ranges

Assume the distribution is given between R_{min} and R_{max}, then

$$p_{dB}(dB) = \frac{1}{R_{max} - R_{min}} \begin{cases} 1, & R_{min} \le R \le R_{max}, \\ 0, & \text{otherwise}, \end{cases}$$

and obtain the distribution of S through the relation

$$S = \frac{A}{R^2}.$$

As in case I, for large max to min range range ratios:

$$SNR_{av} = \frac{1}{N} \frac{TW}{\left[1 + \alpha\ \pi^2/(4N) + \frac{9}{2}\ (N-1)\ R_{min}/R_{max} + 9\beta/SNR_{min\ range}\right]}.$$

Again, assuming the minimum range signal-to-noise ratio is large, and N also:

$$SNR_{av} = \frac{1}{N} \frac{TW}{\left[1 + \frac{9}{2}\ (N-1)\ R_{min}/R_{max}\right]}.$$

A similar conclusion to the uniform distribution in dB case can be reached. The average signal-to-noise ratio decreases as the number of emitters (N). A choice of maximum-to-minimum range of 1000 (60 dB dispersion) gives, in this instance:

$$SNR_{av} = \frac{1}{N}\frac{TW}{\left[1 + .0045(N-1)\right]}.$$

Summarizing, a large number of emitters tends to obscure each emitter's chip rate line. The obscuration increases as 10 log(N) in dB!

APPENDIX VII

NOMOGRAM DETERMINES PROBABILITY OF

Detecting Signals in Noise

By DONALD E. BAILEY
NEIL C. RANDALL
Research Division, Philco Corporation, Philadelphia, Pa.

IN RECEIVING SYSTEMS it is often desirable to determine detection probability for signals in noise. This nomogram gives a method of doing it without solving integral equations[1,2], or using tables[3,4], when dealing with envelope detection of signals with nonfluctuating amplitude accompanied by additive Gaussian noise.

Signal-to-noise ratio S/N is the rms power signal-to-noise ratio, threshold level β is the input voltage above which the detector gives an output, and false-alarm probability P_{fa} is the probability that noise voltage will exceed the threshold. Equation 1 relates threshold level and false-alarm probability, assuming Gaussian noise and normalizing with respect to rms noise current.

Probability P_d that the sum of instantaneous voltages of signal and noise will exceed the threshold, is the integral, from threshold level to infinity, of the probability density function of signal plus noise[1,2], as in Eq. 2, where J_0 is the Bessel function with imaginary argument, and V the envelope of the signal-plus-noise current normalized by rms noise current. Density functions in the figure show typical relationships among P_d, P_{fa}, β and S/N. The nomogram is a semiempirical solution of Eq. 2 for a power S/N ratio measured in the receiver i-f.

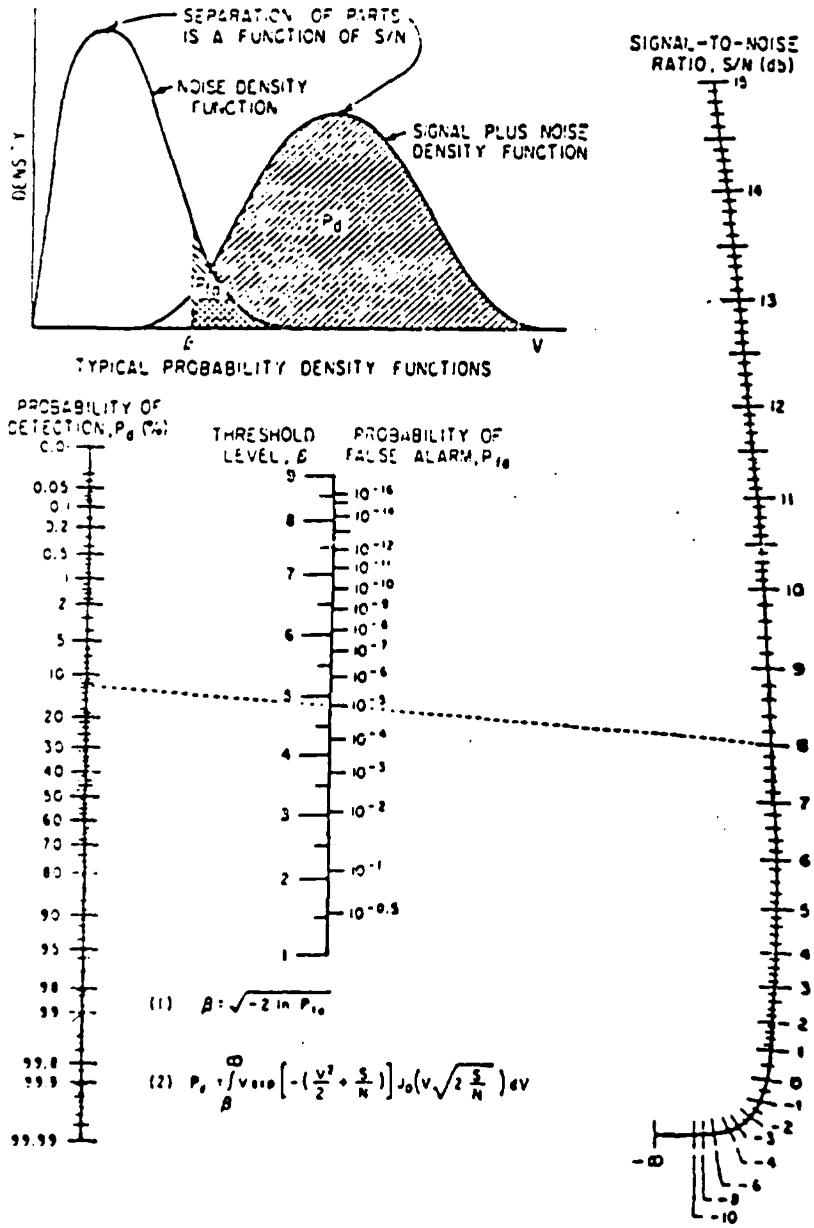

(1) $\beta = \sqrt{-2 \ln P_{fa}}$

(2) $P_d = \int_{\beta}^{\infty} V \exp\left[-\left(\frac{V^2}{2} + \frac{S}{N}\right)\right] J_0\left(V\sqrt{2\frac{S}{N}}\right) dV$

Straight line through points of two known variables will give the third variable, with accuracy ± one division of the S/N scale. If a S/N ratio of 8 db is available and a P_{fa} of 10^{-5} is wanted, a straight line between these points gives the probability of detection as 12.5 percent. Threshold level is about 4.8

REFERENCES

(1) S. O. Rice, Mathematical Analysis of Random Noise, Selected Papers on Noise and Stochastic Processes, ed. Nelson Wax.
(2) M. Schwartz, A Coincidence Procedure for Signal Detection, PGIT, Vol IT-2, Dec 1956.
(3) J. I. Marcum, Table of Q Functions, Project Rand (AD 116551).
(4) Burington and May, Handbook of Probability and Statistics with Tables, Handbook Publishers Inc., 1953.

UNCLASSIFIED

SECURITY CLASSIFICATION OF THIS PAGE

REPORT DOCUMENTATION PAGE

1a. REPORT SECURITY CLASSIFICATION
Unclassified

1b. RESTRICTIVE MARKINGS

2a. SECURITY CLASSIFICATION AUTHORITY

2b. DECLASSIFICATION / DOWNGRADING SCHEDULE

3. DISTRIBUTION / AVAILABILITY OF REPORT
Approved for public release;
distribution unlimited.

4. PERFORMING ORGANIZATION REPORT NUMBER(S)

5. MONITORING ORGANIZATION REPORT NUMBER(S)
ARO 25331.1-EL

6a. NAME OF PERFORMING ORGANIZATION
M/A-COM Government Systems

6b. OFFICE SYMBOL *(If applicable)*

7a. NAME OF MONITORING ORGANIZATION
U. S. Army Research Office

6c. ADDRESS *(City, State, and ZIP Code)*
8619 Westwood Center Drive
Vienna, VA 22180

7b. ADDRESS *(City, State, and ZIP Code)*
P. O. Box 12211
Research Triangle Park, NC 27709-221

8a. NAME OF FUNDING / SPONSORING ORGANIZATION
U. S. Army Research Office

8b. OFFICE SYMBOL *(If applicable)*

9. PROCUREMENT INSTRUMENT IDENTIFICATION NUMBER
DAAL03-87-C-0020

8c. ADDRESS *(City, State, and ZIP Code)*
P. O. Box 12211
Research Triangle Park, NC 27709-2211

10. SOURCE OF FUNDING NUMBERS

PROGRAM ELEMENT NO.	PROJECT NO.	TASK NO.	WORK UN ACCESSION

11. TITLE *(Include Security Classification)*
Detectability of a Direct Sequence Emitter Within a Network of Direct Sequence Emitters

12. PERSONAL AUTHOR(S)
David L. Nicholson and Edgar H. German, Jr.

13a. TYPE OF REPORT
Final Technical

13b. TIME COVERED
FROM 9-15-87 TO 1-14-88

14. DATE OF REPORT *(Year, Month, Day)*
1988 January

15. PAGE COUNT
139

16. SUPPLEMENTARY NOTATION
The view, opinions and/or findings contained in this report are tho of the author(s) and should not be construed as an official Department of the Army posit policy, or decision, unless so designated by other documentation.

17. COSATI CODES

FIELD	GROUP	SUB-GROUP

18. SUBJECT TERMS *(Continue on reverse if necessary and identify by block number)*
Signal Detection, Spread Spectrum Communications,
Low Probability of Intercept

19. ABSTRACT *(Continue on reverse if necessary and identify by block number)*

This report analyzes the ability of unintended intercept receivers to isolate individua Direct Sequence (DS) emitters within a network of DS emitters. The report demonstrates interception over $1/R^4$ propagation paths requires very large, ground-based antennas in to achieve a usable intercept Signal-to-Noise Ratio (SNR). On the other hand, free spac $1/R^2$ propagation paths provide intercept receivers with signal power levels well above thermal noise power even when the intercept antenna is quite small. However, these smal antennas are not able to resolve individual emitters at typical intercept ranges. Ante large enough to resolve individual emitters are too large to put on aircraft as require achieve the necessary free space propagation. Hence, the report finds that the beamwidt of the intercept receiver will typically contain many DS emitters. Therefore the receiv bandwidth will contain many overlapping DS signals each typically with a power level wh is well above the thermal noise power in the intercept bandwidth. This is the intercept context analyzed in this report.

20. DISTRIBUTION / AVAILABILITY OF ABSTRACT
☒ UNCLASSIFIED/UNLIMITED ☐ SAME AS RPT. ☐ DTIC USERS

21. ABSTRACT SECURITY CLASSIFICATION
Unclassified

22a. NAME OF RESPONSIBLE INDIVIDUAL

22b. TELEPHONE *(Include Area Code)*

22c. OFFICE SYMBOL

END
DATED
FILM
8—88
DTIC